



**Synthesis, Coordination chemistry and  
Molecular orbital calculations  
of  
7,8-dihydro-7-oxo-[1,2,4]-triazolo[4,3-a]pyrimidine  
derivative**

**By**

**Sawsan Aref Mohammed Salameh**

**B. Sc. Chemistry / Al-Quds University / Palestine**

**Supervised by:**

**Dr. Mohammad Abul Haj**

**Dr: Omar Deeb**

**Supervisor of experimental and  
Inorganic chemistry**

**Supervisor of Theoretical Chemistry**

**A THESIS**

**Submitted in Partial fulfillment of requirements for the degree of**

**Master of Applied & Industrial Technology**

**Department of Chemistry & Chemical Technology**

**Faculty of Science and Technology**

**Al-Quds University**

**JANUARY, 2005**

**Deanship of Graduate Studies  
Al-Quds University**

**Synthesis, Coordination chemistry and  
Molecular orbital calculations,  
of  
7,8-dihydro-7-oxo-[1,2,4]-triazolo [4,3-a]  
pyrimidine derivative**

**By:**

**Sawsan Aref Mohammed Salameh**

**M.Sc. Thesis**

**Jerusalem- Palestine**

**January 2005**

## ***Declaration***

*I certify that this thesis submitted for the degree of Master is the results of my own research, except where otherwise acknowledged, and that this thesis has not been submitted for a higher degree to any other university or institution.*

## ***Signed:***

*Sawsan Aref Mohammed Salameh*

## ***Date:***

*18/1/2005*

## *Acknowledgement*

*I would like first of all to take the opportunities to appreciate and express my personal and sincere gratitude to my supervisor Dr. Mohammad Abul Haj for his special concern and recommendation on my experiments and analysis whom I respect and admire the most. I would also like to thank my supervisor Dr. Omar Deeb and all the staff members and all my colleagues in Chemistry department at Al-Quds University for their help and advice during my study period.*

*The contribution that Granada University -Spain- has made in helping me in characterization and results analysis was wonderful and helpful therefore I would like to extend my thanks and appreciation.*

*Finally I don't want to forget to thank all the members of my family especially my parents and all my friends whom where by my said through my study period.*

*To all of you I owe special thanks.*

## Abstract

The condensation of 1,2,4-triazole and a pyrimidine ring gives rise to the formation of bicyclic heterocycles known as 1,2,4- triazolopyrimidines. Four different possibilities exist for the relative orientation of both rings, so four different isomeric families of compounds are defined. Among these, 1,2,4-triazolo[1,5-a]pyrimidine derivatives are the thermodynamically more stable and, thus, the most studied ones. Revisions surveying the synthesis, reactivity, spectroscopic characterization and crystallographic studies of 1,2,4-triazolo[1,5-c]pyrimidines, 1,2,4-triazolo[4,3-a]pyrimidine and 1,2,4-triazolo[4,3-c] pyrimidines have also been published.

The studies about the coordination chemistry of triazolopyrimidines have exclusively focused till now in the 1,5-a series. These compounds, which are structurally similar and may be regarded as mimic of isomeric purines, have displayed a rich coordination chemistry, a considerable number of new compounds with interesting structural features having been characterized, including simple mononuclear compounds with monodentately coordinated ligands and di or polynuclear compounds in which either the triazolopyrimidine ligand, or other auxiliary ligands bridge the metal atoms.

On the other hand, we have not found in the bibliography any reference for a coordination compound of any of the other arrangements (1,5-c, 4,3-a or 4,3- c), despite the fact that the different relative orientation of the nitrogen atoms inside the heterocycles could generate a wide number of new structure, specially if dimeric or polynuclear species are formed with bridging heterocycles. A difficulty that has to be taken into account in a study of this type is the lowest stability of these compounds if compared with the 1,5-a derivatives, isomerization processes (Dimroth rearrangement) may take place on heating, possibly catalyzed by acidic or basic pH.

This research and investigation of the coordination chemistry of triazolopyrimidine were the center of our thesis. Following this line of investigation a new derivative 7,8 dihydro-7-oxo-1,2,4-triazolo[4,3-a]pyrimidine was synthesized and characterized, In this thesis we chose the best method through the synthesis and modification to obtain maximum yield. The compound was characterized by usual methods and the results

indicated that the most stable tautomer form is this when the acidic hydrogen was on N8 position, this result was supported by the theoretical study,  $^1\text{H-NMR}$  and  $^{13}\text{C-NMR}$  spectra.  $\text{pK}_a$  value was determined and it was more acidic than analogues purine bases, also from MO calculation there was no preference site of coordination.

This thesis is the first exploration in the coordination chemistry of 1,2,4-triazolo[4,3-a]pyrimidines. This compound comparing with the corresponding 1,5-a isomers, has the change in the position of one of the nitrogen atoms in the triazole ring which is now placed as separated as possible from the pyrimidine ring, with less steric hindrance and contiguous to the other external imidazole nitrogen. Synthesis of metal complexes of the first and second row transition metals (Cu, Ni, and Ag) was carried out, some of these complexes were isolated in pure crystal form, others need further investigation, the complexes were characterized by X-ray crystallography showing that the ligand retain 4,3-a isomer which is less favored thermodynamically. With Cu the ligand form two complexes  $\text{CuL}_2\text{Cl}_2(\text{H}_2\text{O})_3$ , and  $\text{CuL}_2\text{Cl}_2(\text{H}_2\text{O})_5$  these complexes were not isolated in crystal form.

Also two nickel complexes were obtained  $\text{NiL}_2(\text{H}_2\text{O})_5$  and  $\text{Ni}_9\text{L}_8(\text{NO}_3)_4(\text{NH}_3)_4(\text{OH})_6(\text{H}_2\text{O})_{16}$  cluster, for this complex cluster the ligand coordinated in its anionic form through N1, N2 and O without preference of one site over another, this cluster had showed ferromagnetic and antiferromagnetic interaction at lower temperature and also need further investigation since this type of compounds be could used in the field of electronics as data storage materials. Silver crystal complex  $\text{AgL}_2(\text{NO}_3)_2(\text{H}_2\text{O})_2$  were isolated and characterized by X-ray. The coordination mode in N1 and N2 atoms, the acidic hydrogen was situated on N8 the same as in the free ligand.

The most stable thermodynamic 1,5-a compound was also obtained during one of the reaction to prepare cobalt complex with the desired ligand an organic compound had precipitate and the isolated in the form of single crystal, product is in agreement with Dimroth rearrangement

## ملخص الرسالة:

مركبات التريازولوبيريميدين (Triazolopyrimidine) هي مركبات عطرية غير متجانسة وتتكون من حلقتين الأولى هي حلقة سداسية البريميدين (pyrimidine) والآخرى حلقة خماسية تريازول (triazoles), ينتج عن ارتباط الحلقتين اربع مجموعات من المتشكلات تختلف بترتيب ذرات النيتروجين داخل الحلقة السداسية والخماسية اثنين من هذه المتشكلات هي مركبات تتكون بسرعة (Kinetically favor) وهي 4,3-a & 4,3-c ومع العلم انها غير مستقرة من ناحية الديناميكا الحركية, المجموعتان الاخرتان 1,5-a & 1,5-c هما مستقرتان حراريا (thermodynamically stable).

احد هذه المتشكلات (1,5-a) تم دراستها بشكل مستفيض من ناحية التحضير العضوي للمركبات ودراسة تأثيراتها البيولوجية وتحضير معقدات من المركبات وقد وجدت كيمياء التشاركية ثرية بالتشكيلات المختلفة التي تم تحضيرها بسبب أن المركب يمكن أن يتشارك المعدن بطرق وأماكن ارتباط مختلفة تم تحضيرها بسبب أن المركب يمكن أن يكون روابط بطرق وأماكن ارتباط مختلفة مما أدى إلى تحضير مركبات أحادية, ثنائية, ومركبات متسلسلة. بعض هذه المركبات كحان له تأثيرات بيولوجية واضحة وبعضها كان له أهمية من ناحية فيزيائية.

في هذه الرسالة قمنا بتحضير ودراسة المركب 7,8-dihydro-7-oxo-1,2,4-triazolo[4,3-a]pyrimidine, تحضيره وتشخيصه بواسطة التقنيات المختلفة وتحضير مركبات معقدة منه. لا يوجد دراسات سابقة في هذا الموضوع وهذه تعتبر بداية مسار بحثي جديد في الكيمياء التشاركية لهذا المتشكل سيما أن هذا المركب يعتبر غير مستقر من ناحية الديناميكا الحركية, خلال هذا البحث قمنا بدراسة بداية هذا المركب من ناحية نظرية باستخدام طريقة semiempirical والتي هي جزء من موضوع الكيمياء الحاسوبية (Computational chemistry) وقد تم التعرف على (tautomer) الأكثر استقرارا وتم احتساب توزيع الشحنات, الكثافة الإلكترونية و حسابات الأفلاك الجزيئية لهذا المركب ومن هذه الدراسة تبين انه لا يوجد مكان ارتباط مفضل لعمل روابط تشاركية في المعقدات.

بعد تحضير المركب استخدم في تحضير عدد من المعقدات لبعض لمعادن من الدورة الرابعة والخامسة للعناصر الانتقالية و كنتيجة لذلك حصلنا على عدد من المركبات بشكل بلوري مما سمح لنا تشخيصها بواسطة أشعة X

ومن هذه المركبات التي تم تحضيرها  $NiL_2(H_2O)_5$ ,  $CuL_2Cl_2 \cdot (H_2O)$ ,  $CuL_2Cl_2 \cdot (H_2O)_3$ ,  $Ag_2L_2(NO_3)_2 \cdot (H_2O)_2$  فصل منها مركبي الفضة والنيكل على شكل بلوري.

بالنسبة لمركب النيكل  $Ni_9L_8(NO_3)_4(NH_4)_3 \cdot (H_2O)_{16}$  تكون مركب مبعثر (cluster) يتكون من تسع ذرات نيكل وجد أن ligand ارتبط معه بثلاث أماكن مختلفة N1, N2 & O بدون تفضيل احدها على الآخر وهذا يتفق مع الدراسة النظرية, وبعد الدراسات المغناطيسية وجد أن له صفات ferromagnetic & antiferromagnetic وهذه المركبات لها تطبيقات في الالكترونيات في مجال تخزين المعلومات في الحاسوب. وخلال محاولتنا تحضير معقد للكوبالت فصلت مادة على شكل بلوري شخصت باستخدام أشعة X وتبين انه المركب المتشكل الآخر وهو 1,5-a تحول خلال عملية التحضير وذلك حسب الطريقة التي ذكرت هذه العملية (Dimroth rearrangement).



# ***OUT LINE***

	<b>Page</b>
<b>Chapter one: Introduction</b>	1
I.1 Historical background	2
I.2 Synthesis	3
I.2.1 Synthesis of 1,2,4-triazolo[4,3-a]pyrimidine	4
I.2.1.1 Synthesis from pyrimidine	4
I.2.1.2 Synthesis from triazoles	7
I.2.2 Synthesis of 1,2,4-Triazolo[1,5-a]pyrimidine	10
I.2.2.1 Synthesis from 1-Aminopyrimidines	10
I.2.2.2 Synthesis from 2-Aminopyrimidines	11
I.2.2.3 Syntheses from 5(3)-Amino-1,2,4-Triazoles	12
I.2.2.4 Dimroth Rearrangement of 1,2,4-triazolo[4,3-a]pyrimidine	13
I.2.3 1,2,4-triazolo[4,3-c]pyrimidine	16
I.2.3.1 Synthesis from pyrimidine	16
I.2.3.2 Synthesis from triazole	19
I.2.3.3 Synthesis by concurrent formation of both of the 1,2,4- triazole and pyrimidine rings	20
I.2.4 1,2,4-triazolo [1,5-c]pyrimidine	21
I.2.4.1 Open Chain Precursors for Synthesis	21
I.2.4.2 Synthesis from pyrimidine	23
I.2.4.3 Synthesis from triazoles	24
I.2.4.4 Synthesis by concurrent formation of both of the 1,2,4- triazole and pyrimidine rings	25
I.2.4.5 Dimroth Rearrangement of 1,2,4-Triazolo[4,3-c]pyrimidine	26
I.3 The Coordination's Chemistry of the 1,2,4-triazolo[1,5-a]pyrimidine derivatives	28
I.3.1 Compounds without a direct metal-triazolopyrimidine bond	29
I.3.2 Copper(II) complexes	29
I.3.3 Manganese, iron, cobalt, nickel, zinc complexes	32
I.3.4 Mercury(II) and Cadmium(II) complexes	33

I.3.5 Silver(I) and copper(I) complexes	34
I.3.6 Platinum group metal complexes	37
I.4 Applications of Triazolopyrimidines	39
I.4.1 Pharmaceutical uses	39
I.4.2 Agrochemical Uses	41
I.4.3 Photographic uses	42
I.5 Computational Chemistry	42
I.5.1 Quantum Mechanics	43
I.5.2 Molecular Mechanics	44
I.5.2.1 Bonding energies	45
I.5.2.1.1 Bonds and Angles	45
I.5.2.1.2 Bond Angle Bending	46
I.5.2.1.3 Dihedrals (torsion) energy	46
I.5.2.2 Non-bonding energies	46
I.5.2.2.1 Van der Waals energy	46
I.5.2.2.2 Electrostatic energy	47
I.6 Objectives	48
<b>Chapter two: Synthesis ,characterization and theoretical study of 7,8-</b>	49
<b>    dihydro-7-oxo-1,2,4-triazolo[4,3-a]pyrimidine ligand</b>	
II.1 Introduction	50
II.2 Experimental	52
II.2.1 Materials	52
II.2.2 Synthesis of 7,8-dihydro-7-oxo-1,2,4-triazolo[4,3-a] pyrimidine	52
II.3 Characterization	53
II.3.1 Elemental analysis	54
II.3.2 Infrared Spectroscopy	54
II.3.3 Nuclear Magnetic Resonance spectroscopy	57
II.3.4 Potentiometer titration	63
II.3.5 Thermal Analysis	64
II.3.6 X-Ray	66
II.3.7 Molecular Orbital Calculation	66
<b>Chapter three: Coordination chemistry of 7,8 dihydro-7-oxo-1,2,4-</b>	75
<b>    triazolo[4,3-a]pyrimidine ligand with Cu, Ni, and Ag metal</b>	

III.1 Introduction	76
III.2 Experimental	76
III.2.1 Material	76
III.2.2 Instrumentation	76
III.2.3 Crystallography	77
III.3 Results and Discussion	77
III.3.1 Copper complexes	77
III.3.1.1 $\text{CuL}_2\text{Cl}_2(\text{H}_2\text{O})_3$ complex	77
III.3.1.1.1 Synthesis	77
III.3.1.1.3 Elemental analysis	78
III.3.1.1.3 Infrared Spectroscopy	78
III.3.1.1.4 Thermal analysis	80
III.3.1.2 $\text{CuL}_2\text{Cl}_2(\text{H}_2\text{O})_5$ complex	83
III.3.1.2.1 Synthesis	83
III.3.1.2.2 Elemental analysis	83
III.3.1.2.3 Infrared Spectroscopy	83
III.3.1.2.4 Thermal Analysis	85
III.3.2 Nickel Complexes	88
III.3.2.1 $\text{NiL}_2(\text{H}_2\text{O})_5$ complex	88
III.3.2.1.1 synthesis	88
III.3.2.1.2 Elemental Analysis	88
III.3.2.1.3 Infrared Spectroscopy	88
III.3.2.1.4 Thermal Analysis	90
III.3.2.2 $\text{Ni}_9\text{L}_2(\text{NO}_3)_4(\text{NH}_3)_4(\text{OH})_6(\text{H}_2\text{O})_{16}$ complex	93
III.3.2.2.1 Synthesis	93
III.3.2.2.2 Elemental Analysis	93
III.3.2.2.3 Infrared Spectroscopy	93
III.3.2.2.3 Thermal analysis	95
III.3.2.2.4 Crystal structure	98
III.3.2.2.5 Preliminary results of Magnetic Studies	107
III.3.3 Silver complex	108
III.3.3.1 $\text{Ag}_2\text{L}_2(\text{NO}_3)_2(\text{H}_2\text{O})_2$ complex Synthesis	108
III.3.3.2 Elemental analysis	108

III.3.3.3 Infrared spectroscopy	108
III.3.3.4 thermal analysis	110
III.3.3.5 Crystallography	113
<b>Chapter four: Dimroth rearrangement</b>	117
IV. Introduction	118
IV.2 Results and Discussion	120
<b>Chapter five: Conclusion</b>	126
<b>Chapter six: References</b>	129

## Appendix A. Abbreviations

tp	1,2,4-triazolo-[1,5-a]pyrimidine
5mtp	5-methyl-1,2,4-triazolo-[1,5-a]pyrimidine
6mtp	6-methyl-1,2,4-triazolo-[1,5-a]pyrimidine
dmtp	5,7-dimethyl-1,2,4-triazolo-[1,5-a]pyrimidine
dptp	5,7-diphenyl-1,2,4-triazolo-[1,5-a]pyrimidine
5HtpO	4,5-dihydro-5-oxo-1,2,4-triazolo-[1,5-a]pyrimidine
7HtpO	4,5-dihydro-7-oxo-1,2,4-triazolo-[1,5-a]pyrimidine
HmtpO	4,5-dihydro-5-methyl-7-oxo-1,2,4-triazolo-[1,5-a]pyrimidine
H <sub>2</sub> tpO <sub>2</sub>	4,5,6,7-tetrahydro-5,7-dioxo-1,2,4-triazolo-[1,5-a]pyrimidine
en	Ethylendiamine
tn	1,3-diaminopropane
py	pyridine
bpy	2,2'-bipyridine
phen	phenantroline
PPh <sub>3</sub>	triphenylphosphine

## List of Tables

<b>Table</b>	<b>Page</b>
<b>Table 2.1:</b> Theoretical heat of formation energy.	67
<b>Table 2.2:</b> Atomic orbital contributions to the highest energy occupied MO and LUMO, from AM1 calculation for 7,8-dihydro-7-oxo-1,2,4-triazolo[4,3-a]pyrimidine ligand in neutral and ionic form	73
<b>Table 3.1</b> bond lengths [ $^{\circ}$ A] of $\text{Ni}_9\text{L}_8(\text{NO}_3)_4(\text{NH}_4)_3(\text{H}_2\text{O})_{16}$ complex	100
<b>Table 3.2:</b> bond angle [ $^{\circ}$ A] of $\text{Ni}_9\text{L}_8(\text{NO}_3)_4(\text{NH}_4)_3(\text{H}_2\text{O})_{16}$ complex.	102
<b>Table 3.3:</b> bond lengths [ $^{\circ}$ A] of $\text{Ag}_2\text{L}_2(\text{NO}_3)_2 \cdot (\text{H}_2\text{O})_2$ complex.	116
<b>Table 3.4:</b> bond angles [ $^{\circ}$ ] of $\text{Ag}_2\text{L}_2(\text{NO}_3)_2 \cdot (\text{H}_2\text{O})_2$ complex.	116
<b>Table 4.1:</b> bond length [ $^{\circ}$ A] of the rearranged compound.	123
<b>Table 4.2:</b> Bond angle [ $^{\circ}$ ] of the rearranged compound.	124

## List of Figures

Figures	page
<b>Fig. 1.1:</b> View of the $[\text{Cu}(\text{dntp})_4(\text{H}_2\text{O})]^{2+}$ cation	30
<b>Fig.1.2:</b> View of molecular structure of $[\text{Cu}(\text{mtpo})_2(\text{tn})] \cdot 2\text{H}_2\text{O}$	30
<b>Fig.1.3:</b> View of the molecular structure of $[\text{Cu}(\text{5tpO})_4(\text{H}_2\text{O})_2] \cdot 2\text{H}_2\text{O}$	31
<b>Fig.1.4:</b> View of polymeric structure of $[\text{CuCl}_2(\text{tp})_2]$	32
<b>Fig.1.5:</b> View of molecular structure of $[\text{Ni}(\text{NCS})_2(\text{5HtpO})_2(\text{H}_2\text{O})_2]$ complex	33
<b>Fig.1.6:</b> View of Double (left) and single (right) chains present in the crystal structure of $[\text{HgCl}_2(\text{HmtpO})]_2 \cdot \text{H}_2\text{O}$	33
<b>Fig.1.7:</b> View of bidimensional polymeric structure of $\text{FeHg}(\text{SCN})_4(\text{dntp})_2(\text{H}_2\text{O})$	34
<b>Fig.1.8:</b> View of the molecular structure of $[\text{Ag}_2(\text{5HtpO})_2](\text{ClO}_4)_2 \cdot 2\text{H}_2\text{O}$ compound	35
<b>Fig.1.9:</b> View of polymeric chains in $[\text{Ag}_3(\text{mtpO})_2(\text{HSO}_4)(\text{H}_2\text{O})_2] \cdot \text{H}_2\text{O}$	35
<b>Fig.1.10:</b> View of the $[\text{Pt}_2\text{Ag}_2(\text{7tpO})_4(\text{bpm})_2(\text{H}_2\text{O})_2]^{+2}$ cation	36
<b>Fig.1.11:</b> View of the $[\text{Cu}_4\text{Cl}_2(\text{dntp})_4]_2^{2+}$ cation	36
<b>Fig.1.12:</b> View of molecular structure of <i>mer</i> - $[\text{RuCl}_3(\text{dntp})_2(\text{H}_2\text{O})]$ .	37
<b>Fig.1.13:</b> View of molecular structure of the dimer $[\text{Pt}_2(\text{mtpO})_4]$	38
<b>Fig.1.14:</b> View of the dinuclear cation $[(\text{NH}_3)_2\text{Pt}(\text{mtpO})_2\text{Pd}(\text{bpy})]^{2+}$	38
<b>Fig.2.1:</b> IR Diagram for 7,8-dihydro-7-oxo-1,2,4-triazolo[4,3-a]pyrimidine ligand	56
<b>Fig.2.2:</b> Theoretical Chem 3D $^1\text{H}$ -NMR for 7,8-dihydro-7-oxo-1,2,4-triazolo[4,3- a]pyrimidine ligand	59
<b>Fig.2.3:</b> $^1\text{H}$ -NMR for 7,8-dihydro-7-oxo-1,2,4-triazolo[4,3-a]pyrimidine ligand	60
<b>Fig.2.4:</b> Theoretical Chem 3D $^{13}\text{C}$ -NMR diagram for 7,8-dihydro-7-oxo-1,2,4-triazolo[4,3-a]pyrimidine ligand	61

<b>Fig.2.5:</b> $^{13}\text{C}$ -NMR diagram for 7,8-dihydro-7-oxo-1,2,4-triazolo[4,3-a]pyrimidine ligand	62
<b>Fig.2.6:</b> Potentiometric titration curve for 7,8-dihydro-7-oxo-1,2,4-triazolo[4,3-a]pyrimidine ligand	63
<b>Fig.2.7:</b> TG diagrams for 7,8-dihydro-7-oxo-1,2,4-triazolo[4,3-a]pyrimidine ligand	64
<b>Fig.2.8:</b> DSC diagrams for 7,8-dihydro-7-oxo-1,2,4-triazolo[4,3-a]pyrimidine ligand	65
<b>Fig.2.9:</b> Calculated charges of electrostatic potential for 7,8-dihydro-7-oxo-1,2,4-triazolo[4,3-a]pyrimidine ligand in neutral and anion forms	69
<b>Fig.2.10:</b> Electrostatic potential diagram of 7,8-dihydro-7-oxo-1,2,4-triazolo[4,3-a]pyrimidine ligand in the neutral	71
<b>Fig.2.11:</b> Total charge density diagram for 7,8-dihydro-7-oxo-1,2,4-triazolo[4,3-a]pyrimidine ligand in the neutral form	71
<b>Fig.2.12:</b> High molecular orbital (HOMO) and low molecular orbital (LUMO) in neutral and anion forms for 7,8-dihydro-7-oxo-1,2,4-triazolo[4,3-a]pyrimidine ligand	74
<b>Fig.3.1:</b> Infrared spectroscopy of $\text{CuL}_2\text{Cl}_2 \cdot (\text{H}_2\text{O})_3$ complex	79
<b>Fig.3.2:</b> TG diagram of $\text{CuL}_2\text{Cl}_2 \cdot (\text{H}_2\text{O})_3$ complex	81
<b>Fig.3.3:</b> DSC diagram of $\text{CuL}_2\text{Cl}_2 \cdot (\text{H}_2\text{O})_3$ complex.	82
<b>Fig.3.4:</b> Infrared spectroscopy of $\text{CuL}_2\text{Cl}_2 \cdot (\text{H}_2\text{O})_5$ complex	84
<b>Fig.3.5:</b> TG diagram of $\text{CuL}_2\text{Cl}_2 \cdot (\text{H}_2\text{O})_5$ complex	86
<b>Fig.3.6:</b> DSC diagram of $\text{CuL}_2\text{Cl}_2 \cdot (\text{H}_2\text{O})_5$ complex.	87
<b>Fig.3.7:</b> Infrared Spectroscopy of $\text{NiL}_2(\text{H}_2\text{O})_5$ complex.	89
<b>Fig.3.8:</b> TG diagram of $\text{NiL}_2(\text{H}_2\text{O})_5$ complex	91
<b>Fig.3.9:</b> DSC diagram of $\text{NiL}_2(\text{H}_2\text{O})_5$ complex.	92
<b>Fig.3.10:</b> Infrared Spectroscopy of $\text{Ni}_9\text{L}_8(\text{NO}_3)_4(\text{NH}_4)_3 \cdot (\text{H}_2\text{O})_{16}$ complex	94
<b>Fig.3.11:</b> TG diagram of a $\text{Ni}_9(\text{C}_5\text{H}_3\text{N}_4\text{O})_8(\text{NO}_3)_4(\text{NH}_4)_3 \cdot (\text{H}_2\text{O})_{16}$ complex.	96
<b>Fig.3.12:</b> DSC diagram of $\text{Ni}_9(\text{C}_5\text{H}_3\text{N}_4\text{O})_8(\text{NO}_3)_4(\text{NH}_4)_3 \cdot (\text{H}_2\text{O})_{16}$ complex	97



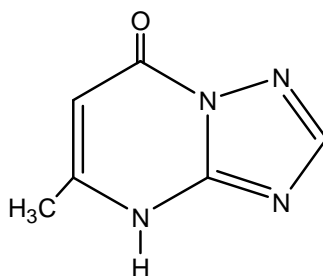
<b>Fig.3.13:</b> Ionic structure of $\text{Ni}_9(\text{C}_5\text{H}_3\text{N}_4\text{O})_8(\text{NO}_3)_4(\text{NH}_4)_3 \cdot (\text{H}_2\text{O})_{16}$ clusture according to X-ray analysis	99
<b>Fig.3.15:</b> Magnetic susceptibility of $\text{Ni}_9(\text{C}_5\text{H}_3\text{N}_4\text{O})_8(\text{NO}_3)_4(\text{NH}_4)_3 \cdot (\text{H}_2\text{O})_{16}$ cluster as a function of temperature	107
<b>Fig.3.16:</b> IR curve of $\text{Ag}_2\text{L}_2(\text{NO}_3)_2 \cdot (\text{H}_2\text{O})_2$ complex	109
<b>Fig.3.17:</b> TG curve of $\text{Ag}_2\text{L}_2(\text{NO}_3)_2 \cdot (\text{H}_2\text{O})_2$ complex.	111
<b>Fig.3.18:</b> DSC curve of $\text{Ag}_2\text{L}_2(\text{NO}_3)_2 \cdot (\text{H}_2\text{O})_2$ complex.	112
<b>Fig.3.19:</b> Molecular structure of the dinuclear compound $[\text{Ag}_2\text{L}_2(\text{NO}_3)_2] \cdot 2\text{H}_2\text{O}$ according to X-ray analysis	115
<b>Fig.4.1:</b> the crystal structure of the rearranged compound.	122

*CHAPTER ONE*

**INTRODUCTION**

## I. 1 Historical background

The chemistry of 1, 2, 4-triazolopyrimidines derivatives started in 1909 when Bulow and Hass <sup>(1)</sup> reported the synthesis of 5-methyl-1,2,4-triazolo[1, 5-a]pyrimidine-7-one (Scheme 1).



**Scheme 1:** Structure of 5-methyl-1, 2, 4-triazolo [1, 5-a] pyrimidine-7-one

Many efforts have been directed toward the synthesis of triazolopyrimidines, because of their chemistry which showed many biological activities as well as medicinal, agrochemical applications and photographic stabilizer emulsions.

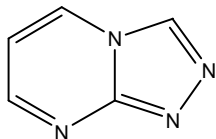
Over the next 50 years, only a few papers and patents on triazolopyrimidine were published, which were included in Mosby's comprehensive monograph on "Heterocyclic systems with Bridgehead Nitrogen Atoms" <sup>(2)</sup>.

The systematic studies reported since 1958 include those of the groups of Sirakawa (1958-1960) <sup>(3)</sup>, Makisumi (1958-1964) <sup>(4)</sup>, Allen and Williams (1959-1962) <sup>(5)</sup>, Levin (1963-1964) <sup>(6)</sup>, Kreutzberger (1966-1979) <sup>(7)</sup>, Reimlinger (1970-1971) <sup>(8)</sup>, Reiter (1987-1993) <sup>(9)</sup>, and the most complete recent revision are those by G. Fischer <sup>(10)</sup>.

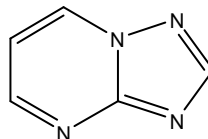
Special aspects of syntheses and reactivity have been covered in reviews by Babichev and Kovtunenکو <sup>(11)</sup>, Tisler <sup>(12)</sup>, Ivashchenko and Gaaricheva <sup>(13)</sup>, Shaben *et al.* <sup>(14)</sup>, G.Fischer <sup>(10)</sup>, Maury <sup>(15)</sup> and in a valuable comparative study of certain azaindolizines by Al ashry <sup>(16)</sup>.

Fusion of 1,2,4-triazolo ring onto a pyrimidine nucleus to form 1,2,4-triazolopyrimidine systems may take place in four different modes that lead

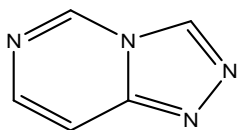
to the following isomeric structures, all of which possess a nitrogen bridgehead atom as seen in (Scheme2).



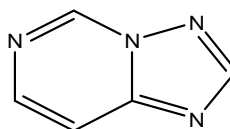
i 1,2,4-triazolo[4,3-a] pyrimidine



ii. 1,2,4-triazolo[1,5-a] pyrimidine



iii. 1,2,4-triazolo[4,3-c]pyrimidine



iv. 1,2,4-triazolo[1,5-c]pyrimidine

**Scheme 2:** Four possible isomer of triazolopyrimidine

## I.2 Synthesis

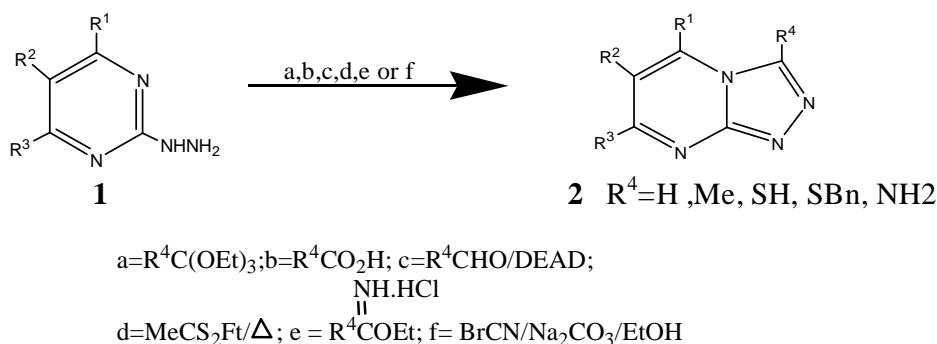
Most synthesis of triazolopyrimidines start either from a 1,2,4-triazolo derivatives or from a pyrimidine residue and need annulations of a second heterocyclic ring. Preferably 5-amino-1,2,4-triazoles and 2-hydrazinopyrimidines. According to the reaction type, these syntheses may be classified as cyclocondensation, cycloadditions, or oxidative cyclizations <sup>(12)</sup>. To some extent triazolopyrimidines are prepared by other transformations of the five-and/or six membered rings.

In some cases, the kinetically favored [4,3-a] and [4,3-c] product is formed initially, this being transformed into the thermodynamically more stable [1,5-a] and [1,5-c] pyrimidines, respectively by the means of Dimroth rearrangement <sup>(18)</sup>.

## I.2.1 Synthesis of 1,2,4-triazolo[4,3-a]pyrimidine

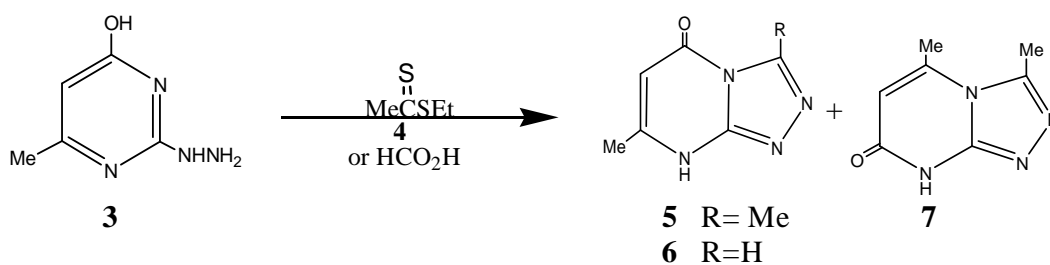
### I.2.1.1 Synthesis from Pyrimidines

The synthesis of this ring system may be achieved by building the diazole onto a preformed pyrimidine ring. Cyclization of a 2-hydrazinopyrimidine with one-carbon-inserting reagents serves as a general route to this ring. Thus, cyclization of 2-hydrazinopyrimidines **1** with formic acid<sup>(17)</sup>, carbon disulfide in boiling pyridine, carbon disulfide in acetonitrile at room temperature<sup>(18)</sup>, ethyl dithioacetate<sup>(19)</sup>, or cyanogen bromide afforded the triazolo[4,3-a]pyrimidines **2**. Reaction of **1** with aldehydes followed by cyclization with diethyl azodicarboxylate (DEAD) gave **2**. Cyclization of 2-hydrazinopyrimidines **1** with ethyl imidate hydrochlorides afforded the 3-substituted 1,2,4-triazolo[4,3-a]pyrimidines **2**. However, when the 2-hydrazinopyrimidine (**1**, R<sup>1</sup>=R<sup>2</sup>=R<sup>3</sup>=H) and 4,6-dimethyl-2-hydrazinopyrimidine (**1**, R<sup>1</sup>=R<sup>3</sup>=Me, R<sup>2</sup>=H) were cyclized with the imidate hydrochlorides, the isomeric triazolo[1,5-a]pyrimidines were formed<sup>(20)</sup> (Scheme 3).



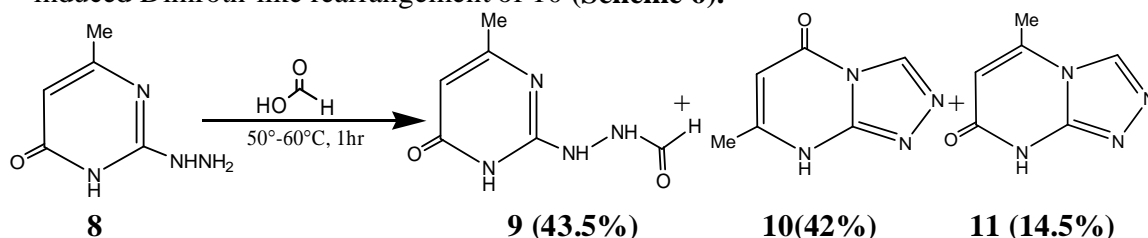
### Scheme 3

Reaction of **3** with ethyl dithioacetate **4** gave a mixture of 3,7(3,5)-dimethyltriazolo[4,3-a]pyrimidinones **5** and **7**<sup>(21)</sup>, whereas the reaction with formic acid gave **6**<sup>(22)</sup> (Scheme 4).

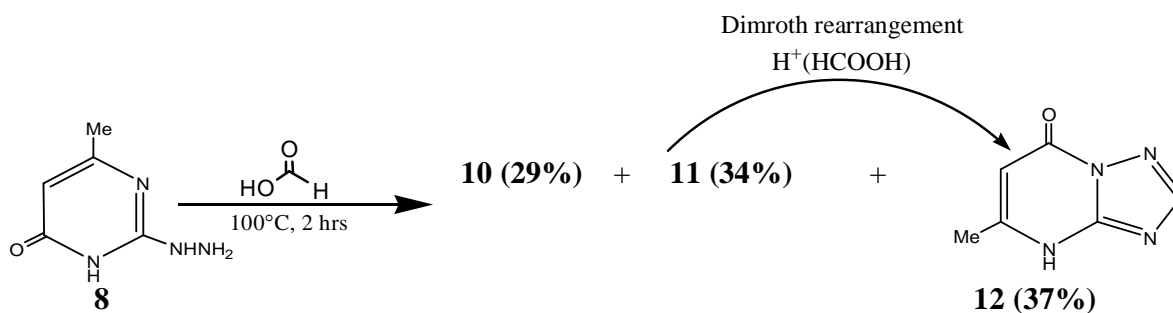


**Scheme 4**

Cyclization of 2-hydrazino-6-methylpyrimidin-4-one **8** with formic acid represents an interesting case, mixtures of products were obtained which varied in number, structures, and relative amounts depending upon the reaction conditions (time, temperature, and pH)<sup>(23)</sup>. The reaction of **8** was carried out with formic acid at 50-60°C for 1 hour and obtained a mixture of the formylhydrazine **9**, (43.5%), 7-methyl-5-oxo-1,2,4-triazolo[4,3-a]pyrimidine (**10**, 42%), and 5-methyl-7-oxo-1,2,4-triazolo[4,3-a]pyrimidine (**11**, 14.5%). Compounds **10** and **11** were formed as a result of dehydrocyclization of hydrazide **9** through nucleophilic attack of the pyrimidine N1 or N3, respectively, onto the formylhydrazino carbonyl carbon (**Scheme 5**). When this reaction was performed at 100°C for 2 hours, the isolated products were **10** (29%), **11** (34%), and 7-methyl-5-oxo-1,2,4-triazolo[1,5-a] pyrimidine (**12**, 37%)<sup>(23)</sup>. The last was formed as a result of acid-induced Dimroth-like rearrangement of **10** (**Scheme 6**).

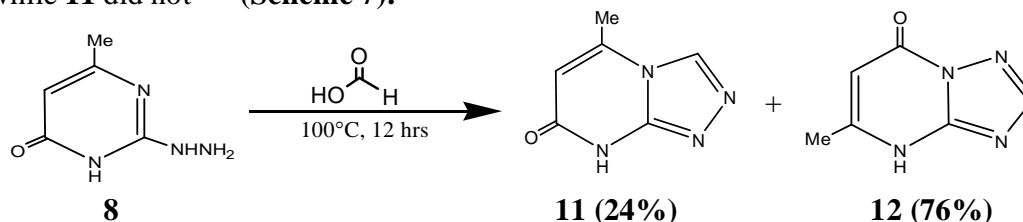


**Scheme 5**



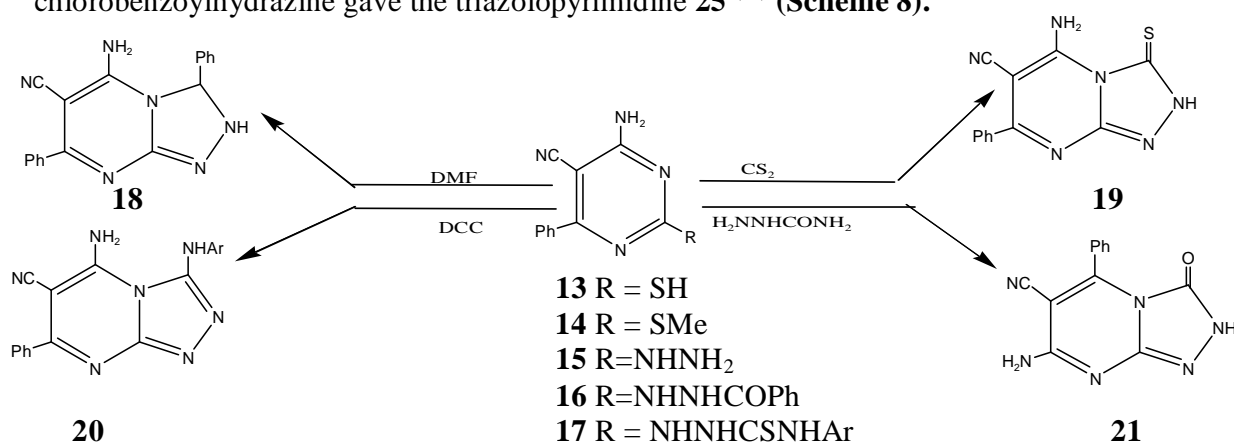
**Scheme 6**

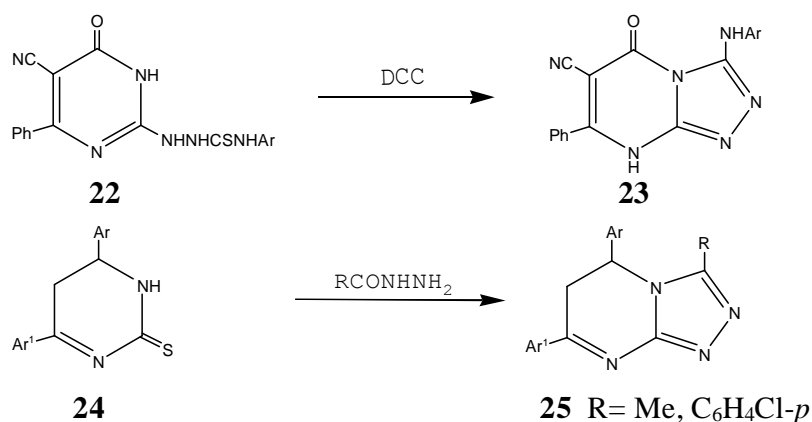
Longer reaction time (12 hours) in the presence of excessive amounts of formic acid gave **11** (24%) and **12** (76%). Under such reaction conditions, **10** completely isomerized to **12** while **11** did not<sup>(23)</sup> (Scheme 7).



**Scheme 7**

The 4-aminopyrimidines **13** and **14** were prepared by the reaction of the benzylidene malononitriles with thiourea or *S*-methylisothiourea, respectively. Nucleophilic substitution at the 2-position of **14** with hydrazine gave the 2-hydrazino derivative **15**, whose treatment with carbon disulfide yielded the triazolopyrimidine **19** rather than its isomeric compound<sup>(24)</sup>. Heating **15** with benzoyl chloride anhydrous dioxane, afforded the *N*-benzoyl derivative **16**, whose ring closure took place upon heating in DMF to give 5-amino-6-cyano-3,7-diphenyl-1,2,4-triazolo[4,3-a]pyrimidine **18**. The latter can also be obtained by direct reaction of **14** with benzoylhydrazine in DMF<sup>(25)</sup>. The isomeric 1,2,4-triazolo-[4,3-a]pyrimidin-3-one **21** was obtained from **14** by reaction with semicarbazide<sup>(26)</sup>. Reaction of **15** with isocyanates gave thiosemicabazides **17** whose cyclodesulfurization with DCC gave **20**<sup>(27)</sup>. Similarly, cyclocondesulfurization of **22** gave **23**. Cyclization of the dihydropyrimidinethione **24** with acetylhydrazine or *p*-chlorobenzoylhydrazine gave the triazolopyrimidine **25**<sup>(28)</sup> (Scheme 8).

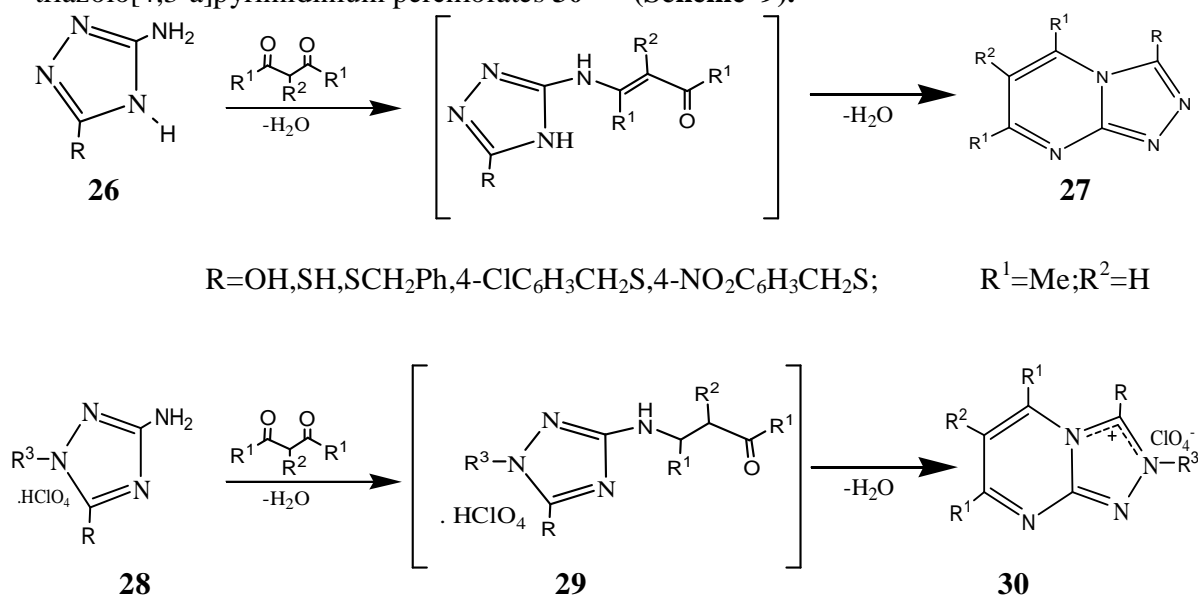




**Scheme 8**

### I.2.1.2 Synthesis from triazoles

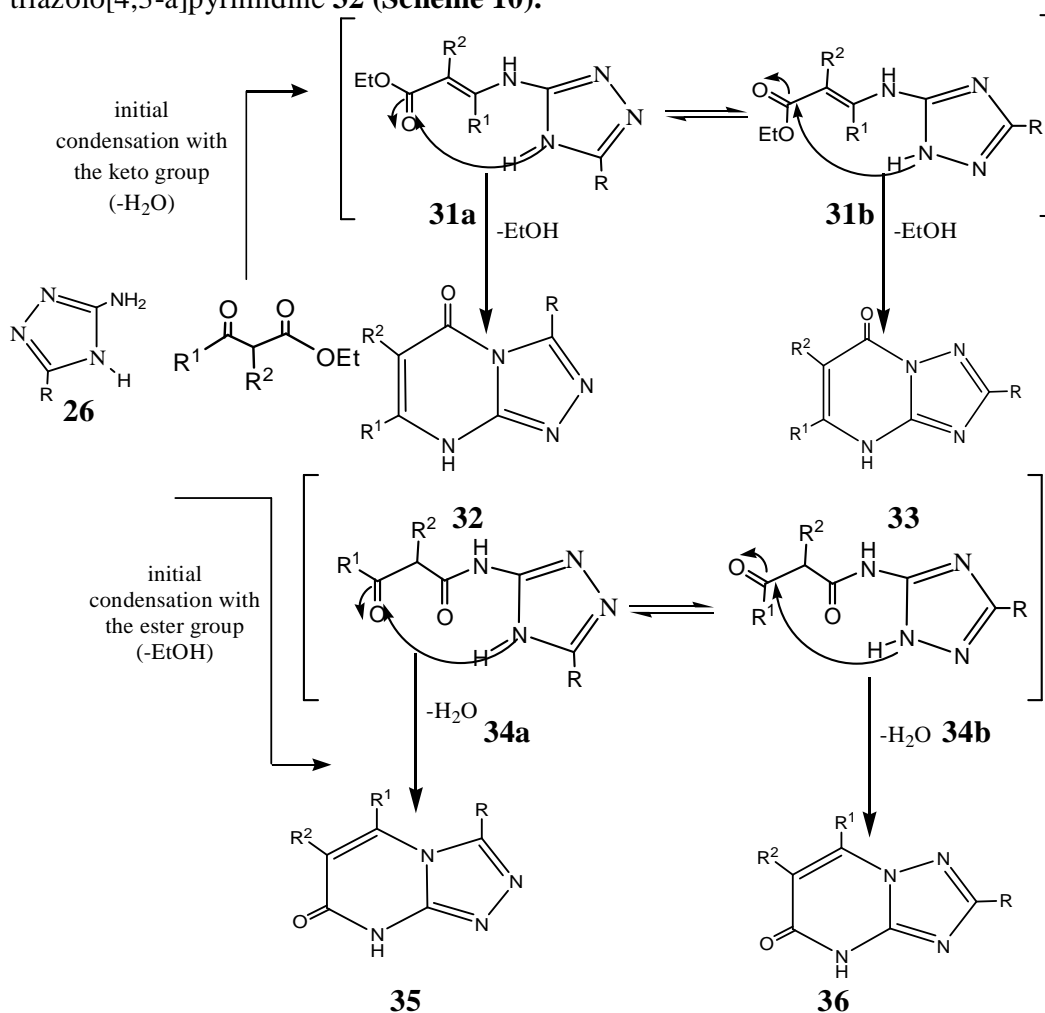
Cyclocondensation of symmetrically substituted 1,3-diketones with 3-amino-5-substituted-1,2,4-triazoles **26** produced the expected 3,5,7-trisubstituted-1,2,4-triazolo[4,3-a]pyrimidines **27** <sup>(29)</sup>. This reaction has been successfully applied to 3-amino-1-benzyl-1,2,4-triazolium perchlorates **28**; the products were the 2-benzyl-1,2,4-triazolo[4,3-a]pyrimidinium perchlorates **30** <sup>(30)</sup> (**Scheme 9**).



**Scheme 9**

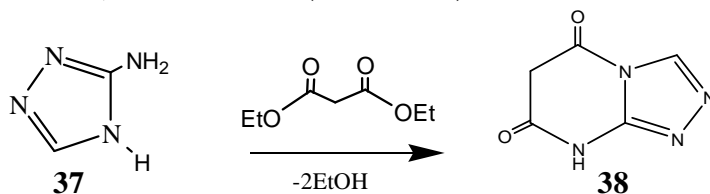


Theoretically, the reaction of 3-amino-1,2,4-triazoles **26** with 1,3-keto-esters may afford the four possible isomeric 1,2,4-triazolopyrimidines **32**, **33**, **35**, and **36**. Formation of these isomers may be explained on the basis of whether the amino group of **26** initially condenses with the keto or ester function of the ketoester to produce the enamine **31** or amide **34** intermediates, respectively <sup>(5)</sup>. Heterocyclization of the enamine intermediates **31a** and **31b** by nucleophilic attack of the triazole N4 or N1 onto the ester carbonyl would afford **32** and/or **33**, respectively. Comparable cyclization of the amide intermediates **34a** and **34b** would lead to the formation of **35** and **36**. However, in practice cyclocondensations of **26** with ethyl acetoacetate <sup>(31)</sup>, ethyl 2-haloacetoacetate <sup>(32)</sup>, or ethyl benzoylacetate <sup>(31)</sup> were found to afford only the corresponding 5-oxo-1,2,4-triazolo[4,3-a]pyrimidine **32** (Scheme 10).



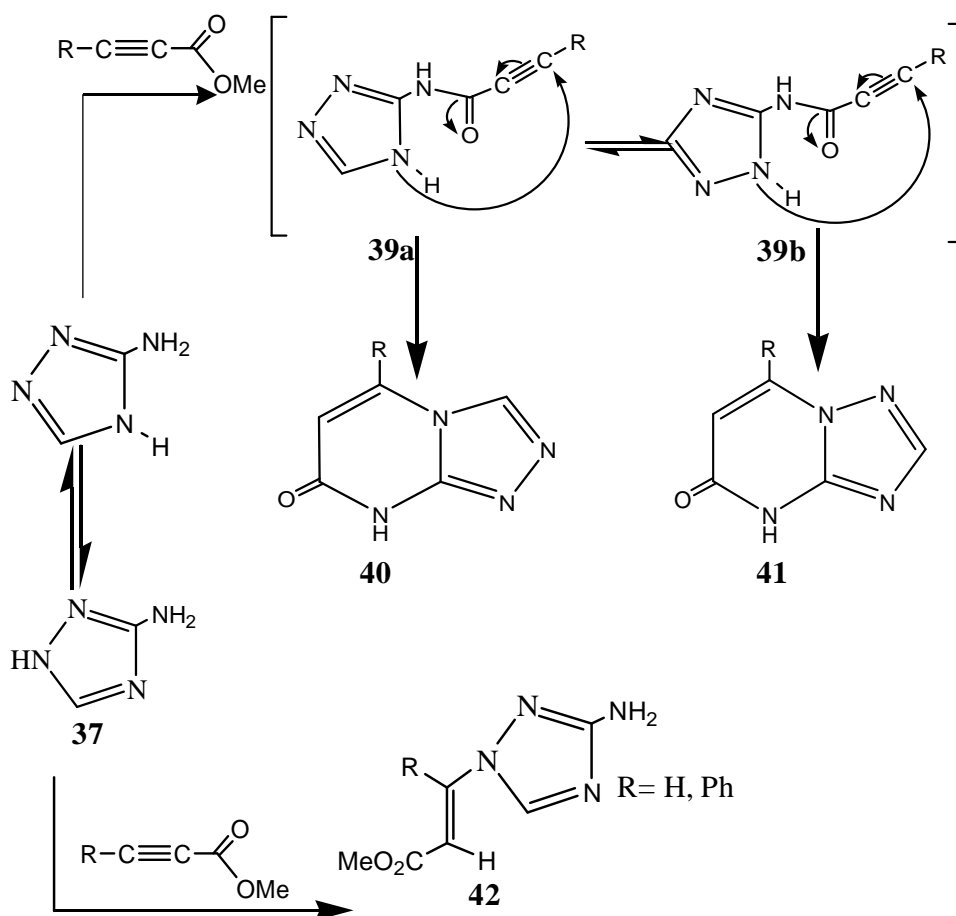
**Scheme 10**

Reaction of diethyl malonate with 3-amino-1,2,4-triazole **37** give the 1,2,4-triazolo[4,3-a]pyrimidine-5,7-diones **38** <sup>(31)</sup> (**Scheme 11**).



**Scheme 11**

Similarly, cyclization of 3-amino-1,2,4-triazoles **37** with methyl propiolate or methyl phenylpropiolate gave a mixture of the 1,2,4-triazolo[4,3-a]pyrimidin-7-ones **40** and the 1,2,4-triazolo[1,5-a]pyrimidin-7-ones **41**. In addition, methyl *trans*-3-(3-amino-1,2,4-triazol-1-yl)acrylates **42** were also obtained. Production of the 1,2,4-triazolopyrimidines **40** and **41** started by condensation of the ester function with the amino group of **37**, followed by cycloaddition of the triazole N4 or N1 of the two tautomeric intermediates **39a** and **39b**, respectively, onto the carbon-carbon triple bond of the side chain. In contrast, formation of the triazolyl acrylates **42** took place through addition only of the triazole N1 onto the propiolate carbon-carbon triple bond. The relative amounts of the products were found to depend on the reaction conditions (temperature, solvent, and time) <sup>(8)</sup> (**Scheme 12**).



**Scheme 12**

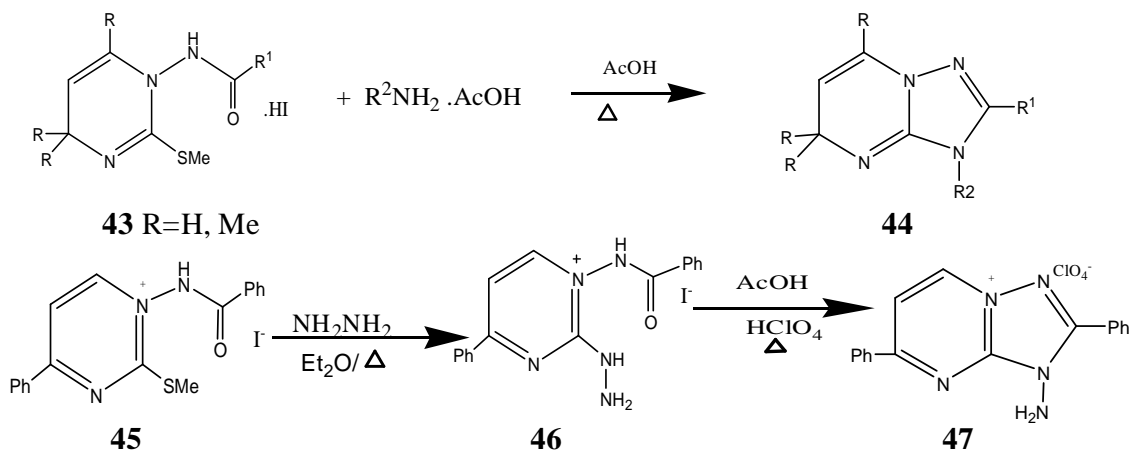
## 1.2.2 Synthesis of 1,2,4-Triazolo[1,5-a]pyrimidines

Synthesis of these compounds is achieved by building of one of the heterocycles followed by using it as a basis to build the other ring onto it or by Dimroth rearrangement of 1,2,4-triazolo[4,3-a] pyrimidines. 1,2-Diaminopyrimidines are generated from 1-amino or 2-aminopyrimidines. The 3- and 5-amino-1,2,4-triazoles are alternative precursors that can act as a source of three carbons to complete the pyrimidine ring.

### 1.2.2.1 Synthesis from 1-Aminopyrimidines

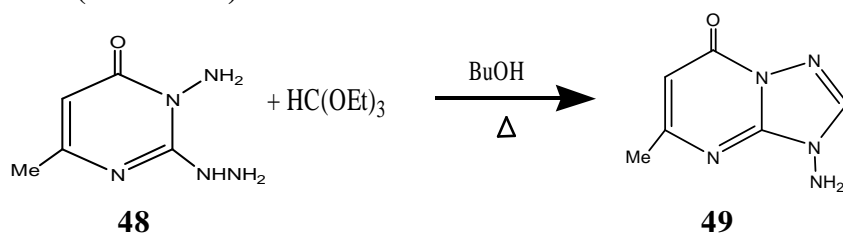
Cyclization of 1-(acylamino)pyrimidine hydroiodides **43** with alkyl ammonium acetates gave 3*H*,5*H*-1,2,4-triazolo[1,5-a]pyrimidines **44** <sup>(33)</sup>. Condensation of the 1-(acylamino)pyrimidinium salt **45** with hydrazine hydrate gave **46**, which upon cyclization

with acetic acid in the presence of perchloric acid afforded the 3-amino-1,2,4-triazolo[1,5-a]pyrimidinium salt **47** <sup>(34)</sup> (Scheme 13).



**Scheme 13**

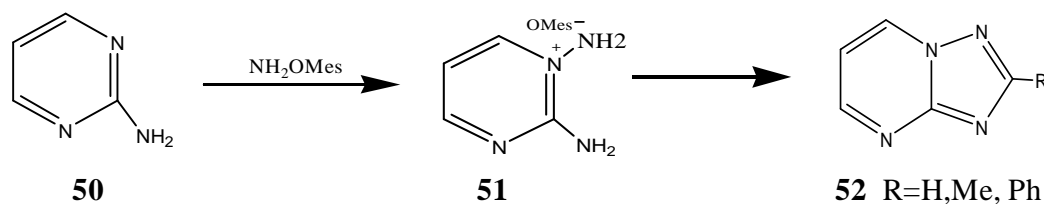
The 1-amino-2-hydrazinopyrimidine **48** can be cyclized with triethyl orthoformate to **49** <sup>(35)</sup> (Scheme 14).



**Scheme 14**

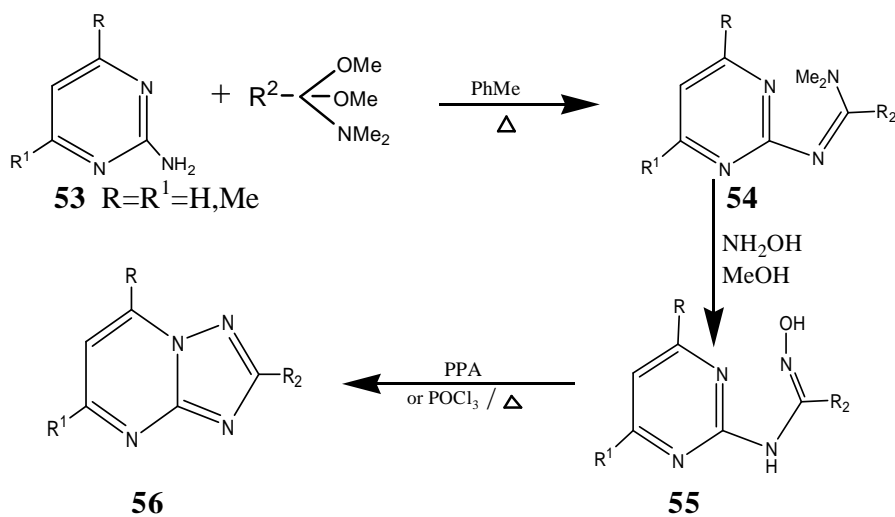
### 1.2.2.2 Synthesis from 2-Aminopyrimidines

Amination of 2-aminopyrimidine **50** with *O*-mesitylenesulfonylhydroxylamine (NH<sub>2</sub>OMes) gave the *N*-aminopyrimidinium salt **51**, which can be transformed into 1,2,4-triazolo[1,5-a]pyrimidines **52** by heating with formic acid, acetic anhydride, and benzoyl chloride <sup>(36)</sup> (Scheme 15).



**Scheme 15**

The synthesis of triazolopyrimidines may be achieved by the cyclization of 2-aminopyrimidines by fusion of a C—N fragment. Thus, the triazolopyrimidines **56** have been prepared by the sequential condensation of 2-aminopyrimidines **53** with  $(\text{MeO})_2\text{CR}^2\text{NMe}_2$  followed by reaction of the resulting derivative **54** with  $\text{NH}_2\text{OH}$  to give the hydroxyiminomethyleneaminopyrimidine **55**, which was cyclized by the action of polyphosphoric acid (PPA) <sup>(37)</sup>. In the case of 2-amino-4-methylpyrimidine as a starting compound, cyclization involved either an N-1 or N-3 atom of the pyrimidine, whereby both isomers were formed in a ratio of 1:5; the major one has  $\text{R}^1 = \text{Me}$  <sup>(38)</sup> (**Scheme 16**).

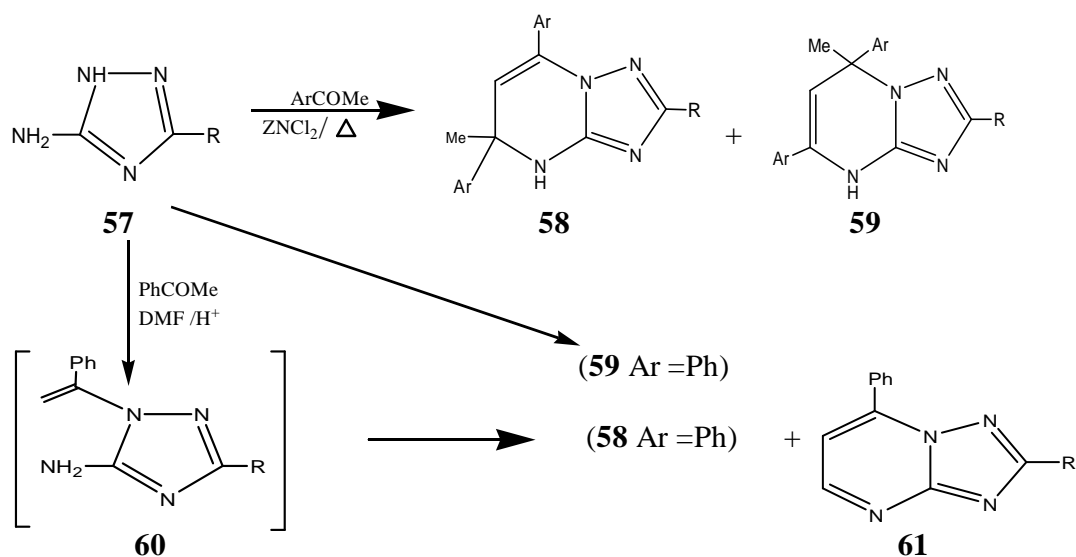


**Scheme 16**

### I.2.2.3 Syntheses from 5(3)-Amino-1,2,4-triazoles

5-Amino-1*H*-1,2,4-triazole and its derivatives are frequently used as precursors for this ring via their reaction with suitable carbonyl compounds. The 5-amino-1,2,4-triazoles **57** prepared from calcium cyanide by hydrolysis to cyanamide followed by condensation with hydrazine <sup>(39)</sup>, reacted with the appropriate acetophenone in the presence of  $\text{ZnCl}_2$  to

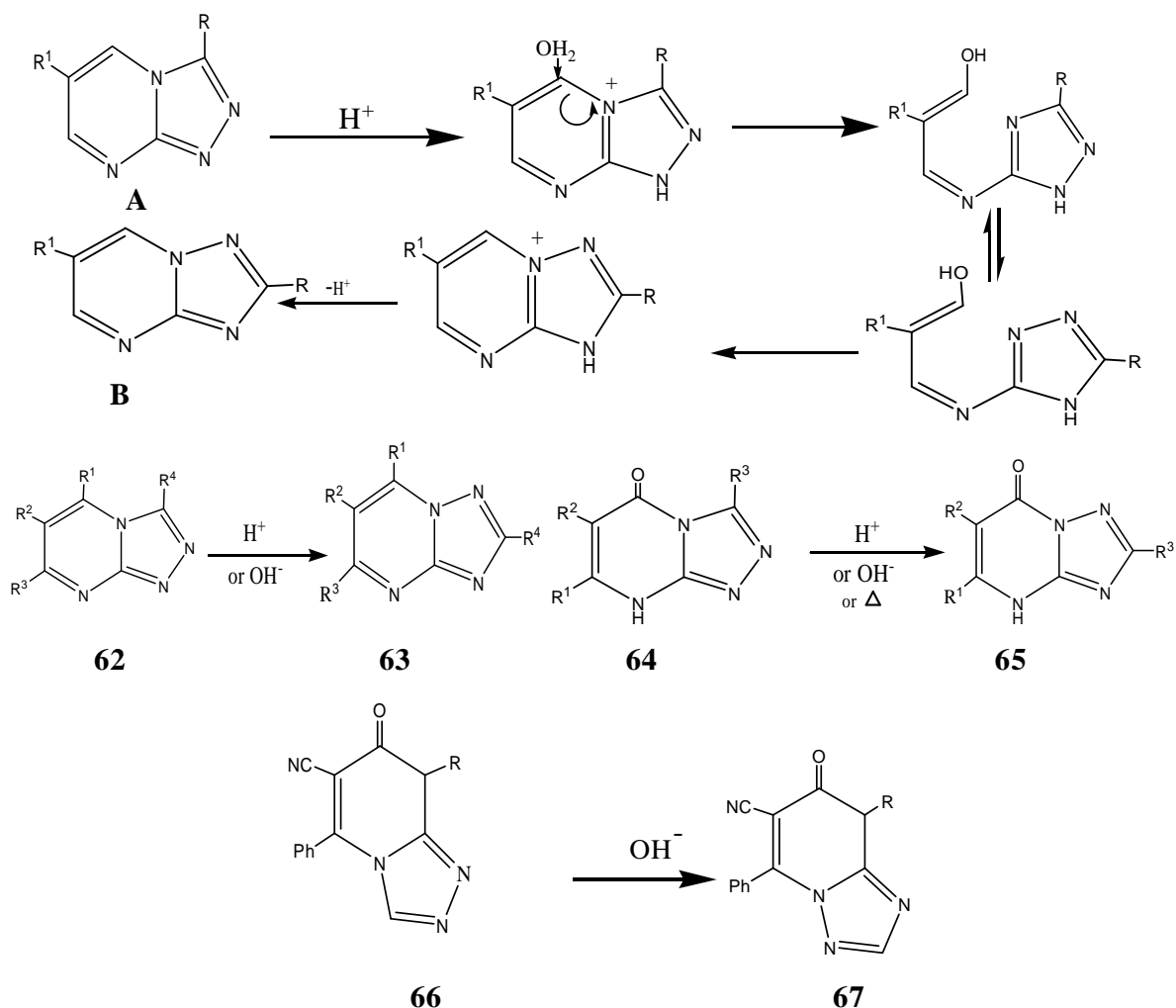
give the dihydrotriazolopyrimidines **58** and **59** <sup>(40)</sup>. Cyclocondensation of **57** with acetophenone in DMF gave the triazolopyrimidines **58** (Ar=Ph) and **61** via the intermediate **60** by participation of either a second acetophenone molecule or a DMF molecule, respectively. The reaction of **57** with PhCMe=CHCOPh in the absence of a catalyst afforded the dihydrotriazolopyrimidines **59** (Ar=Ph) <sup>(41)</sup> (**Scheme 17**).



**Scheme 17**

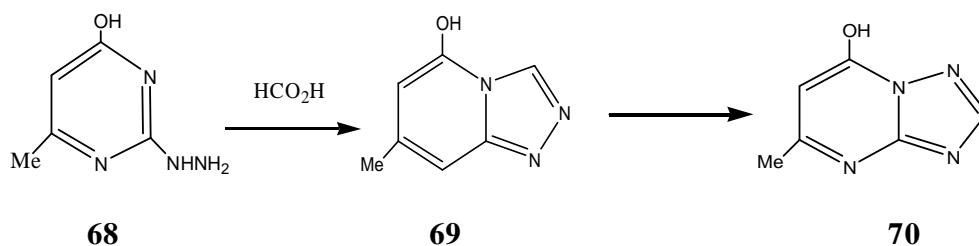
#### I.2.2.4 Dimroth Rearrangement of 1,2,4-Triazolo[4,3-a]pyrimidines

Dimroth rearrangement of 1,2,4-triazolo[4,3-a]pyrimidines (**A**) gave the 1,2,4-triazolo[1,5-a]pyrimidines (**B**) the triazolopyrimidines with various substituents on the ring, as in **62**, **64**, or **66**, underwent rearrangement to give **63**, **65**, and **67** respectively, upon treatment with acid, alkali, or triethylamine, or upon fusion <sup>(18)</sup> (**Scheme 18**).



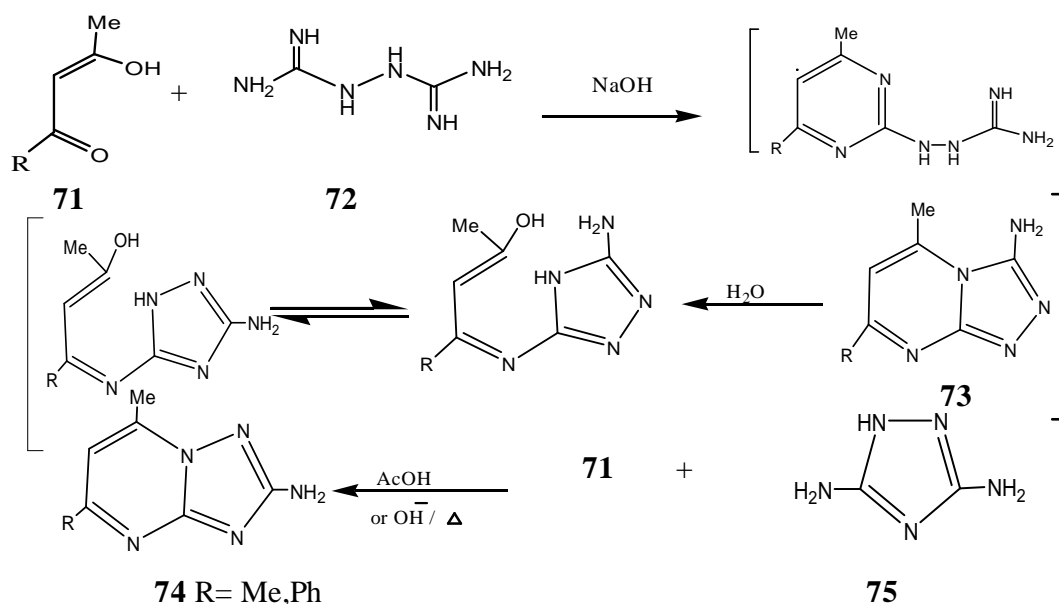
**Scheme 18**

Dimroth rearrangement may be considered to be a disadvantage during the synthesis of the [4,3-a] ring, because this ring system cannot be isolated. However, it is advantageous in cases in which the [1,5-a] ring system is required. Thus, reaction of the hydrazine **68** with formic acid gave **70** via **69** <sup>(5)</sup> (Scheme 19).



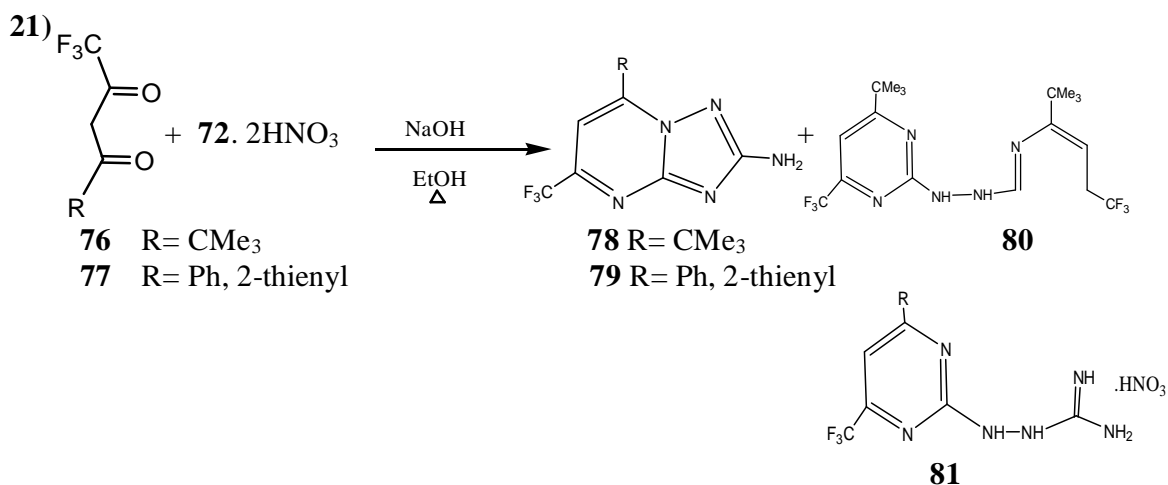
**Scheme 19**

Cyclization of the diamidine **72** with acetyl- or benzoyl-acetone **71** gave 1,2,4-triazolo[1,5-a]pyrimidine **74** via the formation of **73** <sup>(7)</sup>. Alternatively, **74** can be prepared by the reaction **71** with the diaminotriazole **75** <sup>(7)</sup> (Scheme 20).



**Scheme 20**

Reaction of the trifluoromethyl substituted  $\beta$ -diketone **76** with **72** nitrates gave a mixture of the triazolopyrimidine **78** and the pyrimidine **80**; whereas reaction with the aromatic  $\beta$ -diketones **77** gave a mixture of triazolopyrimidines **79** and pyrimidines **81** <sup>(42)</sup> (Scheme 21)



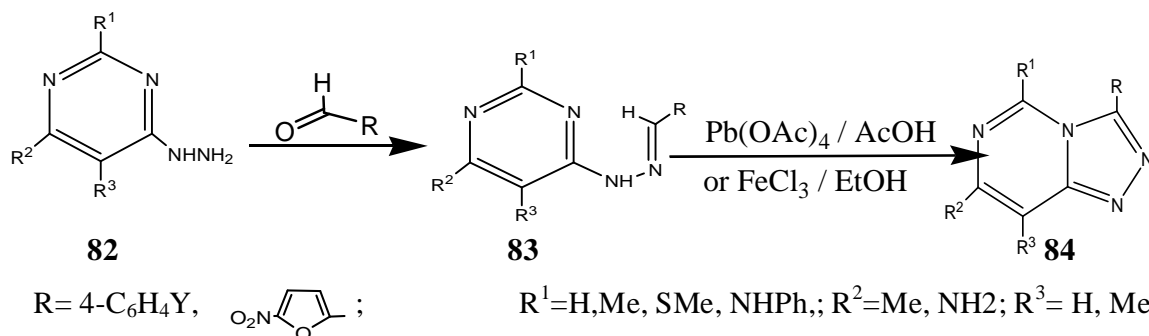
**Scheme 21**



## 1.2.3 1,2,4-Triazolo[4,3-c]pyrimidines

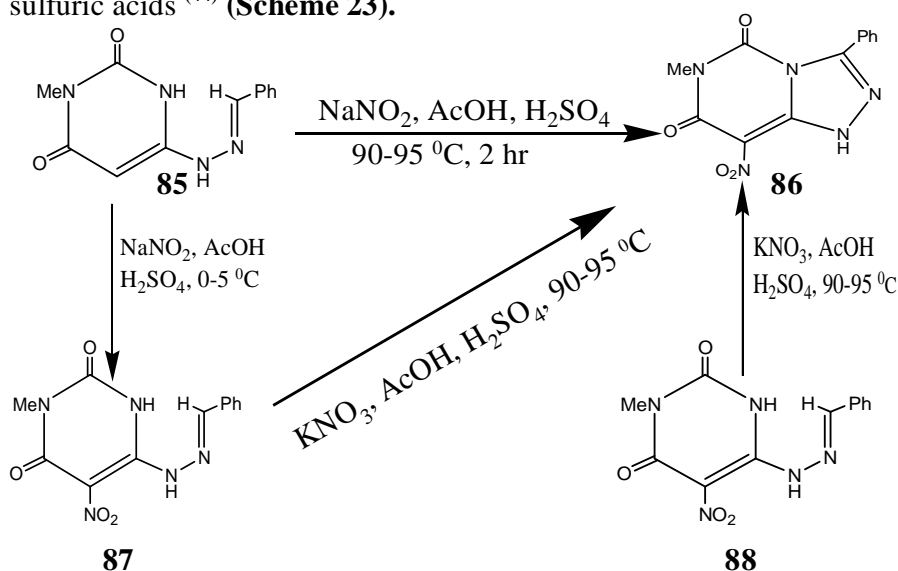
### 1.2.3.1 Synthesis from pyrimidine

Condensation of 4(6)-hydrazinopyrimidines **82** with aryl or heterocyclic aldehydes gave the corresponding 4(6)-arylidenehydrazinopyrimidines **83**. Oxidative cyclization of **83** with lead tetraacetate <sup>(17)</sup>, or with ethanolic iron (III) chloride <sup>(43)</sup> afforded the respective 3-substituted 1,2,4-triazolo[4,3-c]pyrimidines **84** (Scheme 22).



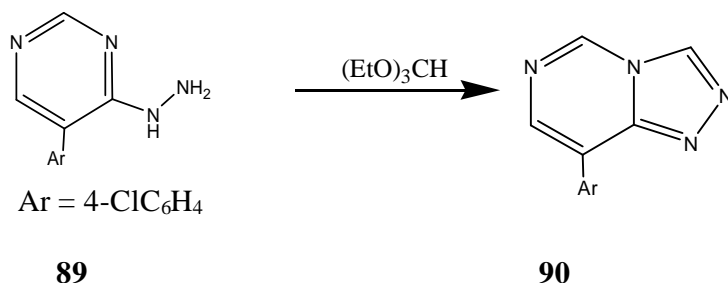
Scheme 22

Nitroization of 6-benzylidenehydrazino-3-methyluracil **85** took place with concurrent cyclization to **86**. The latter was also obtained from the nitroso and the nitro derivatives **87** and **88** upon treatment with a mixture of sodium or potassium nitrate and acetic and sulfuric acids <sup>(44)</sup> (Scheme 23).



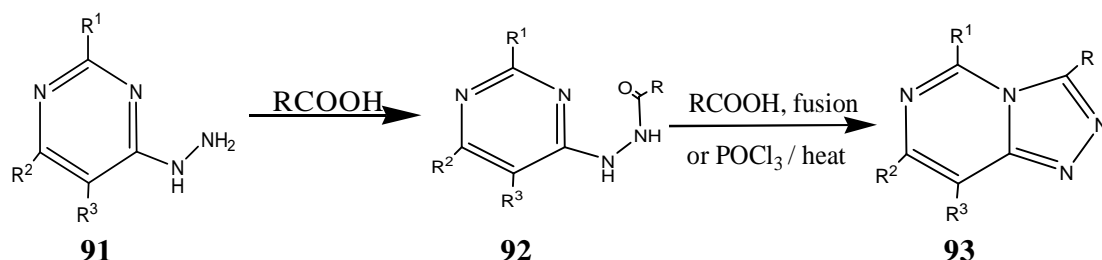
Scheme 23

Aldehyde acetals have also been utilized to accomplish cyclization of 4(6)-hydrazinopyrimidines such as **89** to **90** <sup>(45)</sup> (Scheme 24).



**Scheme 24**

1,2,4-triazolo[4,3-c]pyrimidines **93** were prepared by cyclization of 4-hydrazinopyrimidines carrying various substituents **91** with carboxylic acids. Whereas cyclization with formic acid afforded the 3-unsubstituted **93** (R=H) <sup>(46)</sup>, cyclization with other carboxylic acids gave the 3-substituted **93** (R=alkyl or aryl) <sup>(47)</sup>. This cyclization was also performed with acid chlorides as well as acid anhydrides <sup>(47)</sup>. Occasionally, it was possible to isolate the acylhydrazinopyrimidine intermediates **92** <sup>(47)</sup>, which were dehydrocyclized in a separate step to **93** by further heating with the same carboxylic acid <sup>(46)</sup>, a mineral acid, by fusion <sup>(47)</sup>, or by heating with phosphoryl chloride <sup>(8)</sup> (Scheme 25).

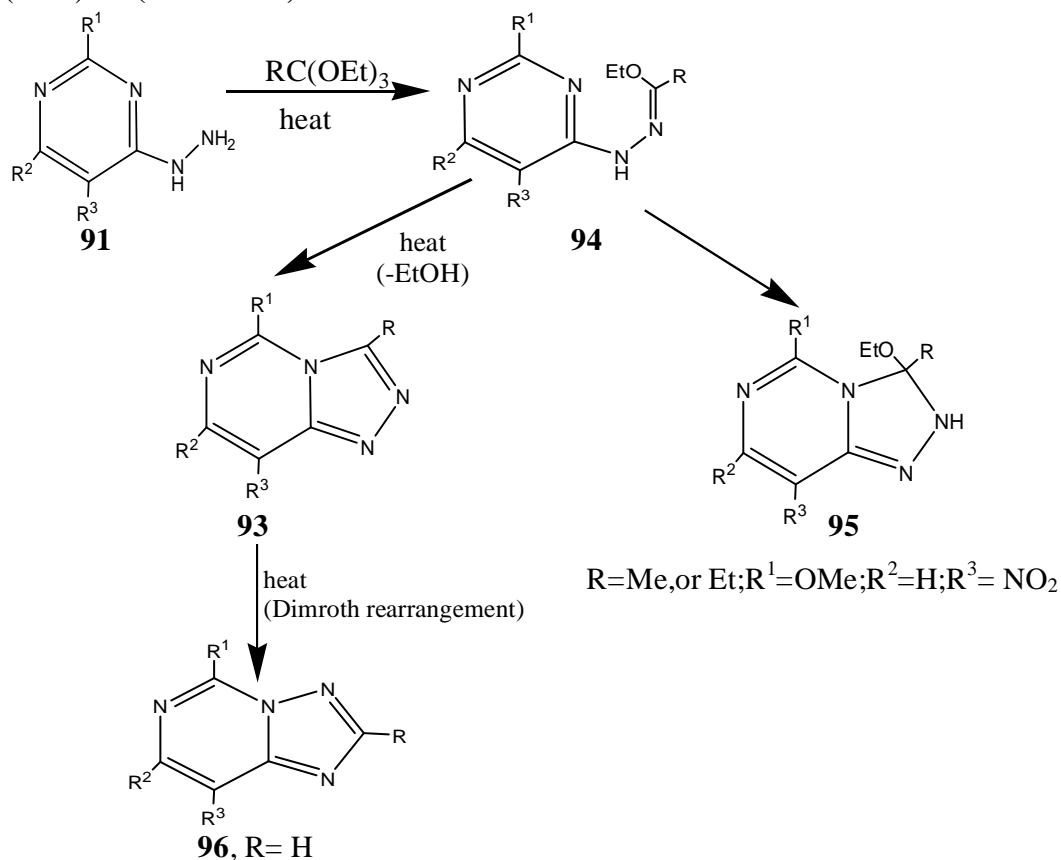


R = H, alkyl, or Ph ; R<sup>1</sup> = OH, SH, or Me ; R<sup>2</sup> or R<sup>3</sup> = H or alkyl

**Scheme 25**

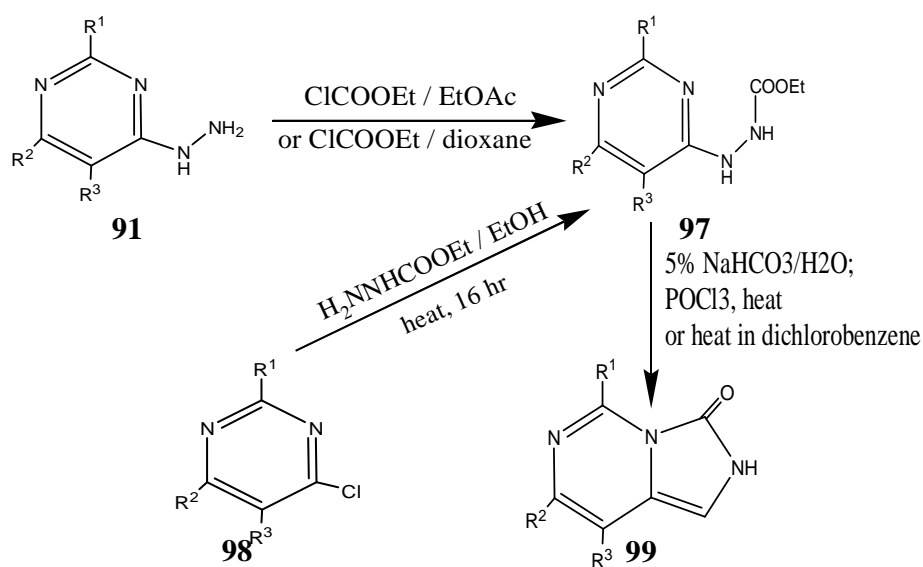
Reaction of **91** with acid orthoesters gave **93** through cyclocondensation of the occasionally isolable 1-ethoxyalkylidene-2-(pyrimidin-4-yl)-hydrazine intermediates **94** <sup>(49)</sup>. In one case, however, the formation of the 3-alkyl-3-ethoxy-2,3-dihydro-1,2,4-triazolo[4,3-c]pyrimidine **95** as a result of intramolecular additive cyclization of the corresponding **94** was reported <sup>(49)</sup>. The 2-unsubstituted 1,2,4-triazolo[1,5-c]pyrimidines

**96** (R=H) were sometimes formed as a result of Dimroth rearrangement of the transient **93** (R=H)<sup>(50)</sup> (Scheme 26).

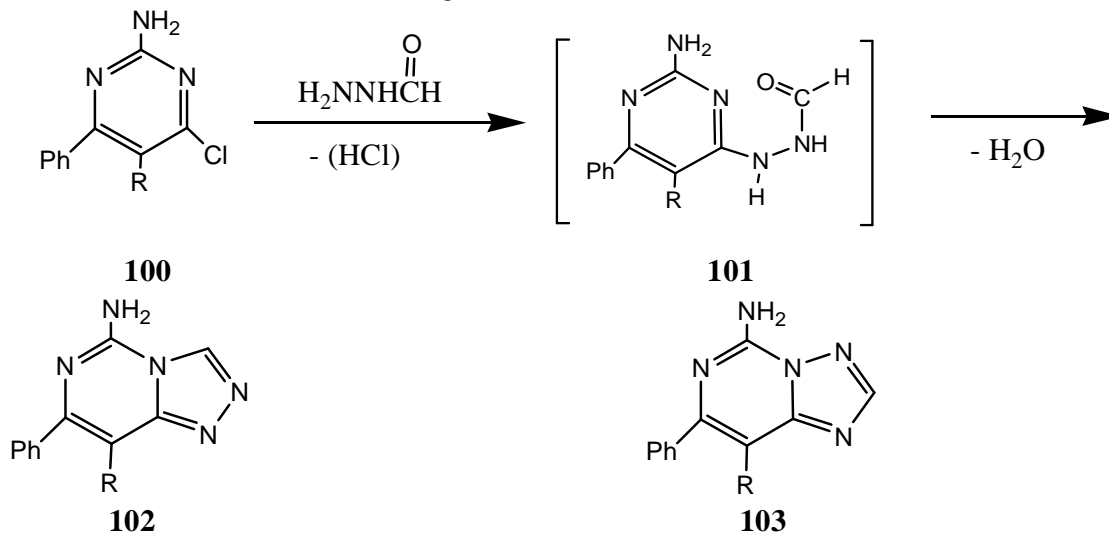


**Scheme 26**

3-Oxo-1,2,4-triazolo[4,3-c]pyrimidines **99** were prepared by cyclization of the 4-(2-ethoxycarbonylhydrazino)pyrimidines **97** by heating with an aqueous solution of sodium hydrogen carbonate<sup>(51)</sup> or phosphoryl chloride or by heating in dichlorobenzene<sup>(52)</sup>. Compounds **97** were synthesized from 4-hydrazinopyrimidines **91** and ethyl chloroformate<sup>(52)</sup>, or from 2-chloropyrimidines **98** and ethoxycarbonylhydrazine<sup>(52)</sup> (Scheme 27).



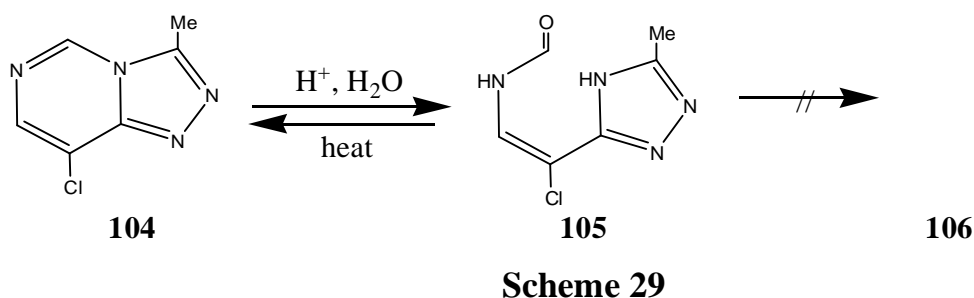
Cyclocondensation of the 2-amino-5-alkyl-4-chloro-5-phenylpyrimidines **100** with formylhydrazine gave the corresponding 1,2,4-triazolo[4,3-c]pyrimidines **102**<sup>(53)</sup> or a mixture of **102** and their [1,5-c] regioisomers **103**<sup>(54)</sup> (Scheme 28).



### 1.2.3.2 Synthesis from Triazole

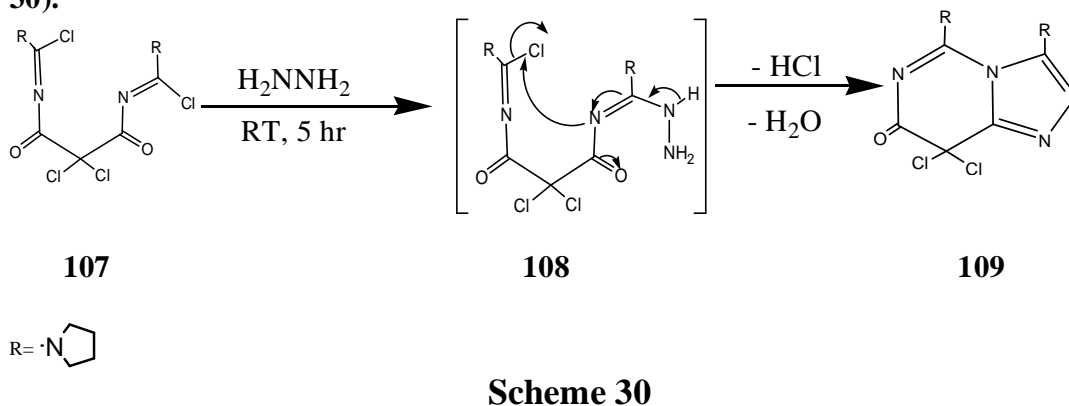
Treatment of the 8-chloro-3-methyl-1,2,4-triazolo[4,3-c]pyrimidine **104** with aqueous

acids caused pyrimidine ring opening to give the 2-chloro-1-formamido-2-(5-methyl-1,2,4-triazolo-3-yl)ethene **105**. The latter underwent thermal dehydrative recyclization to the starting **104** <sup>(55)</sup>. The corresponding 1,2,4-triazolo[1,5-c]pyrimidine regioisomer **106** has not been formed during this reaction probably due to the electron-releasing effect of the C5 methyl group in **105**, which renders the adjacent N4 of the triazole ring more nucleophilic as compared to N2 (Scheme 29).



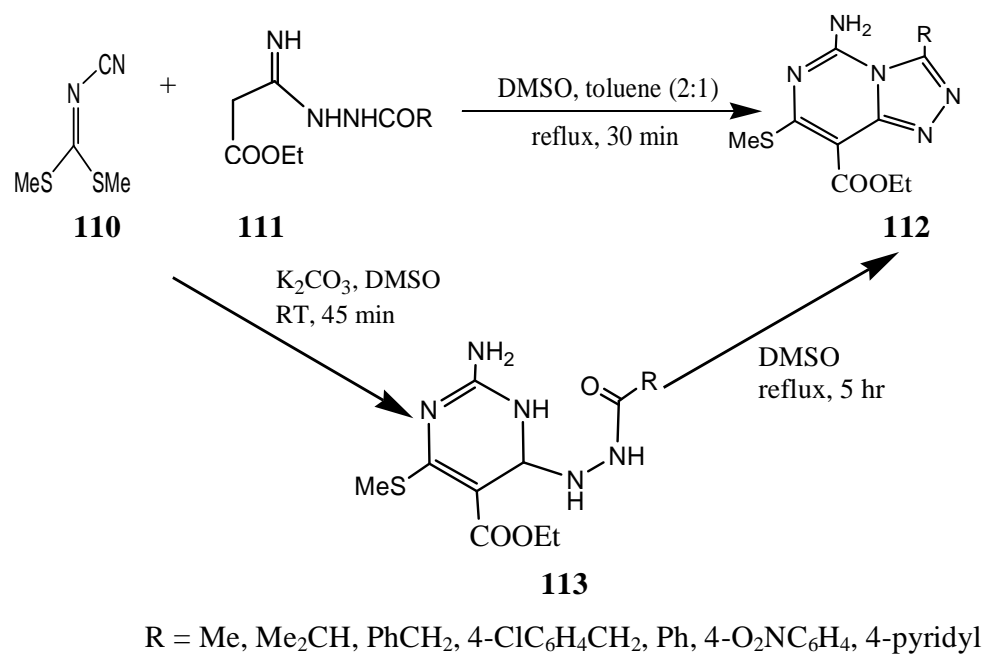
### 1.2.3.3 Synthesis by concurrent formation of both of the 1,2,4-triazole and pyrimidine rings

Cyclization of the 2,2-dichloromalononitrile dipyrrolidine diimidoyl dichloride **107** with hydrazine hydrate caused concurrent double ring closure to afford the 8,8-dichloro-3,5-dipyrrolidino-1,2,4-triazolo[4,3-c]pyrimidin-7(8*H*)-one **109** as explained in <sup>(56)</sup> (Scheme 30).



Reaction of *N*-[bis(methylthio)methylene]cyanamide **110** with the *N*<sup>1</sup>-acylamidrazones **111** at elevated temperature gave directly the corresponding 1,2,4-triazolo[4,3-c]pyrimidines **112**. Carrying out the reaction between **110** and **111** at ambient temperature in the presence of potassium carbonate afforded the 4-acylhydrazino-

pyrimidines **113**, which were dehydratively cyclized to **112** by heating in dimethylsulfoxide<sup>(57)</sup> (**Scheme 31**).



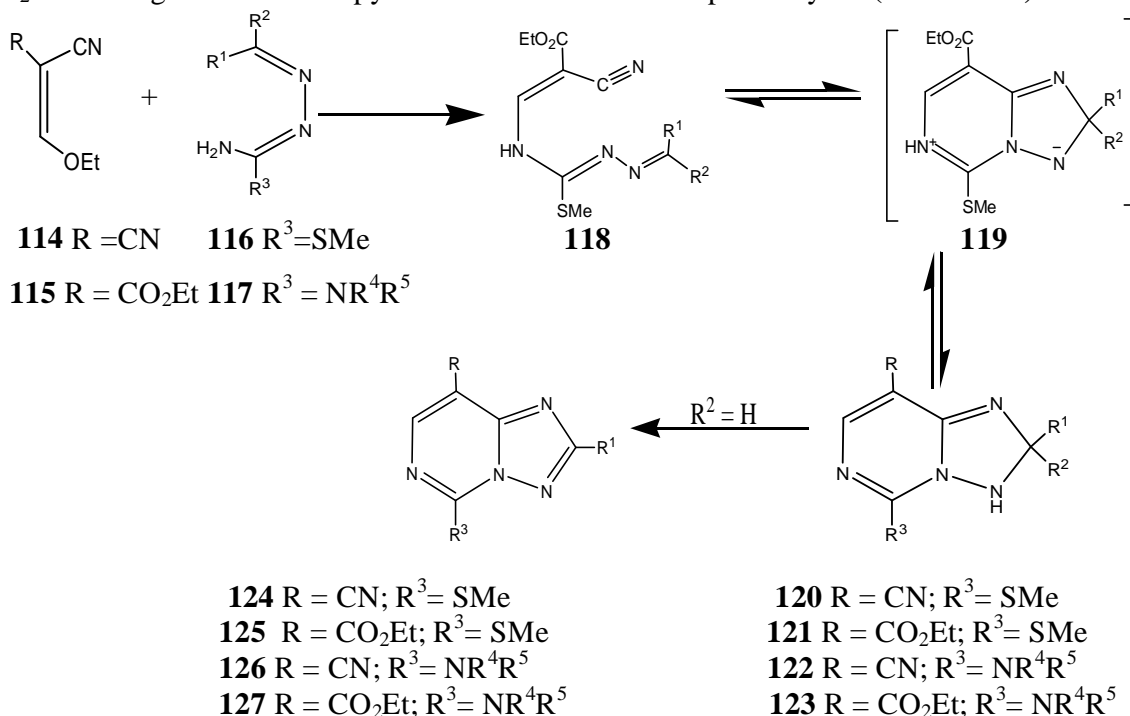
**Scheme 31**

## I.2.4 1,2,4-triazolo [1,5-c]pyrimidine

### I.2.4.1 Open Chain Precursors for Synthesis

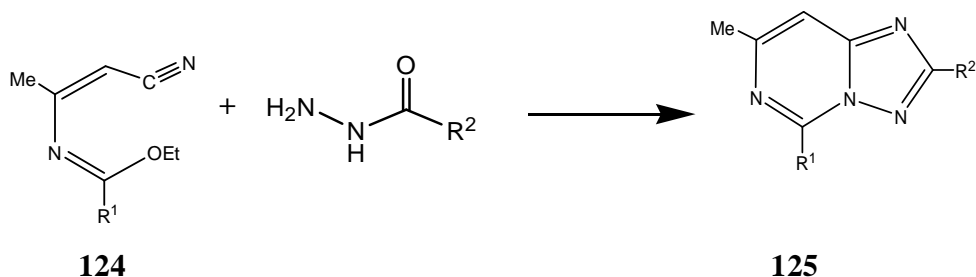
This ring can be prepared by the Cyclization of 4-[2-cyano-2-(ethoxycarbonyl)vinyl]-3-methylisothiosemicarbazones of aromatic aldehydes (**118**; R<sup>2</sup>=H), obtained from the reaction of **115** with **116** by heating in BuOH/DMF/dioxane or in pyridine to give triazolopyrimidines **125** in moderate yields. Competitive formation of ethyl 4-amino-2-(methylthio)-pyrimidine-5-carboxylate takes place. Treatment of the respective aromatic ketones with hot acetic acid or pyridine gave 2,2,5-trisubstituted 2,3-dihydrotriazolopyrimidine-8-carboxylates **121** by intermolecular cycloaddition of **118** via the intermediate **119**. The ring closure of **118** may involve a 10-electron cyclic transition state<sup>(58)</sup>. Condensation of ethoxymethylenemalononitrile **114** with isothiosemicarbazones **116** gave the dihydrocyano analogs **120**, which were readily oxidized in DMSO to the triazolopyrimidines **124**<sup>(59)</sup>. Similarly Condensation of diaminomethylenehydrazones **117**

with **115** and **116** in the presence of MeCN/Et<sub>3</sub>N gave directly the 2,3-dihydro-1,2,4-triazolo[1,5-c]pyrimidines **122** and **123**, respectively. The reaction was initiated by the attack of the amino group of **117** on the ethoxymethine carbon of **114** or **115** followed by an electrocyclic reaction. Compounds **122** and **123** were oxidized with FeCl<sub>3</sub>/AcOH or I<sub>2</sub>/EtOH to give the triazolopyrimidines **126** and **127** respectively <sup>(60)</sup> (Scheme 32).



Scheme 32

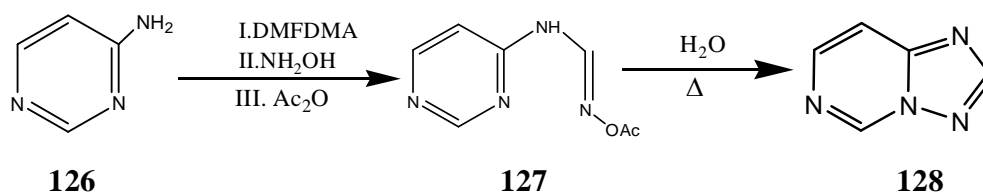
Condensation of the imidates **124** with hydrazides gave 1,2,4-triazolo[1,5-c]pyrimidines **125** <sup>(61)</sup> (Scheme 33).



Scheme 33

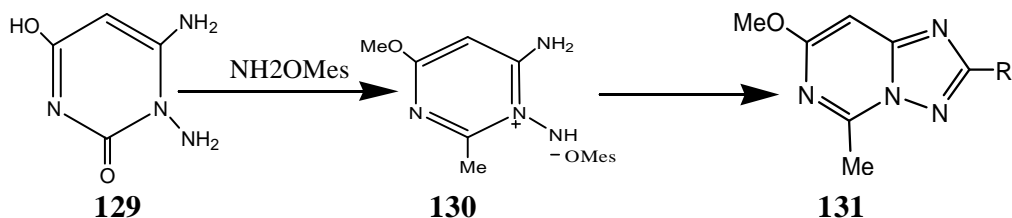
### I.2.4.2 Synthesis from pyrimidines

Reaction of amine **126** with DMF/DMA, followed by hydroxylamine and then acetylation gave the acetoxyiminomethyleneaminopyrimidine **127**, which subsequently cyclized to **128** by heating in water<sup>(45)</sup> (Scheme 34).



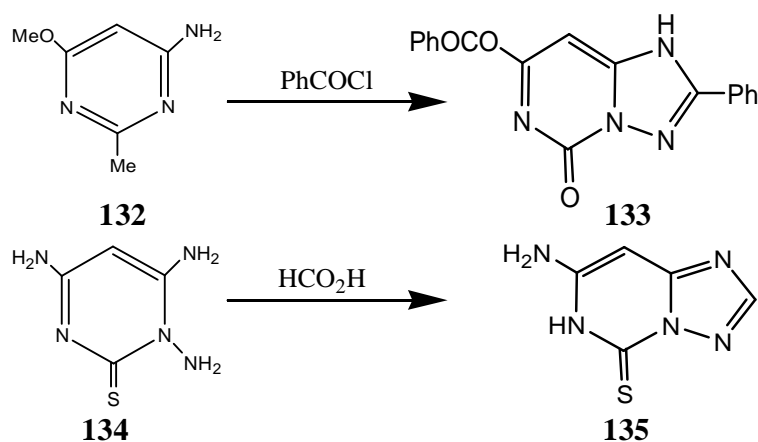
Scheme 34

Amination of the 4-aminopyrimidine **129** with *O*-mesitylenesulfonylhydroxylamine gave the *N*-aminopyrimidinium salt **130**, which was transformed into 1,2,4-triazolo[1,5-*c*]pyrimidines **131** by heating with formic acid, acetic anhydride, or benzoyl chloride<sup>(36)</sup>. Similarly the reactions of 1,6-diaminopyrimidine **132** with benzoyl chloride<sup>(62)</sup>, triamine **134** with formic acid<sup>(63)</sup>, and aminoiminopyrimidine **136** with orthoesters<sup>(64)</sup> gave the triazole[1,5-*c*]pyrimidines **133**, **135**, and **137**, respectively (Schemes 35-37).

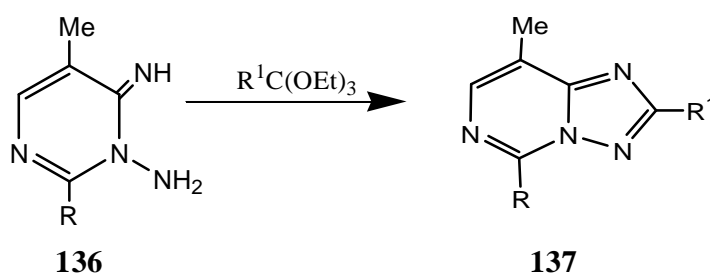


Scheme 35





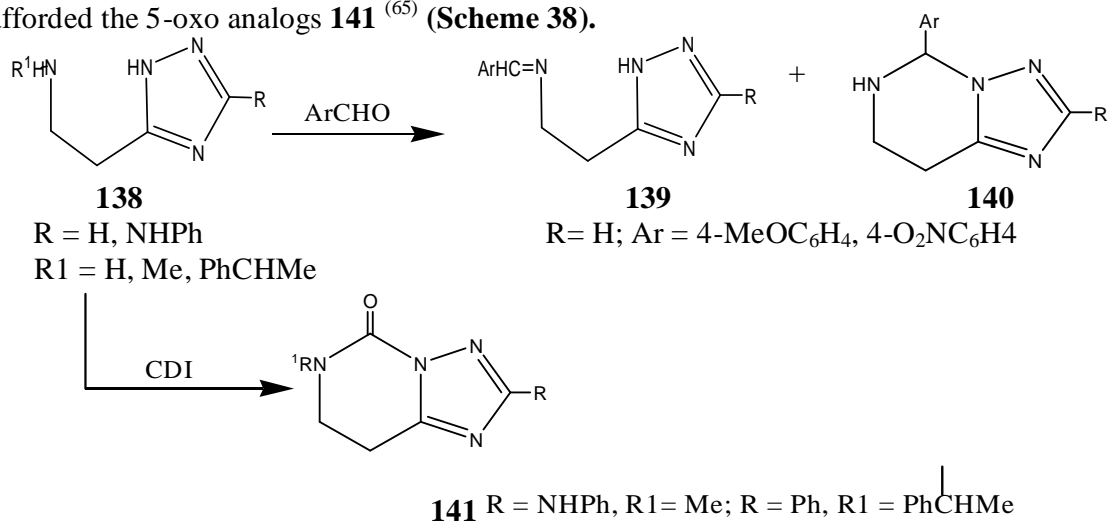
**Scheme 36**



**Scheme 37**

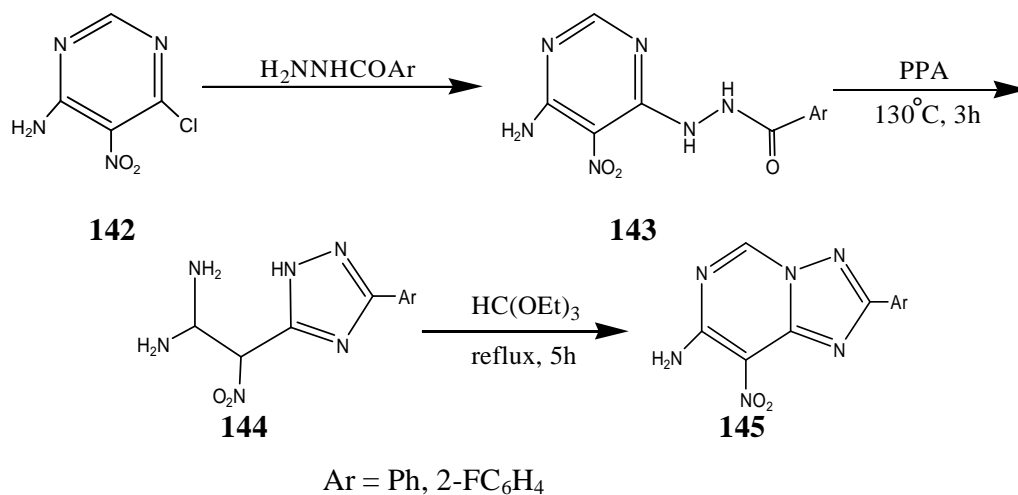
### I.2.4.3 Synthesis from triazoles

Cyclization of the 3-(2-aminoethyl)-1,2,4-triazoles **138** with aromatic aldehydes gave a mixture of the corresponding Schiff bases **139** and the 5,6,7,8-tetrahydro-1,2,4-triazolo[1,5-c]pyrimidines **140**. Cyclization of **138** with carbonyl-1,1'-diimidazole (CDI) afforded the 5-oxo analogs **141**<sup>(65)</sup> (Scheme 38).



**Scheme 38**

Attempted dehydrocyclization of the 6-acylhydrazinopyrimidine **143** by heating with polyphosphoric acid led, instead, to pyrimidine ring rupture, yielding the 1,1-diamino-2-nitro-2-(3-phenyl-1,2,4-triazol-5-yl)ethane **144**. Cyclocondensation of the latter with triethyl orthoformate gave the fully aromatic triazolopyrimidine **145**<sup>(66)</sup> (Scheme 39).

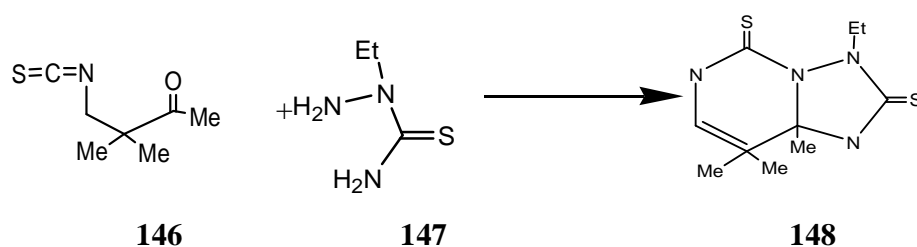


**Scheme 39**

Assignment of the 1,2,4-triazolo[1,5-c]pyrimidine structures to the products obtained from the previously described cyclizations and not the alternative [4,3-c] structures has been rationalized and corroborated on the basis of (a) preference of cyclization at the more nucleophilic triazole ring N2 rather than at its less nucleophilic N4<sup>(67)</sup>, (b) inability of the obtained products to undergo acid- or base-catalyzed Dimroth rearrangement, a property characteristic of the thermodynamically less stable [4,3-c] isomers<sup>(68)</sup> (c) comparison with unequivocally prepared authentics<sup>(67)</sup>, and (d) X-ray crystallographic analysis of the products<sup>(69)</sup>.

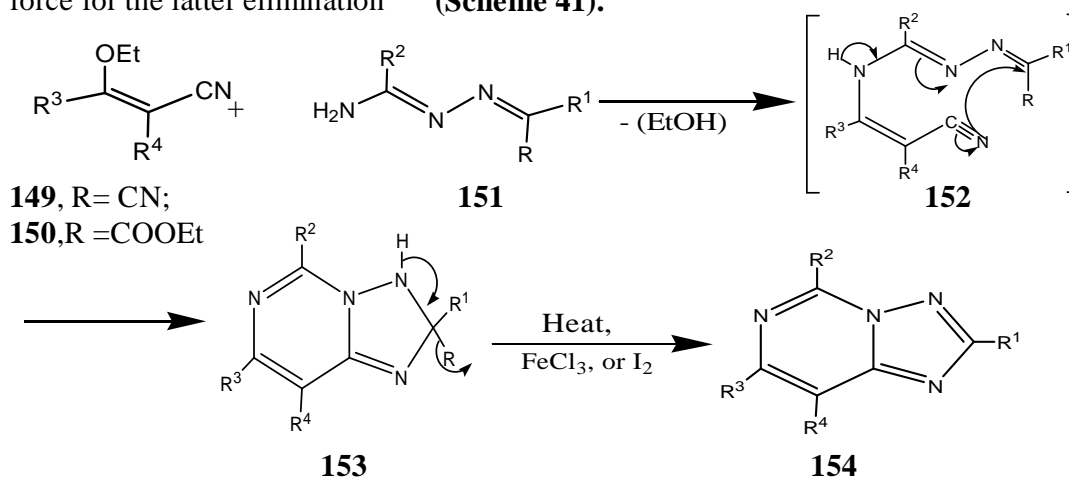
#### I.2.4.4 Synthesis by concurrent formation of both of the 1,2,4-triazole and pyrimidine rings

4-Isothiocyanato-3,3-dimethylbutane-2-one **146** provided the C<sub>4</sub>N<sub>3</sub> fragment that gave, upon reaction with 2-ethylthiosemicarbazide (CN<sub>3</sub> fragment) **147**, the 3-ethyl-1,6,7,8a-tetrahydro-2,5-dithioxo-8,8,8a-trimethyl-1,2,4-triazolo[1,5-c]pyrimidine **148**<sup>(70)</sup> (Scheme 40).



**Scheme 40**

Reaction of ethoxymethylenemalononitriles **149** or ethyl ethoxymethylenecyanoacetates **150** ( $C_3N$  fragments) with hydrazones **151**, derived from aldehydes or ketones and isothiosemicarbazides or aminoguanidines ( $C_2N_3$  fragment), gave the 2,3-dihydro-1,2,4-triazolo[1,5-c]pyrimidines **153** through the occasionally isolable intermediates **152**. Elimination of a hydrogen or the lower alkane molecule from **153** gave the final products **154**<sup>(60)</sup>. Achieving aromaticity and/or alleviating steric crowding at C2 is the mobilizing force for the latter elimination<sup>(58)</sup> (**Scheme 41**).



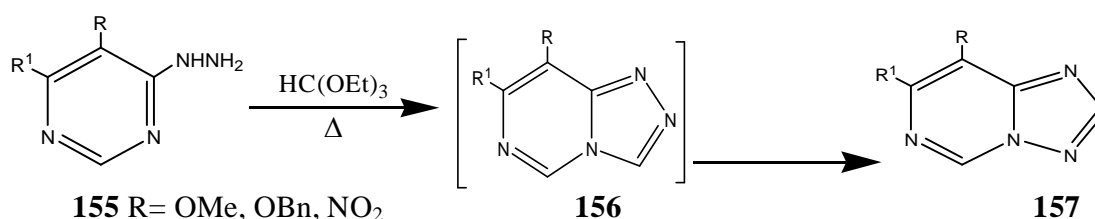
R = H, alkyl, aryl;  $R^1$  = alkyl, aryl;  $R^2$  = SMe, SCH<sub>2</sub>Ph, NHR<sup>5</sup>, NR<sub>2</sub><sup>5</sup>;  $R^3$  = H, Et;  $R^4$  = CN, COOEt

**Scheme 41**

#### 1.2.4.5 Dimroth Rearrangement of 1,2,4-Triazolo[4,3-c]pyrimidines

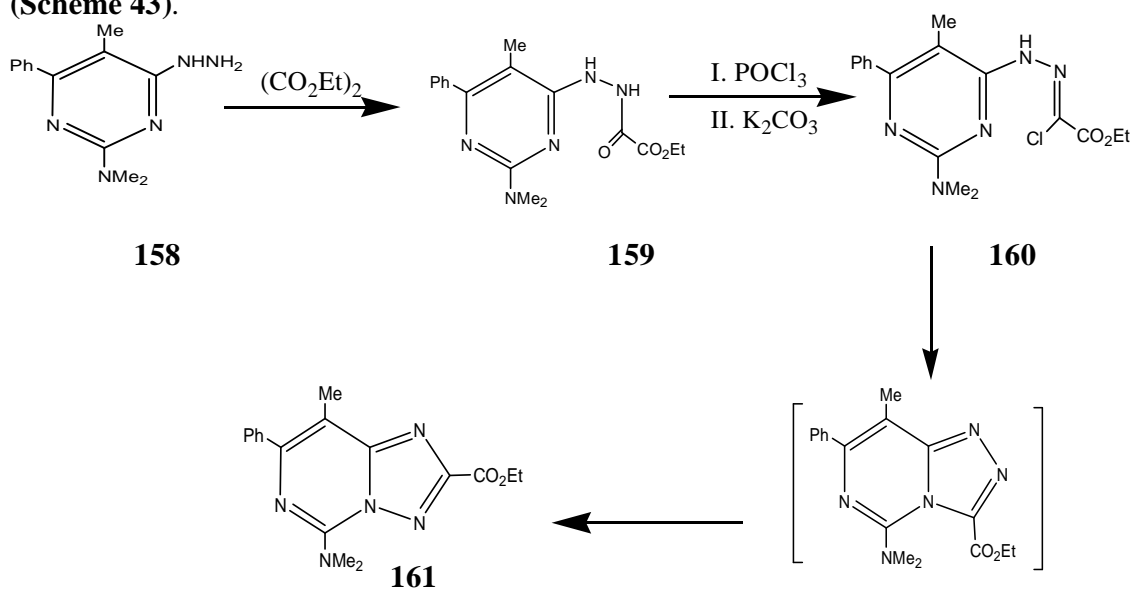
A characteristic feature observed during the cyclization of some hydrazino derivatives of pyrimidines is the rearrangement of the triazolo[4,3-a]pyrimidine intermediate to the triazolo[1,5-c]pyrimidine product.

Cyclization of 5-methoxy(nitro)-4-hydrazinopyrimidines **155** with triethyl orthoformate gave the 1,2,4-triazolo[4,3-c]pyrimidine intermediate **156**, which cannot be isolated due to its conversion to its [1,5-c]isomer **157** by a Dimroth rearrangement. However, the 5-benzyloxy pyrimidine derivative, under the same conditions, afforded a mixture of the 8-benzyloxy derivatives of both [4,3-c] and [1,5-c]isomers **156** and **157**, respectively<sup>(50)</sup>(Scheme 42).



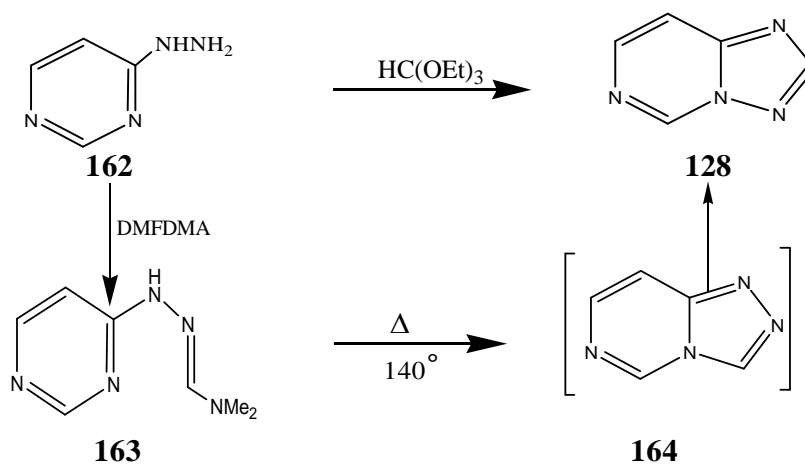
**Scheme 42**

Heating hydrazinopyrimidine **158** in diethyl oxalate gave **159**, which upon chlorination with phosphorus oxychloride yielded (2-ethoxycarbonyl) triazolo[1,5-c]pyrimidine **161**. The intermediate hydrazidoyl chloride **160** can be isolated under mild conditions<sup>(71)</sup> (Scheme 43).



**Scheme 43**

Although the reaction of hydrazinoazines and triethyl orthoformate unusually gives the unrearranged products, the 4-hydrazinopyrimidine **162** afforded with the same reagent the rearranged product 1,2,4-triazolo[1,5-c]pyrimidine **128**<sup>(45)</sup>. The same heterocycle **128** was obtained from the reaction of **162** with DMF/DMA to give the *N,N*-dimethylaminomethylenehydrazono derivative **163**, which thermally cyclized to the 1,2,4-triazolo[4,3-e]pyrimidine **164**, which immediately rearranged into **128**<sup>(72)</sup> (Scheme 44).



Scheme 44

### 1.3 The Coordination's Chemistry of the 1,2,4-triazolo[1,5-a]pyrimidines derivatives

1,2,4-triazolopyrimidine derivatives are ligands that display a great versatility in their interactions with metal ions, not only because they can bind the metal atom through different positions, but also because their presence influence the behavior of other auxiliary ligands, either by electronic or steric reasons, giving rise in some cases to compounds with interesting metal-metal interactions through these auxiliary ligands.

The studies about the coordination chemistry of triazolopyrimidine derivatives have been focused till now in the 1,5-a series which are examples of purine mimics. This type of compound has been used to elucidate the role of metal ions with nucleic acids biochemistry, on the other hand, we have not found in the bibliography any reference for coordination compound of any of the other arrangements (1,5-c, 4,3-a, or 4,3-c). This

thesis regard as the first exploration in the coordination chemistry of 1,2,4-triazolo[4,3-a]pyrimidine isomer.

### I.3.1 Compounds without a direct metal-triazolopyrimidine bond

A few compounds have been described in which there is no direct bond between the metal atom and the triazolopyrimidine derivative. Among these, there are examples with the organic molecule in neutral, cationic (protonated) and anionic form. Thus, three structures have been solved in which tetrakis(thiourea) palladium(II) chloride or tetrakis(thiourea) -platinum(II) chloride cocrystallize with dmtp <sup>(73)</sup> or HmtpO <sup>(74)</sup>. In the cases of  $[\text{Ni}(\text{dmtp})_4(\text{H}_2\text{O})_2](\text{I}_3)_2 \cdot (\text{dmtp})_2$  <sup>(75)</sup>, and  $[\text{HgCl}_2(\text{HmtpO})]_2 \cdot (\text{HmtpO}) \cdot \text{H}_2\text{O}$  <sup>(76)</sup>, both coordinated and non-coordinated triazolopyrimidine molecules coexist in the compound, interacting via stacking or hydrogen bonding.

The protonated form of dmtp has been found as the counterion of complex anions such as  $[\text{CdBr}_4]^{-2}$  <sup>(77)</sup>, and  $[\text{SnCl}_6]^{-2}$  <sup>(78)</sup>. The protonation of dmtp takes place at N3. On the other hand, a compound has also been described in which the anionic form of HmtpO balances the charge of the  $[\text{Cu}(\text{H}_2\text{O})_2(\text{cis-1,2-diaminocyclohexane})_2]^{+2}$  cation <sup>(79)</sup>.

### I.3.2 Copper (II) complexes

As it happens with other ligands, copper(II) is the metal ion of which more complexes have been characterized. Many of these compounds are mononuclear, An example of this type of compounds is the  $[\text{Cu}(\text{dmtp})_4(\text{H}_2\text{O})](\text{PF}_6)_2$  <sup>(80)</sup> which is displayed in **(Fig. 1.1)**.

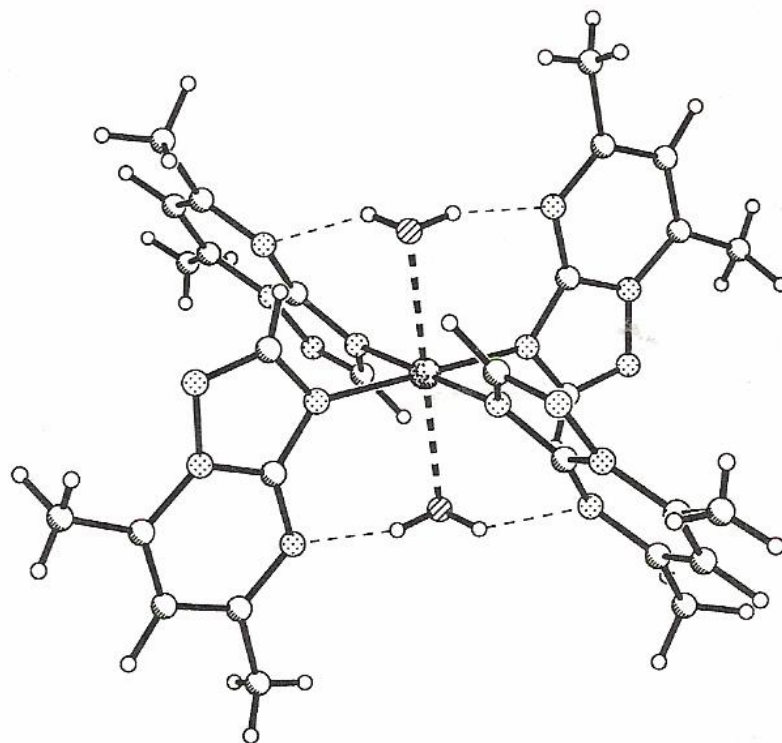


**Fig.1.1.** View of the  $[\text{Cu}(\text{dntp})_4(\text{H}_2\text{O})_2]^{2+}$  cation Adapted from Favre *et al.*.

Some of the molecular coordinate complex were characterized to coordinated with the ligand in a bidentate coordination mode  $[\text{Cu}(\text{mtpo})_2(\text{tn})] \cdot 2\text{H}_2\text{O}$  <sup>(81)</sup> is an example for this type (**Fig. 1.2**).

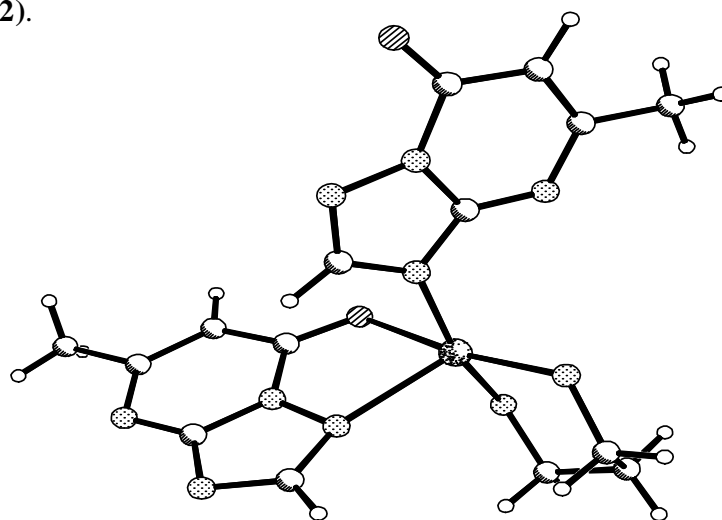


**Fig.1.2.** View of Molecular structure of  $[\text{Cu}(\text{mtpo})_2(\text{tn})] \cdot 2\text{H}_2\text{O}$  Adapted from Navarro *et al.*

On the other hand, bidentate N3-N4 behavior, has been observed for Cu(II) in the dimeric compound as an example  $[\text{Cu}_2(5\text{tpO})_4(\text{H}_2\text{O})_2] \cdot 2\text{H}_2\text{O}$  (**Fig. 1.3**).<sup>(82)</sup>, in which a strong antiferromagnetic coupling ( $2J = -104.9 \text{ cm}^{-1}$ ) takes place through the triazolopyrimidine moieties, Dimeric compounds have also been characterized in which the auxiliary anions bridge the metallic atoms this is observed for  $[\text{Cu}_2\text{Br}_4(\text{dmtp})_2] \cdot 2\text{H}_2\text{O}$ <sup>(83)</sup>, in which the copper atoms are antiferromagnetically coupled with  $2J = -21.1 \text{ cm}^{-1}$ : in this work, the value of  $2J$  is correlated with the structure for a number of bromine bridged copper dimers.

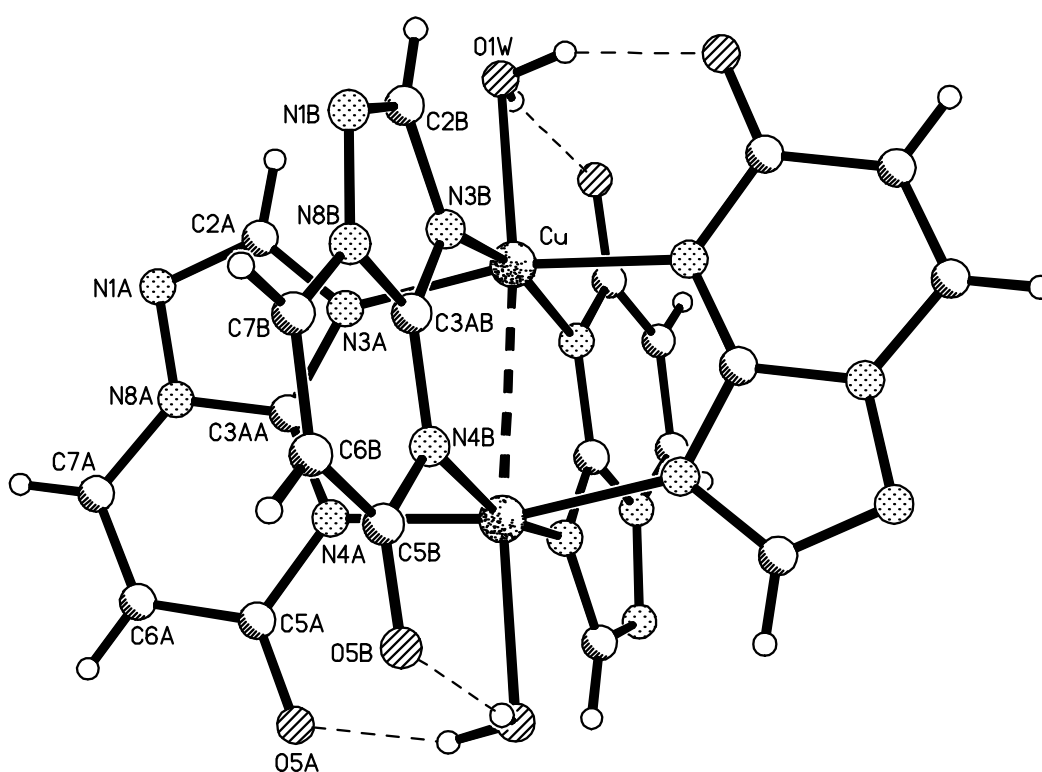


**Fig.1.3:** View of the molecular structure of  $[\text{Cu}_2(5\text{tpO})_4(\text{H}_2\text{O})_2] \cdot 2\text{H}_2\text{O}$ ; atoms are represented as 50% probability thermal ellipsoids. Adapted from M. Abul Haj.



In some cases, Cu(II) complexes have coordinated through N3 and NI to generate two-dimensional polymers as an example for this case  $[\text{CuCl}_2(\text{tp})_2]$ <sup>(84)</sup> (**Fig. 1.4**).

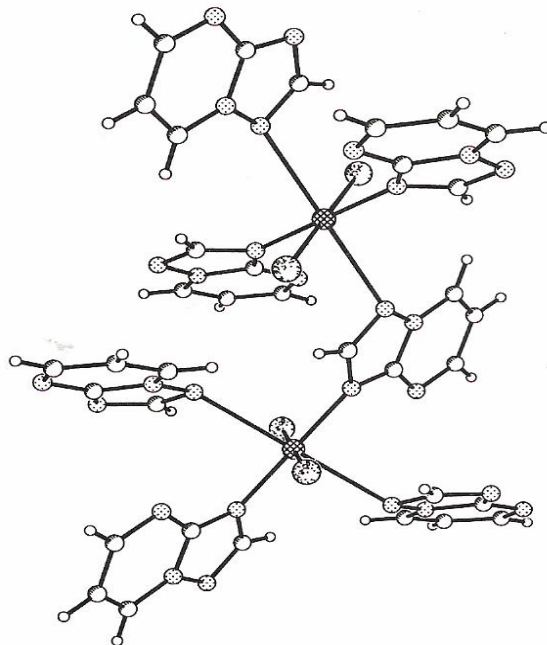
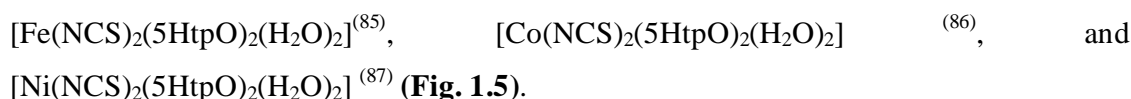


**Fig.1.4.** View of Polymeric structure of  $[\text{CuCl}_2(\text{tp})_2]$ . Adapted from Biagini-Cingi *et al.*

### I.3.3 Manganese, iron, cobalt, nickel, zinc complexes

A number of Mn(II), Fe(II), Co(II), Ni(II), and Zn(II), complexes with triazolo-[1,5-a]pyrimidine derivatives have been prepared and the crystal structures of some of them have been determined by single crystal X-ray diffraction.

The most frequent geometry found in the structural analysis is octahedral with two (or four) triazolo-[1,5-a]pyrimidine ligands monodentately coordinated via the nitrogen atom in position 3. The coordination sphere is completed by water molecules, auxiliary amine ligands or  $\text{NCS}^-$  anions, other anions balancing the charge of cationic complexes. The following compounds are examples obey those schemes:



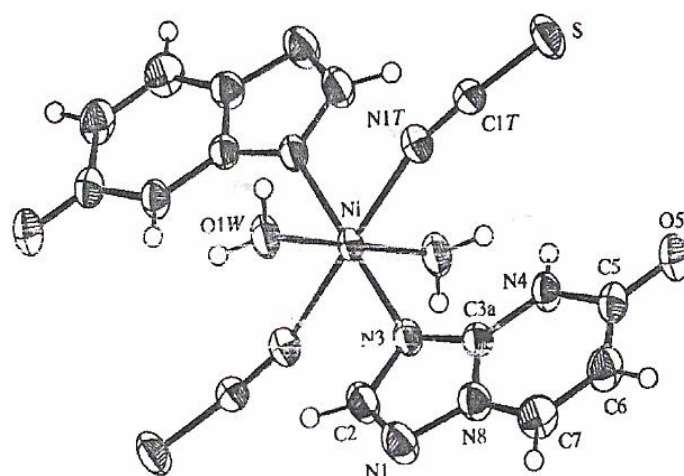


**Fig.1.5:** View of molecular structure of  $[\text{Ni}(\text{NCS})_2(5\text{HtpO})_2(\text{H}_2\text{O})_2]$  complex. Adapted from Biagini-Cingi *et al.*

### I.3.4 Mercury(II) and Cadmium(II) complexes

A special case is  $[\text{HgCl}_2(\text{HmtpO})]_2 \cdot \text{H}_2\text{O}$  <sup>(76)</sup>, the structure of which is built trigonal geometry comprising two chlorine atoms and a nitrogen atom NI from a monodentate HmtpO moiety, this coordination mode being unique for this ligand **Fig. 1.6**.

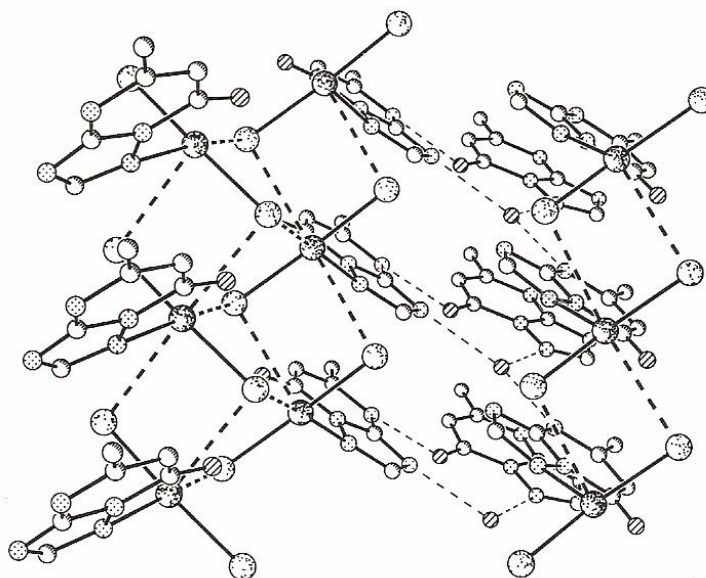


**Fig.1.6.** View of Double (left) and single (right) chains present in the crystal structure of  $[\text{HgCl}_2(\text{HmtpO})]_2 \cdot \text{H}_2\text{O}$ . both chains are linked via hydrogen bonds with the non coordinated HmtpO molecules and the water molecule. Adapted from Salas *et al.*

Some Heterometallic Hg(II) complex characterized with the ligand dmtp have been described; examples for these complexes are:  $[\text{FeHg}(\text{NCS})_4(\text{dmtp})_2(\text{H}_2\text{O})]$  <sup>(88)</sup>,  $[\text{CoHg}(\text{NCS})_4(\text{dmtp})_3(\text{H}_2\text{O})]_2$  <sup>(89)</sup> and  $[\text{CuHg}(\text{NCS})_3(\text{dmtp})_2]$  <sup>(90)</sup>.

In all cases, Hg-SCN-M bridges are present which generate either dimeric (cobalt compound) or polymeric structures (the rest, see for example **(Fig. 1.7)** and the dmtp ligands coordinate monodentately via N3.

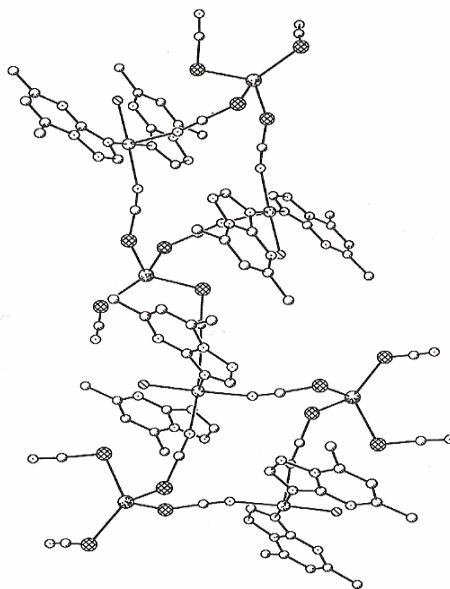


**Fig.1.7.** View of Bidimensional polymeric structure of  $[\text{FeHg}(\text{SCN})_4(\text{dmtp})_2(\text{H}_2\text{O})]$ . Adapted from Biagini-Cingi *et al.*

### I.3.5 Silver(I) and copper(I) complexes

The basic structural unit in most of these silver complexes is an eight-member ring -Ag-N-C-N-Ag-N-C-N- generated by the coordination of two triazolopyrimidine moieties to two silver atoms through the nitrogen atoms in positions 3 and 4. as an example the crystal structure of silver complex  $[\text{Ag}_2(5\text{HtpO})_2](\text{ClO}_4)_2 \cdot 2\text{H}_2\text{O}$  <sup>(91)</sup> are binuclear compound with two ligands bridging two silver atoms (**Fig. 1.8**).

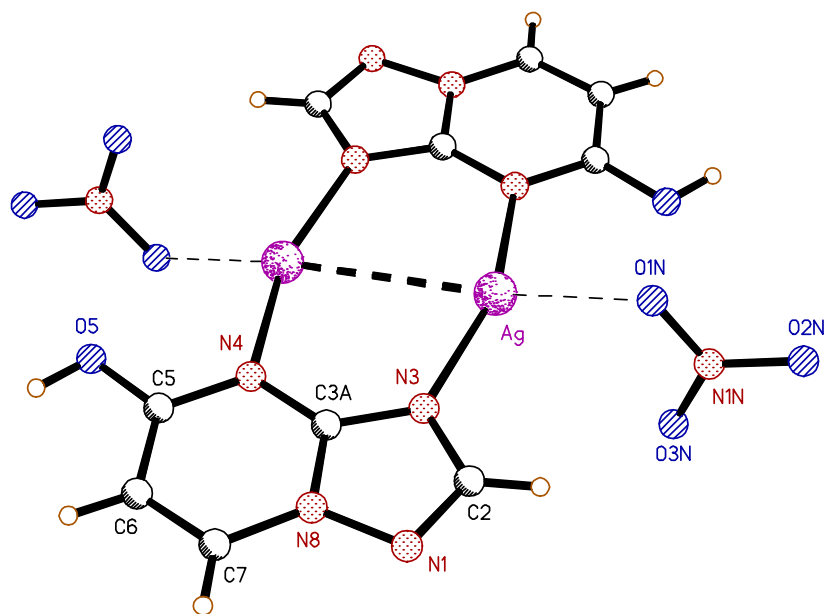


**Fig.1.8:** View of the molecular structure of  $[\text{Ag}_2(5\text{HtpO})_2](\text{ClO}_4)_2 \cdot 2\text{H}_2\text{O}$  compound. Adapted from M. Abul Haj *et al.*

Also polymer silver complexes are isolated as an example  $[\text{Ag}_3(\text{H}\text{SO}_4)(\text{mtpO})_2(\text{H}_2\text{O})_2] \cdot \text{H}_2\text{O}$  <sup>(92)</sup>, the dimeric units are linked by weak bonds of silver atoms with the N1 and O7 atoms of neighboring units, whereas a third silver atom is present in coordinated to the N1 and O7 atoms of two different dimeric units, generating a linear polymer in this way (**Fig. 1. 9**).

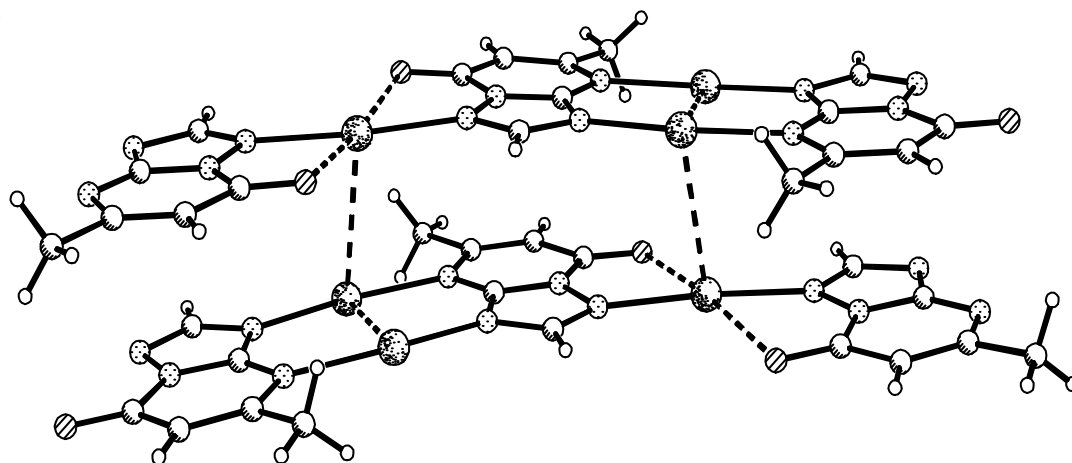


**Fig.1.9.** View of polymeric chains in  $[\text{Ag}_3(\text{mtpO})_2(\text{HSO}_4)(\text{H}_2\text{O})_2] \cdot \text{H}_2\text{O}$ . Bisulphate anions and water molecules are omitted for clarity. Adapted from Navarro *et al.*

A heterometallic tetranuclear compound  $[\text{Pt}_2\text{Ag}_2(7\text{tpO})_4(\text{bpm})_2(\text{H}_2\text{O})_2] \cdot (\text{NO}_3)_2 \cdot \text{H}_2\text{O}$  <sup>(93)</sup> is described where the four metal ions are bridge the bpm-bipyrimidine and 7tpO<sup>-</sup> (**Fig. 1.10**).

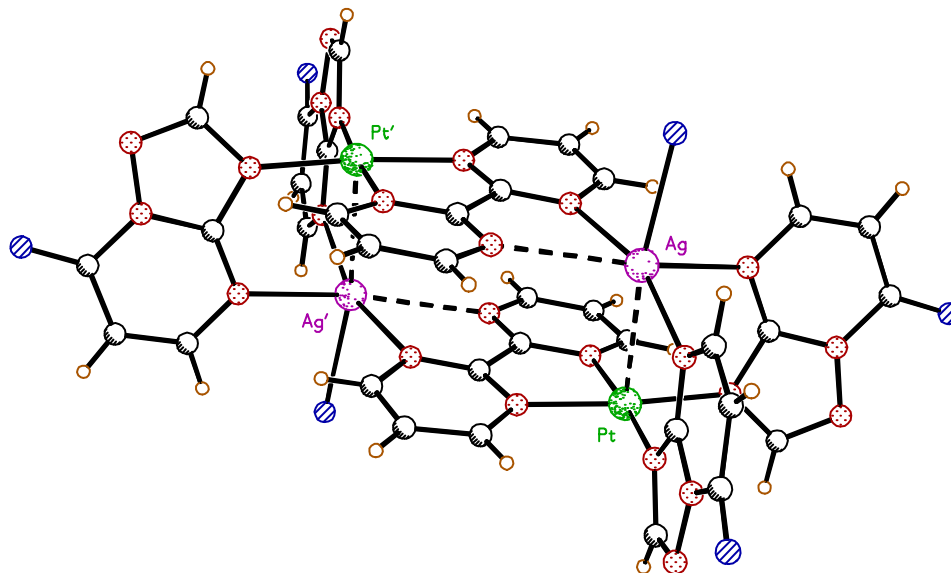


**Fig.1.10:** View of the  $[\text{Pt}_2\text{Ag}_2(7\text{tpO})_4(\text{bpm})_2(\text{H}_2\text{O})_2]^{+2}$  cation, as deduced from the X-ray data. Only a few selected atom are labeled for clarity. Adapted from M. Abul. Haj *et al.*

Finally, there is only one copper(I) compound, the structure of which has been solved,  $[\text{Cu}_4\text{Cl}_2(\text{dmtP})_4][\text{Cu}_2\text{Cl}_4]$  <sup>(94)</sup>. It is built by two dimeric units, analogous to the silver(I) previously described with a Cu-Cu distance of 2.909 °A, linked by two bridging chlorine atoms (**Fig. 1.11**).

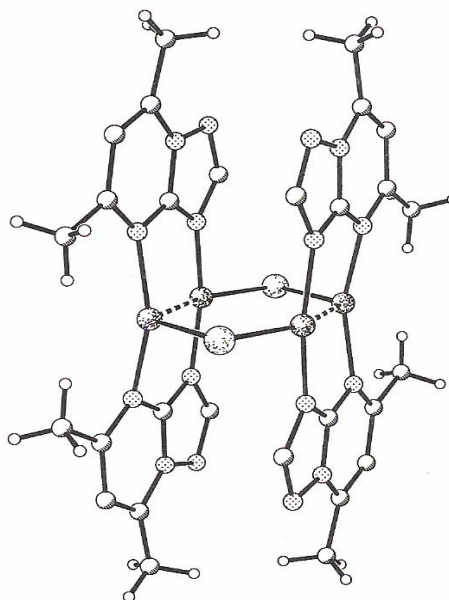


**Fig.1.11.** View of the  $[\text{Cu}_4\text{Cl}_2(\text{dmtP})_4]^{2+}$  cation. Adapted from Hassnoot *et al.*

### I.3.6 Platinum group metal complexes

The study of the interaction of platinum group metals with 1,2,4-triazolo-[1,5-a]pyrimidine ligands is dominated by the formation of Pt(II) and Pd(II) complexes, with only one example for a Ru(III) compound.

For the ligand dntp, that has not any ionizable hydrogen atom, the structures of only three mononuclear complexes have been reported: *mer*-[RuCl<sub>3</sub>(dntp)<sub>2</sub>(H<sub>2</sub>O)]<sup>(95)</sup>, and [Pt(dntp)<sub>4</sub>][Pt(SCN)<sub>6</sub>]<sup>(96)</sup> (**Fig. 1.12**).

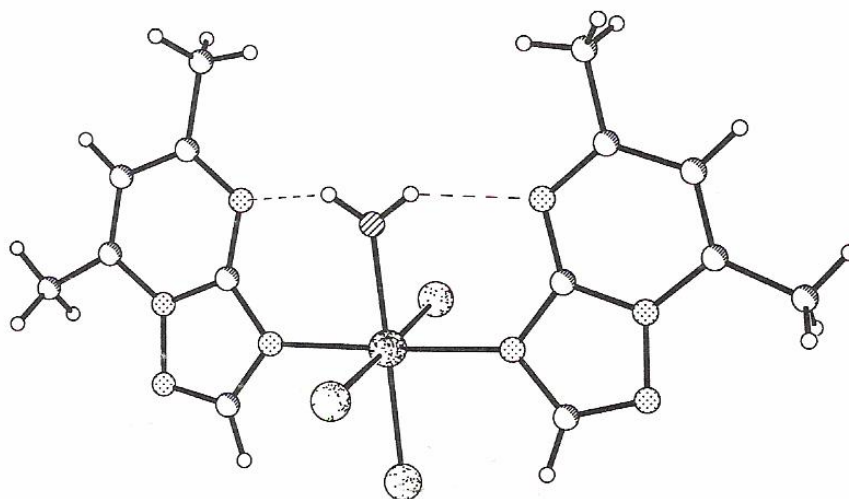


**Fig.1.12.** View of molecular structure of *mer*-[RuCl<sub>3</sub>(dntp)<sub>2</sub>(H<sub>2</sub>O)]. Adapted from velders *et al.*

On the other hand, because of the presence of an ionizable hydrogen at N4, HmtpO is a well suited ligand for the preparation of multinuclear metal complexes, since it provides up to four potential binding sites, N3 and N4 being adequate to coordinate soft atoms such as Pt(II) and Pd(II). In a first stage in acidic media, the mononuclear species monodentately coordinated via N3 are formed, *cis*-[PtCl<sub>2</sub>(HmtpO)<sub>2</sub>]<sub>2</sub>H<sub>2</sub>O<sup>(97)</sup>, and *cis*-[Pt(NH<sub>3</sub>)(HmtpO)<sub>2</sub>](NO<sub>3</sub>)<sub>2</sub>·2H<sub>2</sub>O<sup>(98)</sup> having been characterized crystallographically.

If the pH is raised up to 7, deprotonation of HmtpO at N4 occurs and the monomeric compound *cis*-[PtCl<sub>2</sub>(HmtpO)<sub>2</sub>] condensate with itself yielding the dinuclear product [Pt<sub>2</sub>(mtpO)<sub>4</sub>]<sup>(99)</sup> (**Fig. 1.13**).

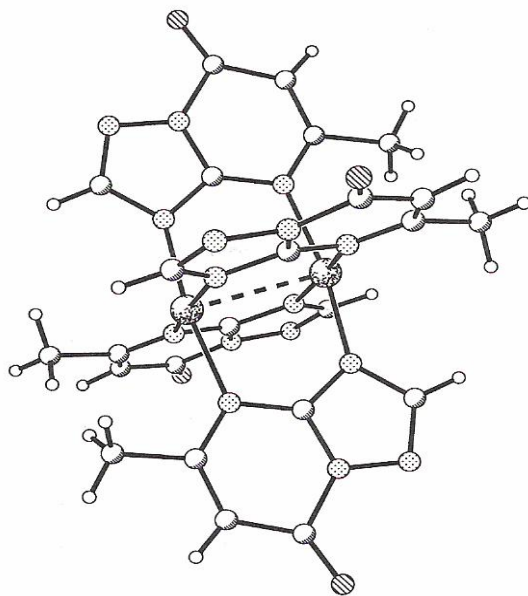


**Fig.1.13.** View of molecular structure of the dimer  $[\text{Pt}_2(\text{mtpO})_4]$ . Adapted from Navarro *et al.*

The reaction of  $\text{cis-}[\text{Pt}(\text{NH}_3)_2(\text{HmtpO})_2](\text{NO}_3)_2 \cdot 2\text{H}_2\text{O}$  with palladium electrophiles of the type  $[\text{Pt}(\text{H}_2\text{O})_2(\text{L-L})]^{2+}$  (where L-L is a bidentate diamine) affords heterobinuclear complexes of formula  $[(\text{NH}_3)_2\text{Pt}(\text{mtpO})_2\text{Pd}(\text{L-L})](\text{NO}_3)_2$ <sup>(98)</sup> (**Fig. 1.14**).

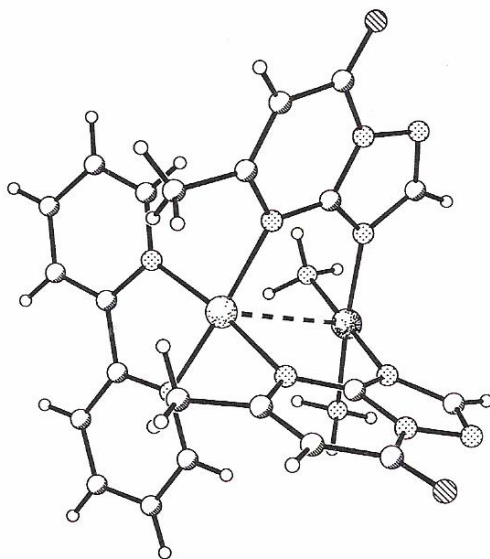


**Fig.1.14.** View of the dinuclear cation  $[(\text{NH}_3)_2\text{Pt}(\text{mtpO})_2\text{Pd}(\text{bpy})]^{2+}$ . Adapted from Navarro *et al.*

## I.4 Applications of Triazolopyrimidines

### I.4.1 Pharmaceutical uses

Many triazolopyrimidines have been tested to know their possible biological activity as potential growth inhibitors of microorganisms ranging from antiviral activities (7-pyrrolyl(indolyl)triazolopyrimidinum salts) <sup>(100)</sup>, antifungal and antibacterial (6,7-dihydro-tetrazolo-[1,5-a]pyrimidine) <sup>(16)</sup>. Some compounds of this system were found to amplify the action of the antibiotic (7-Amino-3-[2-(3,4-dihydroxy-benzenesulfonylmethyl)-5-methyl-1,2,4-triazolo[1,5-a]pyrimidin-7-ylsulfanylmethyl]-8-oxo-5-thia-1-aza-bicyclo[4.2.0]oct-2-ene-2-carboxylic acid) <sup>(101)</sup>, Nucleosides carrying a 1,2,4-triazolo[1,5-c]pyrimidin-5(6H)-one nucleosides base showed antiprotozoal activity against amastigotes of *Leishmania donovani* <sup>(102)</sup>.

In connection with their medicinal applications and activities to the respiratory system they showed antiallergic (2,5,6-trialkyl-1,2,4-triazolo[1,5-a]pyrimidin-7-ylamine) <sup>(16)</sup>, antihistaminic 5,7,8-Trimethyl-[1,2,4]triazolo[1,5-c]pyrimidin-2-one <sup>(103)</sup>, bronchodilatory (8-(4-Chloro-phenyl)-1,2,4-triazolo[4,3-c]pyrimidine) <sup>(104)</sup>.

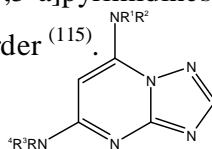
Toward the cardiovascular and urinary tract, these compounds offer applications as antiangiogenic (Diethyl-(5-methyl-1,2,4-triazolo[1,5-a]pyrimidin-7-yl)-amine) <sup>(1053)</sup>, anticholesteremics (2-Methyl-1,2,4-triazolo[1,5-a]pyrimidine) <sup>(106)</sup>, hypotensive (Diethyl-(5-methyl-2-[(phenyl-propyl-amino)-methyl]-1,2,4-triazolo[1,5-a]pyrimidin-7-yl)-amine) <sup>(107)</sup>, calcium blockers (**3-Oxo-2,3,5,8-tetraalkyl-1,2,4-triazolo[4,3-a]pyrimidine-6-carboxylic acid**) <sup>(108)</sup>, oral antihypertensive (8-aryl-1,2,4-triazolo[1,5-c]pyrimidine-2-thiol) <sup>(109)</sup>, angiotensin II receptor antagonist (1,8a-Dihydro-2H-1,2,4-triazolo[4,3-c]pyrimidin-3-one) <sup>(109)</sup>, inhibits aortic smooth muscle proliferation {2-[4-(4-Chloro-phenyl)-piperazin-1-ylmethyl]-5-methyl-1,2,4-triazolo[1,5-a]pyrimidin-7-yl}-diethyl-amine) <sup>(107)</sup>, treatment of circulatory disease such as stroke and arteriosclerosis (5-Butyl-4-(2'-triazolylbiphenylmethyl-1,2,4-triazolo[1,5-a]pyrimidine-7-one) <sup>(110)</sup>, and used as cardiac insufficiency and disease of the arterial wall (5-butyl-4(2'-triazolylbiphenylmethyl)-1,2,4-triazolo[1,5-a]pyrimidine-7-one) <sup>(111)</sup>, increased renal blood flow and urine



output (5-Azido-8-(2-ethoxy-ethyl)-7-phenyl-1,2,4-triazolo[1,5-c]pyrimidine)<sup>(112)</sup>, diuretics (8-Methyl-7-phenyl-1,2,4-triazolo[1,5-c]pyrimidin-5-ylamine), and also as antiarrhythmic disorders (1-(2-hydroxyethyl)triazolo[4,3-c]pyrimidine)<sup>(113)</sup>.

Antiulcer agents (2,5,6-trialkyl-1,2,4-triazolo[1,5-a]pyrimidin-7-ylamine, the amine derivatives of 1,2,4-triazolo[1,5-a]pyrimidine-5,7-diamine have antineoplastic activity. Thus, effects are found for (NR<sup>1</sup>R<sup>2</sup> = NHBn; NR<sup>3</sup>R<sup>4</sup> = NHNH<sub>2</sub>) against AK755, while (NR<sup>1</sup>R<sup>2</sup> = NHBn; NR<sup>3</sup>R<sup>4</sup> = morpholino) against sarcoma 37, and (NR<sup>1</sup>R<sup>2</sup> = NR<sup>1</sup>R<sup>2</sup> = phthalamidoethylthio) against Lewis Lung Cancer<sup>(114)</sup>.

In addition 7-phenoxyalkyl-1,2,4-triazolo[1,5-a]pyrimidines were prepared for possible treatment of seizures and neurological disorder<sup>(115)</sup>.



Many of the isolated metal complexes of triazolo[1,5-a]pyrimidines complexes were shown to possess very interesting biological activities. In this way, several divalent metal complexes of 5,7-dimethyl-1,2,4-triazolo[1,5-a]pyrimidine have been tested as inhibitors of the growth of different Gram(+) and Gram(-) bacteria and the fungus *Candida albicans*. Some cobalt(II) complexes show an appreciable activity against *Micrococcus*, *Staphylococcus* and *Proteus*<sup>(116)</sup>, and some copper(II) compounds present MIC (minimum inhibitory concentration) values lower than 50 µg cm<sup>-3</sup> towards the Gram (-) bacteria *E. coli* and *Salmonella Sp*<sup>(83)</sup>. Likewise, MIC values of 20 µg cm<sup>-3</sup> have been found for [Ni(5,7-dimethyl-1,2,4-triazolo[1,5-a]pyrimidine)(SO<sub>4</sub>)(H<sub>2</sub>O)].4H<sub>2</sub>O against *Streptococcus Faecalis* and [Cd(5,7-dimethyl-1,2,4-triazolo[1,5-a]pyrimidine)X<sub>2</sub>(H<sub>2</sub>O)], (where X=Cl, Br) against *Streptococcus faecalis* and *Bacillus megaterium*<sup>(77)</sup>.

The effect of several metal complexes of 4,7-dihydro-5-methyl-7-oxo-1,2,4-triazolo[1,5-a]pyrimidine isomer against *Phytomonas staheli* (promastigote form)<sup>(117)</sup> has also been studied showing that some of them inhibit parasite growth by nearly 90%; these complexes have also displayed good results against analogous parasites like *Trypanosoma cruzi* and *Leishmania donovani*. Transmission electron microscopy studies have been carried out to evaluate the morphological changes that these complexes cause in

different cell or ganelles, comparing the cell structure of treated and nontreated *P. staheli* (118).

The effect of (*cis*-[Pt(4,7-dihydro-7-oxo-1,2,4-triazolo[1,5-a]pyrimidine)<sub>2</sub>Cl<sub>2</sub>]) addition at different concentrations to cultured human cell lines MCF-7 breast carcinoma and A121 ovarian carcinoma has been tested (93). The results indicates a high antitumour activity against the latter, this complex being less active than cisplatin but more than carboplatin. Some 5,7-dimethyl-1,2,4-triazolo[1,5-a]pyrimidinecomplexes with Ru(II) are also being tested for antitumour activity (119).

#### I.4.2 Agrochemical Uses

Triazolopyrimidines are used as pesticide, fungicides, nitrification inhibitors, growth regulators, and especially herbicides. 1,2,4-triazolo[1,5-a] pyrimidinesulfonamides are used as herbicides, and plant growth inhibitors (120), and they show activity against acetolactate syntheses (121).

Compound (7-Methoxymethyl-5-methyl-1,2,4-triazolo[1,5-a]pyrimidine-2-sulfonic acid arylamide) acts as a selective herbicide against dicotyledonous weeds, such as *Galium*, *Matricaria*, *Galinsoga*, and *Mercurialis Spp* (122) in beets (its herbicidal activities vary with the position of the substituent on the phenyl ring). The (2-(Arylthio)-1,2,4-triazolo[1,5-a]pyrimidines 2-(Arylthio)-1,2,4-triazolo[1,5-a]pyrimidines) and (5,7-Dichloro-[1,2,4]triazolo[1,5-a]pyrimidine) are also useful as herbicides (123).

Compounds (2,5,6-trialkyl-1,2,4-triazolo[1,5-a]pyrimidin-7-ylamine) and (5,7-dihalo-1,2,4-triazolo[1,5-a]pyrimidines) act as agrochemical fungicides and cause protection against *Plasmopara viticola* (124). (7-Amino-2-methyl-[1,2,4]triazolo[1,5-a]pyrimidine-6-carbonitrile) compound are superior fungicides(125). (5-Fluoromethyl-7-methoxy-1,2,4-triazolo-[1,5-a]pyrimidine-2-sulfonamides) are useful for the control of pigweed (126). Where (5,7-Dialkyl-[1,2,4]triazolo[1,5-a]pyrimidine-2-sulfonic acid phenylamide) are useful as herbicides and inhibitors of nitrification of amino nitrogen in soil, and they are used for the control of *Echinochloa crusgalli* without damage to rice (126).

### 1.4.3 Photographic uses

5-methyl-1,2,4-triazolo[1,5-a]pyrimidine-7-one (MOT) discovered by Birr in 1935<sup>(1)</sup>, and used as "stabilizing" activity, this discovery made it possible for the first time to stabilize the sensitometric properties of photographic materials during storage. Even today MOT is an inherent constituent of nearly every photographic product. Numerous derivatives have been synthesized: none is substantially more effective than MOT. 5-or-7-one-1,2,4-triazolo[1,5-a]pyrimidines derivatives adding to silver halide photographic materials to provide high contrast, which is suitable for graphic arts use<sup>(101)</sup>, and good shelf life under high temperature and high humidity<sup>(127)</sup>. Compound 2,5,6-Trialkyl-[1,2,4]triazolo[1,5-a]pyrimidin-7-one were prepared as a photosensitive photographic element<sup>(128)</sup>. Silver halide emulsion layers containing the substituted **5(7)-one-1,2,4-triazolo[4,3-a]pyrimidine** derivatives are used as a photosensitive photographic materials<sup>(127)</sup>. Comprehensive theory of stabilization does not exist.

## 1.5 Computational Chemistry

Computational chemistry is a new discipline. Its advent and popularity have paralleled improvements in computing power during the last several decades. As with other disciplines in chemistry, computational chemistry uses tools to understand chemical reactions and processes. Scientists use computer software to gain insight into chemical processes. Although computational chemists frequently develop and refine software tools, their primary interest is in applying software tools to enhance chemical knowledge.

In general software program uses two types of methods in calculations: molecular mechanics and quantum mechanics. The quantum mechanics methods include semi-empirical and *ab initio*. The molecular mechanics and semi-empirical quantum mechanics methods have several advantages over *ab initio* methods. Most importantly, these methods are fast. While this may not be important for small molecules, it is certainly important for biomolecules. Another advantage is that for specific and well-parameterized molecular systems, these methods can calculate values that are closer to experiment than lower level *ab initio* techniques.

The accuracy of a molecular mechanics or semi-empirical quantum mechanics method depends on the database used to parameterize the method. This is true for the type of molecules and the physical and chemical data in the database. Frequently, these methods give the best results for a limited class of molecules or phenomena. A disadvantage of these methods is that you must have parameters available before running a calculation. Developing parameters is time-consuming. The *ab initio* method may overcome this problem.

### I.5.1 Quantum Mechanics

*Ab initio* quantum mechanics methods have evolved for many decades. The speed and accuracy of *ab initio* calculations have been greatly improved by developing new algorithms and introducing better basis functions.

In quantum mechanics, the Schrödinger equation (1) gives the wave functions and energies of a molecule.

$$H\Psi = E\Psi \quad (1)$$

Where H is the molecular Hamiltonian,  $\Psi$  is the wave function, and E is the energy. The molecular Hamiltonian is composed of the following operators: the kinetic energy of the nuclei (N) and electrons (E), nuclear-nuclear (NN) and electron-electron repulsions (EE), and the attraction between nuclei and electrons (NE) (equation 2).

$$H = (\text{Kinetic energy})_N + (\text{Kinetic energy})_E + (\text{repulsion})_{NN} + (\text{repulsion})_{EE} + (\text{attraction})_{NE} \quad (2)$$

Nuclei have many times more mass than electrons. During a very small period of time when the movement of heavy nuclei is negligible, electrons are moving so fast that their distribution is smooth. This leads to the approximation that the electron distribution is dependent only on the fixed positions of nuclei and not on their velocities. This approximation allows two simplifications of the molecular Hamiltonian. The nuclear kinetic energy term drops out (equation 3).

$$H = (\text{Kinetic energy})_E + (\text{repulsion})_{NN} + (\text{repulsion})_{EE} + (\text{attraction})_{NE} \quad (3)$$

Since the nuclear-nuclear repulsion is constant for a fixed configuration of atoms, this term also drops out. The Hamiltonian is now purely electronic.

$$H = (\text{Kinetic energy})_E + (\text{repulsion})_{EE} + (\text{attraction})_{NE} \quad (4)$$

After solving the electronic Schrödinger equation (equation 4), to calculate a potential energy surface, you must add back nuclear nuclear repulsions (equation 5).

$$H_{\text{electronic}} \Psi_{\text{electronic}} = E_{\text{electronic}} \Psi_{\text{electronic}}$$

$$V_{\text{PES}} = E_{\text{electronic}} + (\text{repulsion})_{NN} \quad (5)$$

Generating the potential energy surface (PES) using this equation requires solutions for many configurations of nuclei. In molecular mechanics, the electronic energy is not evaluated explicitly. Instead, these methods solve the potential energy surface by using a force field equation. The force field equation represents electronic energy

## I.5.2 Molecular Mechanics

Molecular mechanical force fields use the equations of classical mechanics to describe the potential energy surfaces and physical properties of molecules. A molecule is described as a collection of atoms that interact with each other by simple analytical functions. This description is called a *force field*. One component of a force field is the energy arising from compression and stretching a bond.

This component is often approximated as a harmonic oscillator and can be calculated using Hooke's law.

$$V_{\text{spring}} = \frac{1}{2} K_r (r - r_0)^2 \quad (6)$$

The bonding between two atoms is analogous to a spring connecting two masses. Using this analogy, equation 7 gives the potential energy of the system of masses,  $V_{\text{spring}}$ , and

the force constant of the spring,  $K_r$ . The equilibrium and displaced distances of the atoms in a bond are  $r_0$  and  $r$ . Both  $K_r$  and  $r_0$  are constants for a specific pair of atoms connected by a certain spring.  $K_r$  and  $r_0$  are force field *parameters*.

The potential energy of a molecular system in a force field is the sum of individual components of the potential, such as bond, angle, and van der Waals potentials (equation 8). The energies of the individual bonding components (bonds, angles, and dihedrals) are functions of the deviation of a molecule from a hypothetical compound that has bonded interactions at minimum values.

$$E_{\text{Total}} = \text{term}_1 + \text{term}_2 + \dots + \text{term}_n \quad (7)$$

The absolute energy of a molecule in molecular mechanics has no intrinsic physical meaning;  $E_{\text{Total}}$  values are useful only for comparisons between molecules. Energies from single point calculations are related to the enthalpies of the molecules. However, they are not enthalpies because thermal motion and temperature dependent contributions are absent from the energy terms (equation 7).

Unlike quantum mechanics, molecular mechanics does not treat electrons explicitly. Molecular mechanics calculations cannot describe bond formation, bond breaking, or systems in which electronic delocalization or molecular orbital interactions play a major role in determining geometry or properties.

### **I.5.2.1 Bonding energies**

#### **I.5.2.1.1 Bonds and Angles**

This term is associated with deformation of a bond from its standard equilibrium length. For small displacements from equilibrium, a harmonic function is often used:

$$E_{\text{bond}} = \sum_{\text{bonds}} K_r (r - r_0)^2 \quad (8)$$

A larger value for the stretch force constant  $K_r$  leads to a greater tendency for the bond to remain at its equilibrium distance  $r_0$ . Higher powers of  $r - r_0$ , giving cubic, quadric, or higher terms are also common.

### I.5.2.1.2 Bond Angle Bending

This term is associated with the deformation of an angle from its normal value. For small displacements from equilibrium, a harmonic function is often used:

$$E_{\text{bond angle}} = \sum_{\text{angles}} K_{\theta} (\theta - \theta_0)^2 \quad (9)$$

A larger value for the bending forces constant  $K_{\theta}$  leads to a greater tendency for the angle to remain at its equilibrium value  $\theta_0$ . There may be cubic, quartic, etc. terms as with the corresponding bond stretch term in addition to the quadratic term shown here.

### I.5.2.1.3 Dihedrals (torsion) energy

This term is associated with the tendency of dihedral angles to have a certain  $n$ -fold symmetry and to have minimum energy for the *cis*-, *gauche*-, or *trans*-conformation, etc.

$$E_{\text{dihedral}} = \sum_{\text{dihedral}} \frac{V_n}{2} [1 + \cos(n\phi - \phi_0)] \quad (10)$$

The period of the interaction is  $360/n$ . The phase angle  $\phi_0$  shifts the curve to the left or right. For  $n=1$  and  $\phi_0=0$ , the curve represents the situation where the energy is a minimum for the *trans*-conformation with a barrier of  $V_n$  to the highest energy *cis*-conformation. A phase angle of  $\phi_0=180$  represents the opposite situation with a minimum at the *cis*-conformation and a maximum at the *trans*-conformation.

## I.5.2.2 Non-bonding energies

### I.5.2.2.1 Van der Waals energy

This term describes the repulsive forces keeping two nonbonded atoms apart at close range and the attractive force drawing them together at long range.

$$E_{\text{vanderWaals}} = \sum_{ii \in \text{vdW}} \left[ \frac{A_{ij}}{R_{ij}^{12}} - \frac{B_{ij}}{R_{ij}^6} \right] \quad (11)$$

i and j represent two different atoms

A<sub>ij</sub> and B<sub>ij</sub> are derived from atomic constants A<sub>ii</sub> and B<sub>ii</sub>

R<sub>ij</sub> is the distance between the two atoms i and j

The first positive term is the short range repulsion energy between two atoms which depends inversely on the distance ( $r^{-12}$ ) while the second negative term is the long range attraction energy between the two atoms and is a less sensitive function of the distance ( $r^{-6}$ ).

#### I.5.2.2.2 Electrostatic energy

This term describes the classical nonbonded electrostatic interactions of charge distributions.

$$E_{\text{electrostatic}} = \sum_{ii \in \text{electrostatic}} \left[ \frac{q_i q_j}{\epsilon R_{ij}} \right] \quad (12)$$

The above potential describes the monopole-monopole interactions of atomic charges  $q_i$  and  $q_j$  a distance  $R_{ij}$  apart. Normally these charge interactions are computed only for nonbonded atoms. The dielectric constant  $\epsilon$  used in the calculation is sometimes scaled or made distance-dependent, as described in the next section. Electrostatic terms other than the simple charge interactions above are commonly included in molecular mechanics calculations, particularly dipole-dipole interactions. More recently, second-order electrostatic interactions like those describing polarizability have been added to some force fields.

So equation (7) can be represented as the sum of these bonding and nonbonding energies as (equation 14):

$$E_{\text{total}} = E_{\text{bond}} + E_{\text{bond angle}} + E_{\text{dihedral}} + E_{\text{vanderwaals}} + E_{\text{electrostatic}} \quad (13)$$



## I.6 Objectives

- (1) Synthesis of the new derivatives triazolopyrimidine 7,8 dihydro-7 oxo-[1,2,4]-triazolo [4,3-a] pyrimidine, and characterization of this ligands by means of suitable techniques.
- (2) Determine the crystal structure by x-ray diffraction of the isolated ligand in the crystal form.
- 3) Carry out theoretical study of the ligand 7,8-dihydro-7-oxo-[1,2,4]-triazolo[4,3-a] pyrimidine in its molecular form as well in the anionic form, taking in consideration all the tautomeric forms by quantum mechanics calculations of the type RHF/AM1 through the program HyperChem (Hypercube, Inc.). The standard mode geometry to be modeled by the use of the same program, auto consistently with the molecular orbital calculations. The charges over the atoms will be calculated using mulliken method.
- (4) Preparation of metal complexes and metal clusters with the previously studied ligand (7,8 dihydro-7-oxo-[1,2,4]-triazolo[4,3-a]pyrimidine)
- (5) Characterize this complex by suitable techniques (Infrared spectroscopy, elemental analysis, thermogravimetric studies(TG), differential scanning calorimetric(DSC),  $^1\text{H}$  and  $^{13}\text{C}$  nuclear magnetic resonance )
- (6) Solve X-ray structure of the isolated complex in the crystal form

## *CHAPTER TWO*

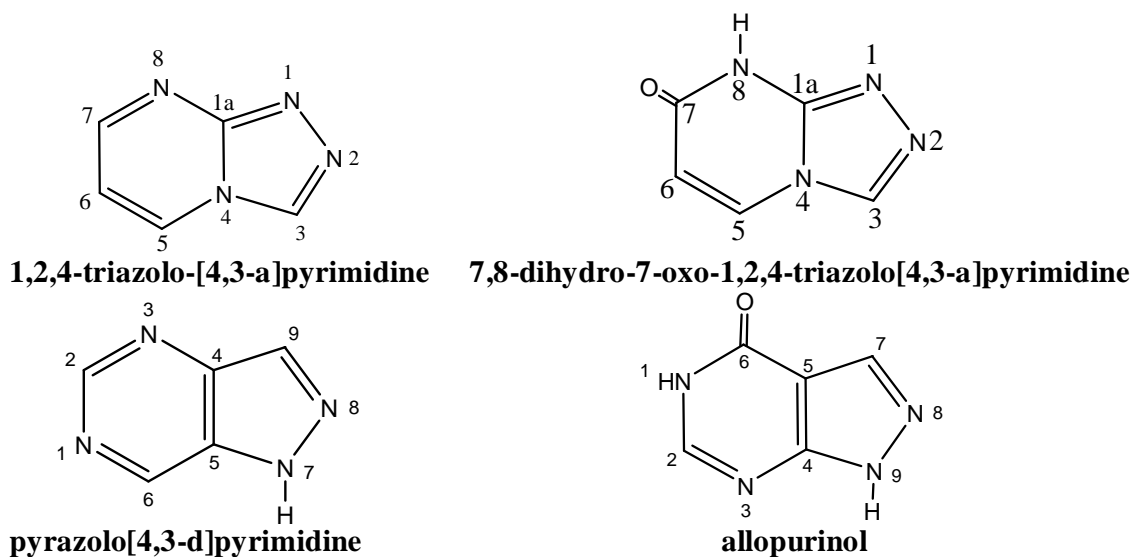
*Synthesis, characterization, and  
theoretical study  
of  
7,8- dihydro-7-oxo-1,2,4-triazolo[4,3-a]  
pyrimidine ligand*

## II.1 Introduction

Until the present the study of the coordination compounds of the triazolopyrimidines had focused on the 1,5-a isomer, many derivatives of the 1,5-a isomer were extensively studied. None of the other triazolopyrimidines arrangements [(1,5-c), (4,3-a), 4,3-c)] were studied for its coordination behavior.

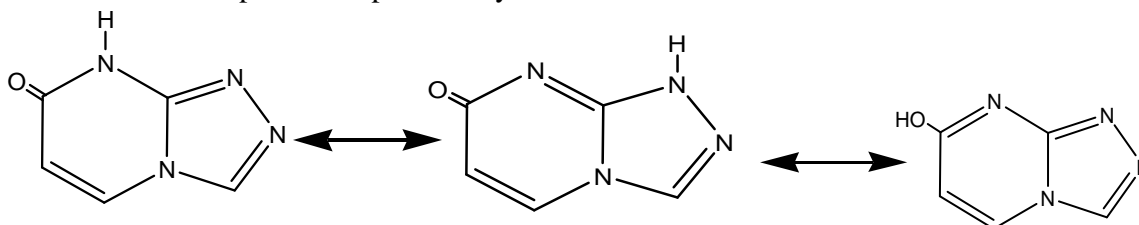
This thesis is the first attempt to study the coordination compounds of the 1,2,4-triazolo[4,3-a]pyrimidine derivative. Prior to this study we have to prepare and characterize this derivative by the usual technique; in addition a theoretical study was done to complete the experimental work.

This heterocyclic isomer has a structure similar to that pyrazolo[4,3-d]pyrimidine, their fused ring system differing in having the pyrimidine nitrogen atom in a bridgehead position with disappearance of the acidic H-proton of the five-member ring. Whereas 7,8-dihydro-7-oxo-1,2,4-triazolo[4,3-a]pyrimidine isomer may be considered an analogue of the natural occurring nucleobase pyrazolo[4,3-d]pyrimidines, the most outstanding of which is allopurinol. The following (**Scheme 45**) below compares these two systems, depicting the IUPAC numbering scheme used for the 7,8-dihydro-7-oxo-1,2,4-triazolo[4,3-a]pyrimidine ligand and the biochemical numbering schemes used for pyrazolo[4,3-d]pyrimidines and allopurinol. Because of the similarity of both systems, coordination compounds of triazolopyrimidin isomers can be considered as model systems for various naturally occurring metal coordination compounds.



**Scheme 45**

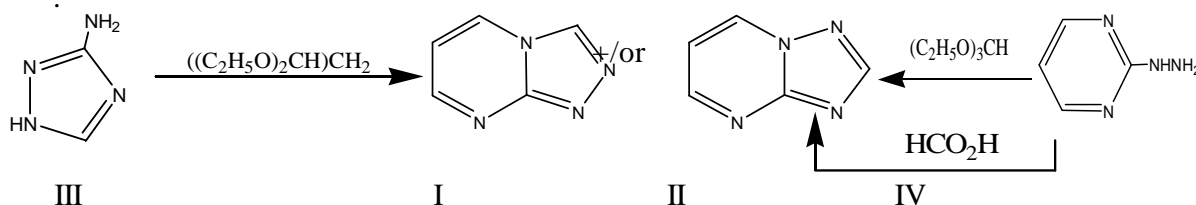
Tautomerism plays an important role in the chemical properties of heterocyclic bases which contain exocyclic oxygen atom. The 7,8-dihydro-7-oxo-1,2,4-triazolo[4,3-a]pyrimidine isomer may exist in a one lactim or two lactam forms (**Scheme 46**) depending on the position to which the acidic protons are attached. Nevertheless, one of these forms usually is much more stable than the others. The relative stabilities of this tautomer in the gaseous state may be estimated by mean of semiempirical calculation. At the end of this chapter a complete study will describe the most stable tautomer.



**Scheme 46**

The synthesis of 1,2,4-triazolo[4,3-a]pyrimidine (I) and of 1,2,4-triazolo[1,5-a]pyrimidine (II) can be accomplished by two different routs, either starting with 3-amino-1,2,4-triazolo (III) or with 2-hydrazinopyrimidine (IV) <sup>(2)</sup>. The former of these reactions can, in theory, produce either I or II, or both of these compounds, depending upon whether N2 or N4 of the 3-amino-1,2,4-triazolo is involved in the cyclization reaction <sup>(3,5)</sup>. In some cases, the kinetically favored [4,3-a] product is formed initially, this

being transformed into the thermodynamically more stable [1,5-a] isomer by mean of the Dimroth rearrangement [7], which can also be obtained directly from IV with formic acid (129).



**Scheme 47**

The major argument in favor of structures of [1,5-a] appears to be based upon the statement that ethyl orthoformate and 2-hydazinopyrimidine yield only the non-rearranged compound 1,2,4-triazolo[4,3-a]pyrimidines which can be rearranged under different conditions to the 1,2,4-triazolo[1,5-a]pyrimidines<sup>(3,5)</sup>.

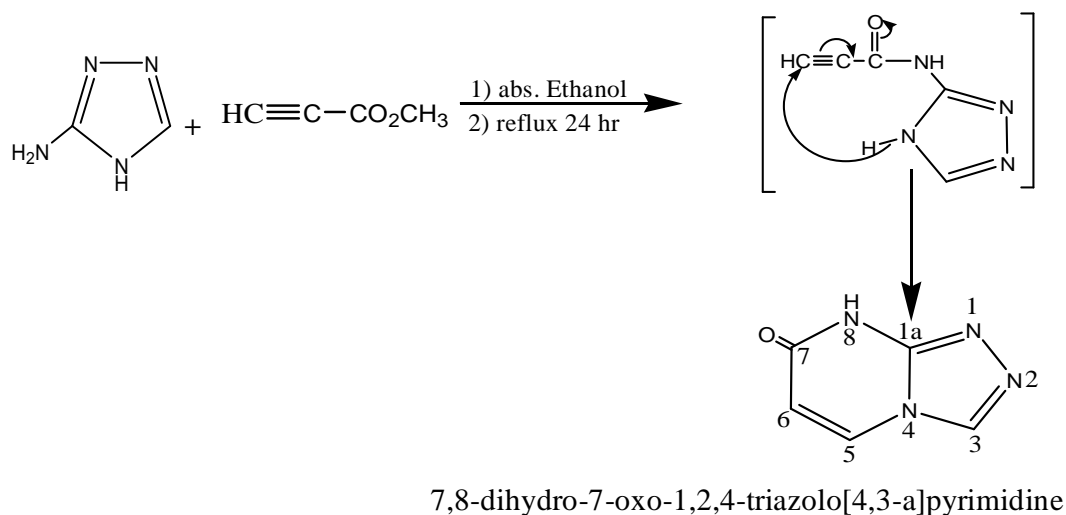
## II.2 Experimental

### II.2.1 Materials

3-amino-1,2,4-triazole, hydroquinone, methyl propiolate and absolute ethanol were purchased from Aldrich and used as received. All preparative manipulations were carried out in open atmosphere.

### II.2.2 Synthesis of 7,8-dihydro-7-oxo-1,2,4-triazolo[4,3-a]pyrimidine

The synthesis was done as described by Reimlinger et al.<sup>(8)</sup> 4.2 g of 3-amino-triazole were dissolved in 40 ml absolute ethanol at 78°C, 0.1 g of hydroquinone (as catalyst) and 5g of methyl propiolate were then added and the resulting solution was refluxed on oil bath with vigorous stirring (colorless crystals were appeared after 30 min) for 24 hr. After cooling down the resulting yellow precipitate was filtered and recrystallized from water. The overall yield 50.8%.



**The mechanism of the reaction is:**

- 1- Nucleophilic attachment of the amino group to the ester group of the methyl propiolate to form the amid intermediate
- 2- Intramolecular conjugate addition of the triazole N4 onto the carbon-carbon triple bond of the side chain

**II.3 Characterization**

**The compound was characterized by:**

1. Elemental analysis
2. Infrared spectroscopy (IR)
3. <sup>1</sup>H-NMR and <sup>13</sup>C-NMR
4. Thermal analysis study (Thermogravimetry (TG) and Differential Scanning Calorimetry (DSC))
5. pKa
6. Crystal study determining by X-ray diffraction)

Also the theoretical study semiempirical study was done to determine molecular orbitals, electron and charge distribution, as well as to predict characteristic bands in the IR, <sup>1</sup>H and <sup>13</sup>C NMR spectra.

### II.3.1 Elemental analysis

Microanalyses of C, H, and N were performed in a Fisons Instruments EA-1008 analyser. Elemental analysis percentage of the  $C_5H_4N_4O \cdot 1/2H_2O$ : Found C, 41.7; H, 3.6; N, 39.0, Calculated: C, 41.38; H, 3.45; N, 38.62.

### II.3.2 Infrared Spectroscopy

From the previous study the infrared spectra of 1,2,4-triazolo[4,3-a]pyrimidines bearing a potential hydroxyl group adjacent rather than OH absorptions. This indicated the predominance of the amide over the imidic acid tautomers of these compounds in the solid state <sup>(5)</sup>. Whereas an amide-carbonyl group attached to the 1,2,4-triazolo[4,3-a]pyrimidin-3-ones was reported to absorb at 1680-1733  $cm^{-1}$  <sup>(130)</sup>, the amide-carbonyl groups attached to the pyrimidine subunit in 1,2,4-triazolo[4,3-a]pyrimidine-5- or 7-ones usually absorb in the region 1640-1755  $cm^{-1}$  <sup>(27)</sup>. Saturation of the pyrimidine ring of 1,2,4-triazolo[4,3-a]pyrimidin-5-ones produces shifts to lower amide absorptions due to lack of conjugation. 1,2,4-triazolo[4,3-a]pyrimidin-5-ones have been differentiated from 1,2,4-triazolo[4,3-a]pyrimidin-7-ones by their amide-carbonyl absorption; the latter absorb at a lower frequency by  $\sim 10-15 cm^{-1}$  than the former <sup>(5)</sup>. Williams proposed that the infrared spectra of 1,2,4-triazolo[4,3-a]pyrimidin-5-ones contain an extra strong absorption band at 1563-1575  $cm^{-1}$  <sup>(131)</sup>.

In our experiment IR spectra were recorded in the 4000-500  $cm^{-1}$  range on a Perkin Elmer 983 spectrophotometer using KBr and polyethylene pellets.

As in (**Fig. 2.1**) the IR spectrum of the free 7,8-dihydro-7-oxo-1,2,4-triazolo[4,3-a]pyrimidine ligand in neutral form displaying an intense band in the region of around 3457  $cm^{-1}$  assignable to  $\nu(OH)$  from water and NH of the ligand, a single band at 1314  $cm^{-1}$  are assignable for the C-O stretching. The presence of the hydrogen bond associated acidic hydrogen atom in the free ligand is reflected in its IR spectrum as a number of bands in the 3100-2300  $cm^{-1}$  regions are assignable for carbon-carbon bonds.

The vibrational activity of the carbonyl group (C=O) appeared at  $1712\text{ cm}^{-1}$  (ca.  $1800\text{ cm}^{-1}$ ), whereas the pyrimidine and triazole ring showed at  $1577$  and  $1507\text{ cm}^{-1}$  (ca.  $2571$  and  $1523\text{ cm}^{-1}$ ) respectively. Other bands appeared at  $755$  and  $520\text{ cm}^{-1}$  assignable to rocking and wagging water modes<sup>(132)</sup>.



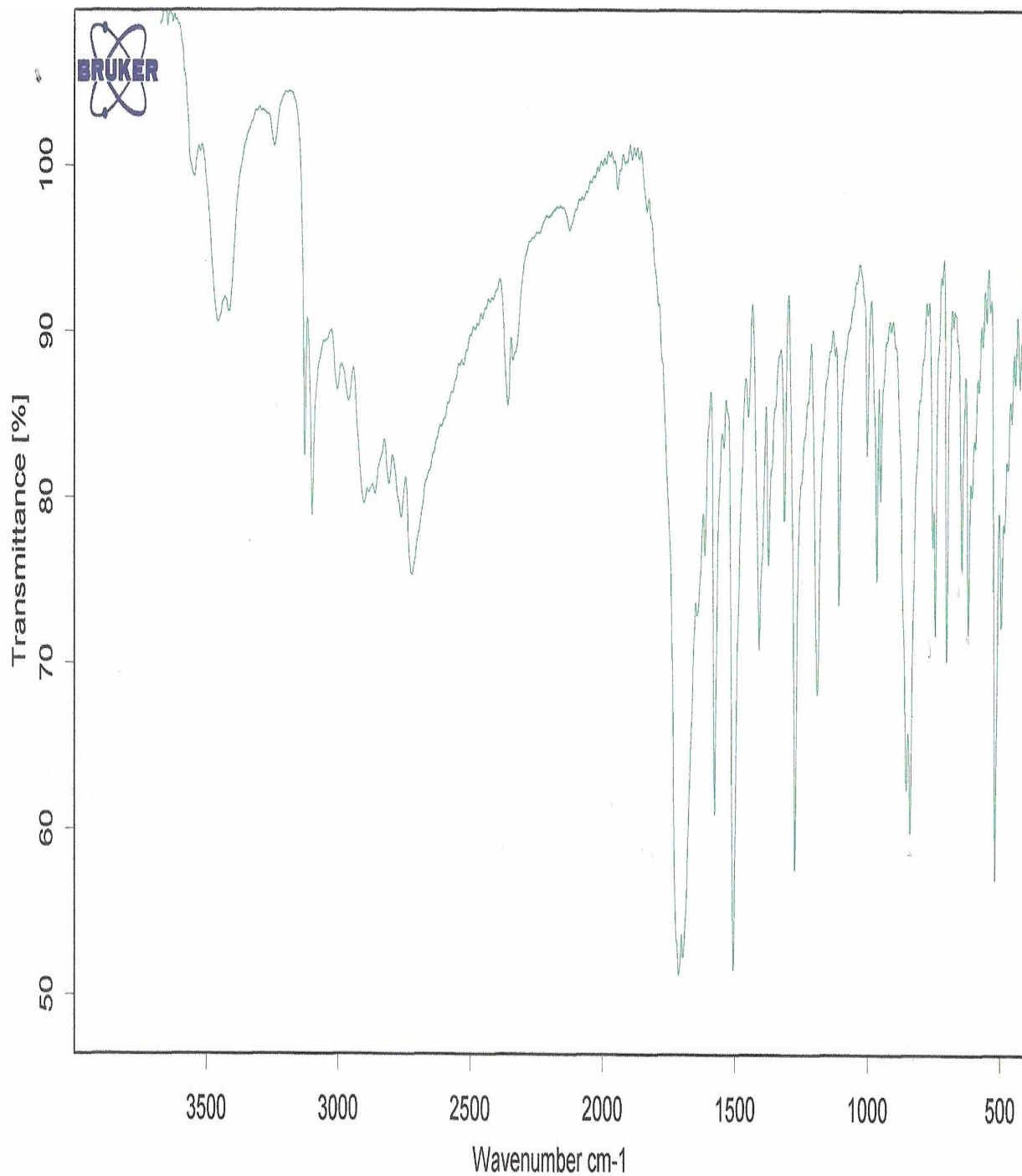


**Fig.2.1** IR Diagram for 7,8-dihydro-7-oxo-1,2,4-triazolo[4,3-a]pyrimidine  
ligand

### II.3.3 Nuclear Magnetic Resonance spectroscopy

From the previous study as a rule, the order of chemical shift of the methine protons of 1,2,4-triazolo[4,3-a]pyrimidine was found to be  $\delta$  (ppm)  $H3 > H5 > H7 > H6$ <sup>(132)</sup>.

In harmony with this order is also the order of chemical shifts of the methane protons of 3-<sup>(133)</sup>, 5-<sup>(133)</sup>, 6-<sup>(134)</sup>, and 7<sup>(133)</sup>-substituted-1,2,4-triazolo[4,3-a]pyrimidines

3-Substituted 1,2,4-triazolo[4,3-a]pyrimidines  $\delta$   $H5 > H7 > H6$

5-Substituted 1,2,4-triazolo[4,3-a]pyrimidines  $\delta$   $H3 > H7 > H6$

6-Substituted 1,2,4-triazolo[4,3-a]pyrimidines  $\delta$   $H3 > H5 > H7$

7-Substituted 1,2,4-triazolo[4,3-a]pyrimidines  $\delta$   $H3 > H5 > H6$

The <sup>1</sup>H and <sup>13</sup>C NMR spectra of the 7,8-dihydro-7-oxo-1,2,4-triazolo[4,3-a]pyrimidine ligand were recorded on a Bruker AM300 equipment using DMSO-d<sub>6</sub> as solvent.

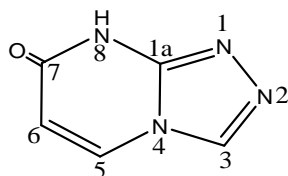
Theoretically the calculation of <sup>1</sup>H NMR spectra were recorded by using chem. draw ultra 7 program<sup>(135)</sup> (**Fig. 2.2**) in this figure the spectra show four sets of signals at  $\delta$  8, 8.3, 6.5, and 5.7 associated to H8, H3, H6 and H5 respectively.

The spectrum of <sup>1</sup>H-NMR (**Fig. 2.3**) display the expected 4 sets of signals, integrated for 4 protons, one singlet at  $\delta$ 8.65 associated to H3, and the two pyrimidine protons H6 and H5 split one another into two doublets signals one centered at  $\delta$ 6.15 other at  $\delta$ 8.35 ppm with a coupling constant equal 7.7 Hz . The most downfield broadening singlet is that at  $\delta$  12.7 for acidic N8 proton.

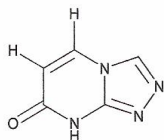
The order of chemical shifts for the carbons of 1,2,4-triazolo[4,3-a]pyrimidines was found to vary according to the type and positions of substituents attached to their skeleton.

From the theoretical study <sup>13</sup>C-NMR spectra which recorded by using chem. Draw ultra 7 (**Fig. 2.4**) show four set of signal at 108, 135, 148, 148, 164 ppm associated for four different carbon atom C6, C5, C3, C8a and C7 respectively.

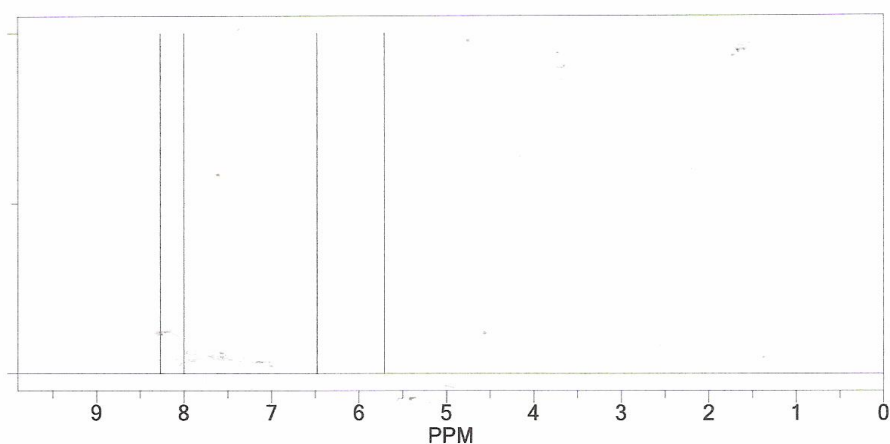
$^{13}\text{C}$ -NMR spectrum of the 7,8-dihydro-7-oxo-1,2,4-triazolo[4,3-a]pyrimidine ligand (**Fig. 2.5**), displayed five signals corresponding to different carbon atom. The pyrimidine ring carbons C5 is found at 136.9 ppm whereas the other carbon C6 found upfield at 109.7 ppm because it is attached to carbonyl group, while the triazole ring carbon C3 is found at 134.1 ppm. The bridgehead carbon C8a shown at more downfield position (148.8 ppm) due to deshielding by the nearby pyrimidine ring. The most downfield signal is that at  $\delta$  161.4 ppm is assigned to the carbonyl group carbon. Assignments are straightforward with the aid of the DEPT spectrum, the signals associated to H6, H5, and H3 integrates clearly for just one proton and that assigned to C6, C5, and C3 appears positive at the DEPT spectrum (as expected for CH).



ChemNMR H-1 Estimation



Estimation Quality: blue = good, magenta = medium, red = rough



Protocol of the H-1 NMR Prediction:

Node	Shift	Base + Inc.	Comment (ppm rel. to TMS)
NH	8.0	8.00	sec. amide
CH	8.3	8.27	1,2,4-triazole
	?		1 unknown substituent(s) from 1-pyrrole
	?		1 unknown substituent(s) from 2-pyrrole
			-> 2 increment(s) not found
H	6.5	5.25	1-ethylene
		1.23	1 -C(=O)N gem
		?	1 unknown substituent(s)
			-> 1 increment(s) not found
H	5.7	5.25	1-ethylene
		0.46	1 -C(=O)N trans
		?	1 unknown substituent(s)
			-> 1 increment(s) not found

**Fig.2.2:** Theoretical Chem 3D  $^1\text{H}$ -NMR for 7,8-dihydro-7-oxo-1,2,4-triazolo[4,3-a] pyrimidine ligand

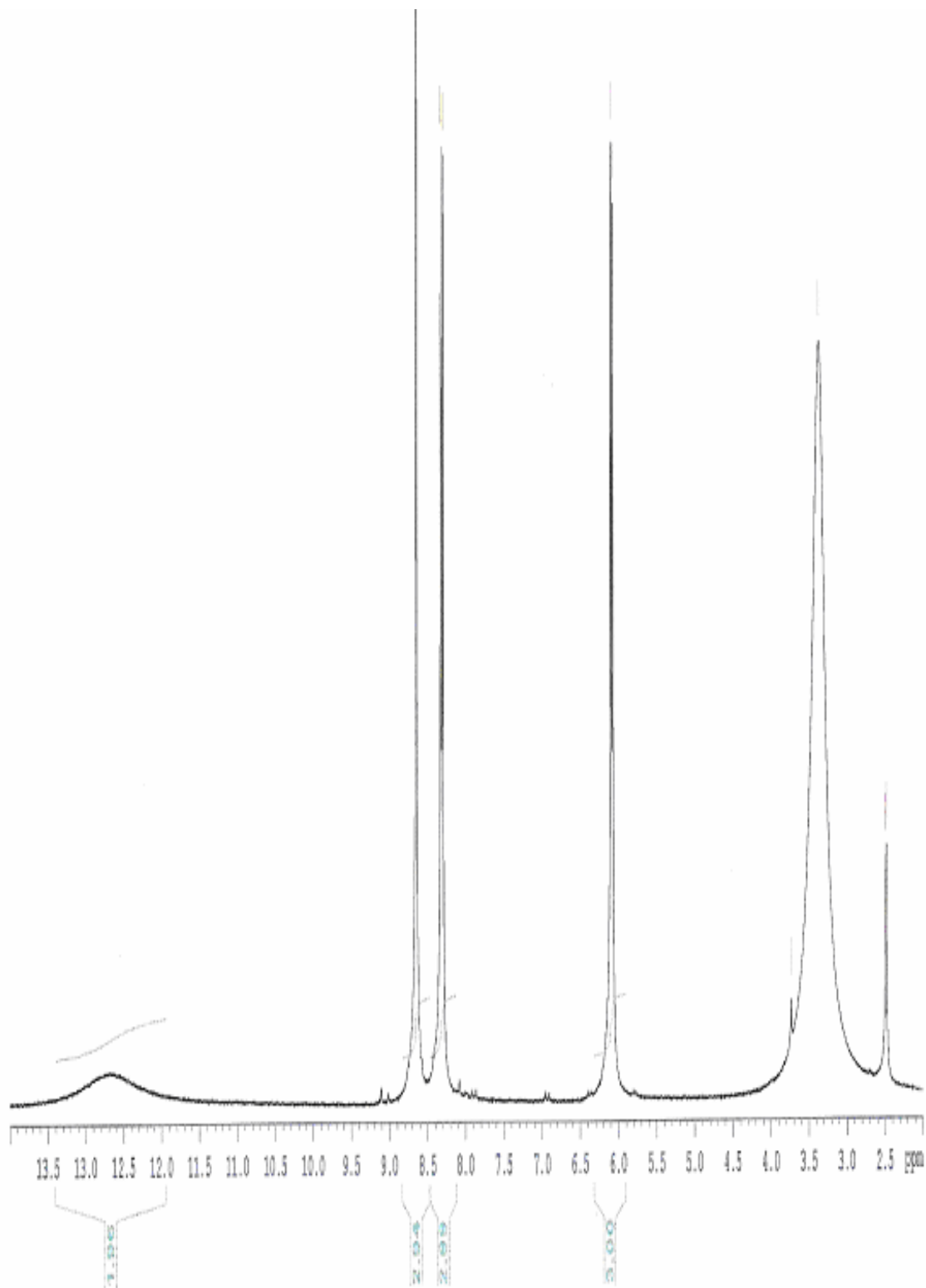
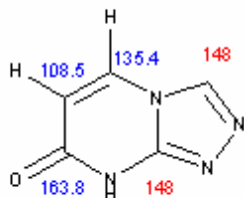
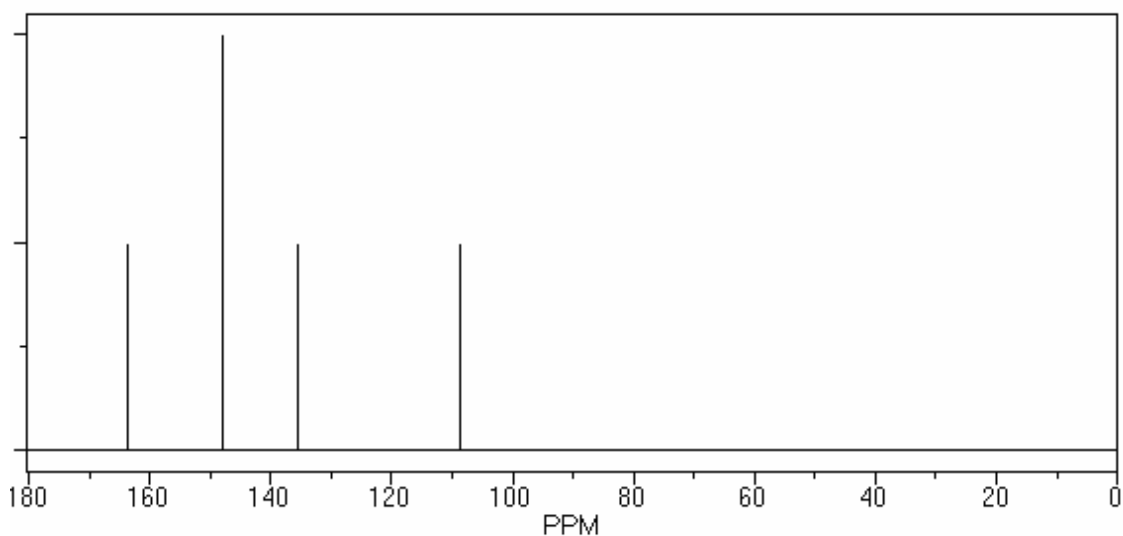


**Fig.2.3:**  $^1\text{H-NMR}$  for 7,8-dihydro-7-oxo-1,2,4-triazolo[4,3-a]pyrimidine ligand

ChemNMR C-13 Estimation



Estimation Quality: blue = good, magenta = medium, red = rough



Protocol of the C-13 NMR Prediction:

Node Shift Base + Inc. Comment (ppm rel. to TMS)

C	148	147.9	1,2,4-triazole
C	163.8	165.0	1-amide
		3.3	1-C=C
		-4.5	1-C <sup>α</sup> R from N-amide
CH	108.5	123.3	1-ethylene
		7.5	1-C(=O)N
		-22.3	1-1:N-R <sup>α</sup> R <sup>β</sup> R <sup>γ</sup> R-1
CH	135.4	123.3	1-ethylene
		5.8	1-C(=O)N
		6.3	1-1:N-R <sup>α</sup> R <sup>β</sup> R <sup>γ</sup> R-1
CH	148	147.9	1,2,4-triazole

**Fig.2.4:** Theoretical Chem3D 13C-NMR diagram for 7,8-dihydro-7-oxo-1,2,4-triazolo[4,3-a]pyrimidine ligand

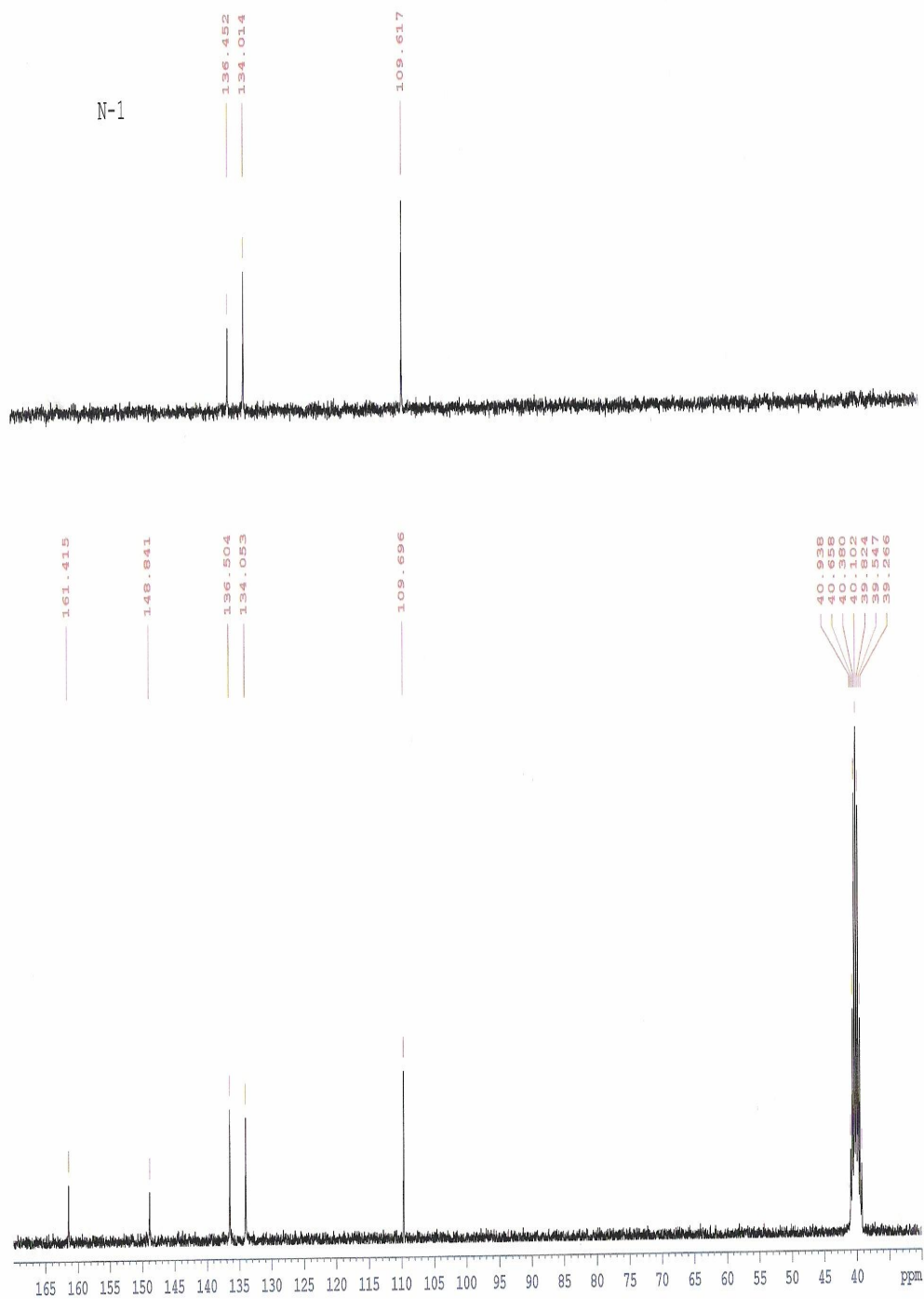


**Fig.2.5:**  $^{13}\text{C}$ -NMR diagram for 7,8-dihydro-7-oxo-1,2,4-triazolo[4,3-a]pyrimidine ligand.

### II.3.4 Potentiometer titration

For the determination of the  $K_a$  value of the compound,  $1 \times 10^{-3}$  mol (0.145 g) of it were dissolved in the stoichiometric amount of 0.25 M NaOH, distilled water was added to get 10 ml to of 0.1 M solution of the sodium salt. This was titrated at 25 °C with 0.1 M HCl. The acidity constant of the compound have been determined by titrating the volume of HCl and calculated the  $pK_a$  by best square fit method values 5.6 ( $K_a = 2.5 \times 10^{-6}$ ) this value being appreciably lower than those found for analogous pyrazolo[4,3-d]pyrimidine<sup>(136)</sup>, for example, the  $pK_a$  value for allopurinol is 8.9. This enhanced acidity of triazolopyrimidine if compared with pyrazolo[4,3-d]pyrimidine can be attributed to better delocalization of the negative charge in their conjugated anion.

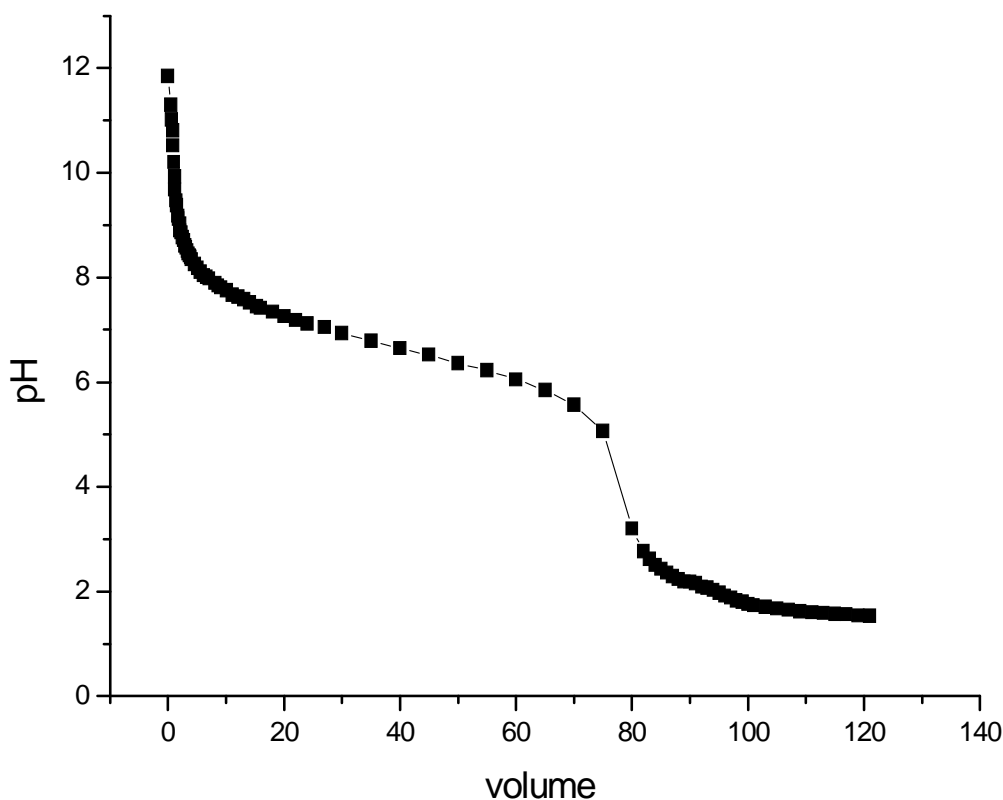


**Fig.2.6.** Potentiometric titration curve for 7,8-dihydro-7-oxo-1,2,4-triazolo[4,3-a]pyrimidine ligand



### II.3.5 Thermal Analysis

The thermal behavior of the ligand has been studied from the TG and DSC curves (Fig. 2.7 and 2.8), which show that the dehydration process take place in three steps in the 42-700 °C temperature range, in the first step ½ mole H<sub>2</sub>O were lost (experimental weight loss 5.61% and theoretical weight 6.21%, loss), this process appears in the DSC diagram as a sharp endothermic peak centered at 64.48 °C, with an associated enthalpy change of 5.034 kJ/mol of water. Avery weight loss effect appearing in the range 320-710 °C.

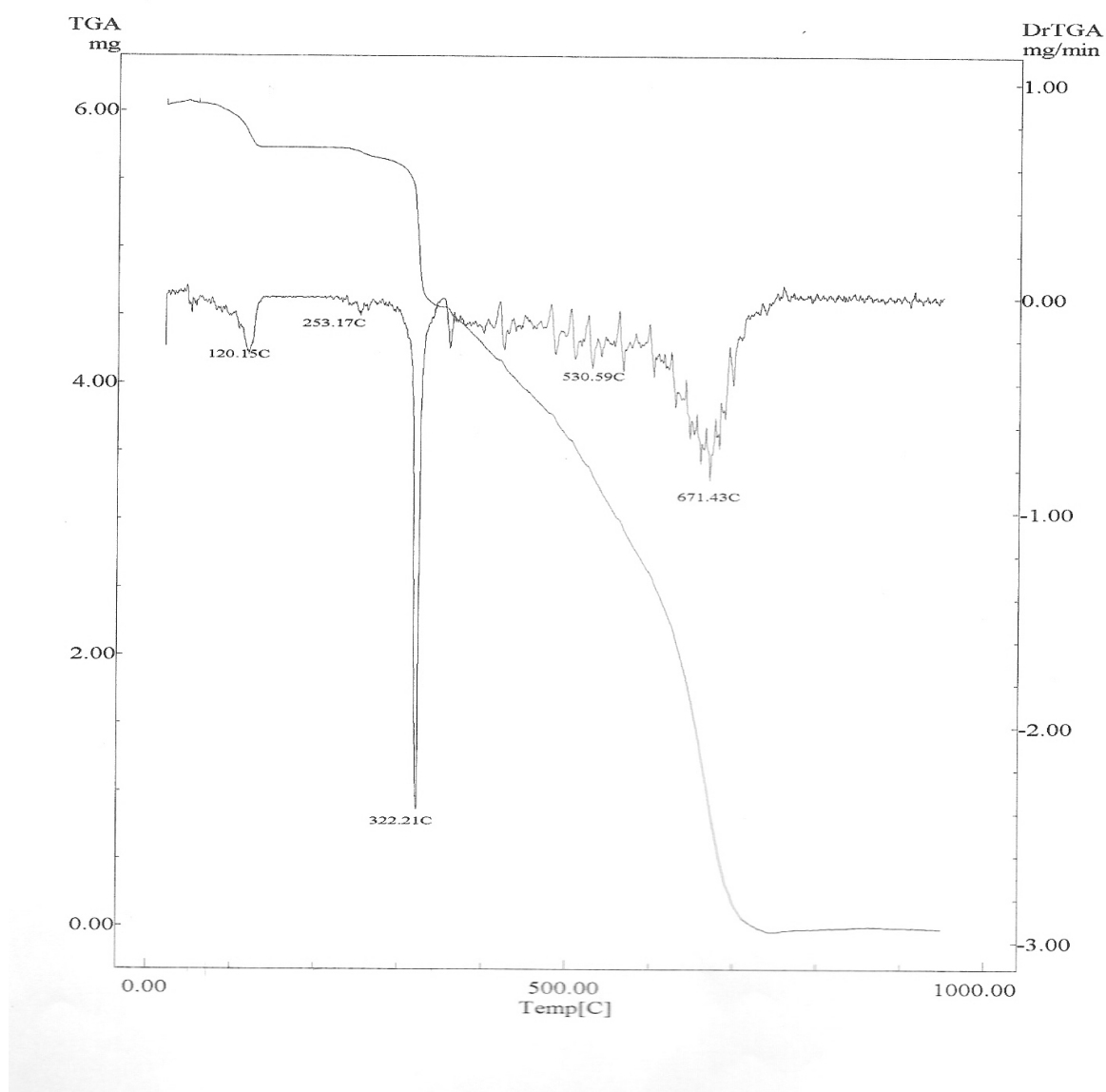


**Fig.2.7.** TG diagrams for 7,8-dihydro-7-oxo-1,2,4-triazolo[4,3-a]pyrimidine ligand

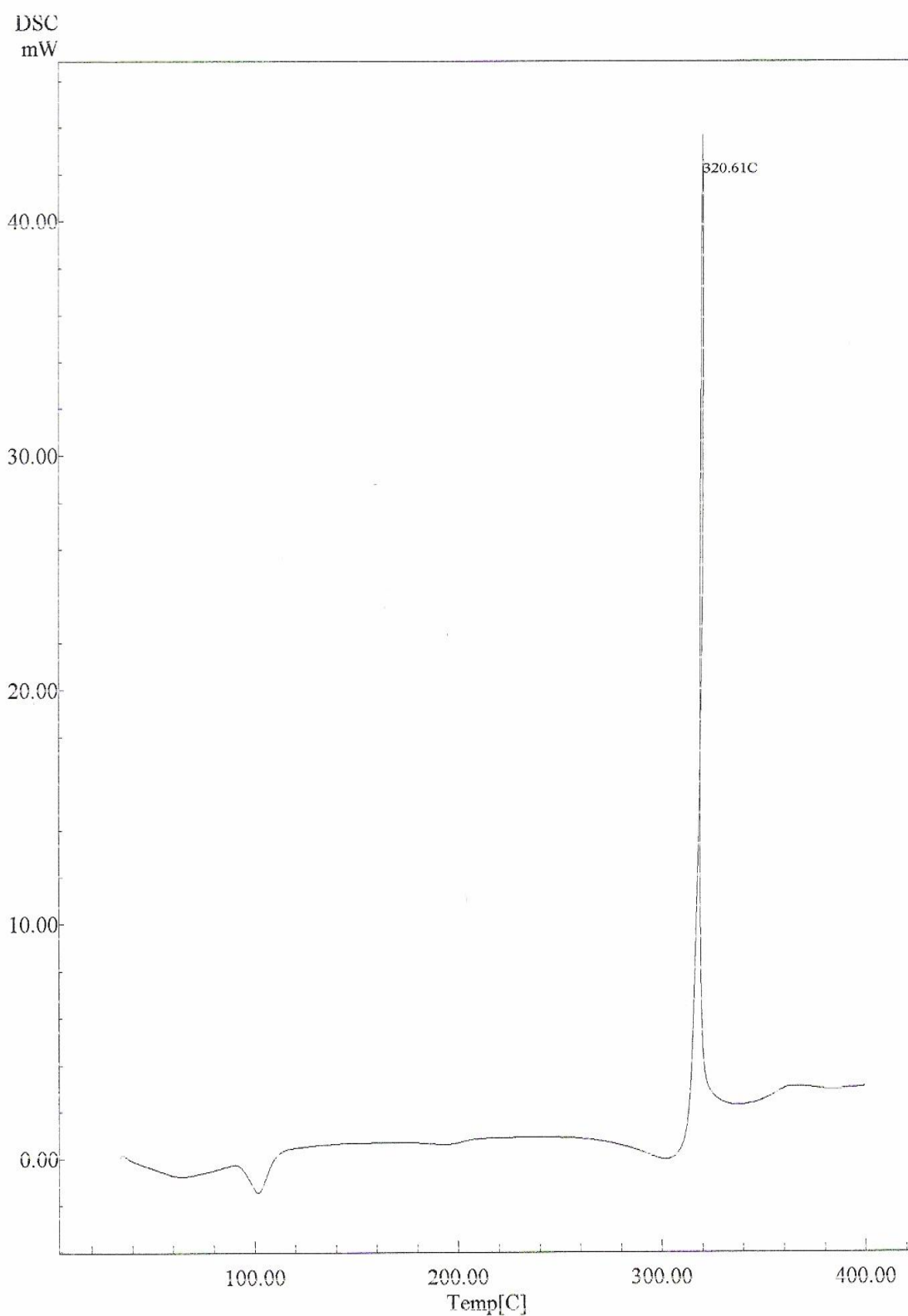


**Fig.2.8:** DSC diagrams for 7,8-dihydro-7-oxo-1,2,4-triazolo[4,3-a]pyrimidine ligand

### II.3.6 X-Ray

The 7,8-dihydro-7-oxo-1,2,4-triazolo[4,3-a]pyrimidine ligand was not isolated in crystal form. In metal complexes of nickel and silver which were isolated in the crystal form and the structure was dissolved by diffraction method, the structure was obtained, complete description of the expected structure, will be shown in chapter 3.

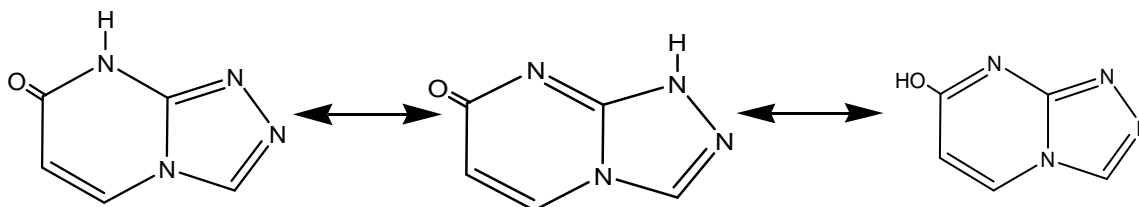
### II.3.7 Molecular Orbital Calculation

The general approach in theoretical study is as follows: we first construct the molecule by using HyperChem, an interactive molecular graphics program for building and manipulating Molecular mechanical calculations. These are applied in order to improve the molecular geometry (optimization), quantum mechanical calculations are then employed for the improved structures in order to study their electronic properties and to verify the preferences of low energy conformers.

Also a theoretical study "semiempirical" study was done to determine molecular orbitals (MO), electron distribution, charge distribution as well as to predict characteristic bands in the IR, NMR ( $^1\text{H}$  and  $^{13}\text{C}$ ), and UV spectra. Semiempirical molecular orbital calculation types RHF/AM1 have been performed for different tautomeric forms of 7,8-dihydro-7-oxo-1,2,4-triazolo[4,3-a]pyrimidine and their conjugated anions. Full geometry optimization was performed with the MO calculation. Net charges on the atoms were calculated according to fits to the molecular electrostatic potential as implemented in the Hyperchem 5.1 program <sup>(137)</sup>, and Chem Draw Ultra 7 <sup>(135)</sup>, in order to make proper assignments of the IR bands, both AM1 and PM3 Semiempirical methods, were used to calculate the corresponding theoretical vibrational spectrum of the free ligand

7,8-dihydro-7-oxo-1,2,4-triazolo[4,3-a]pyrimidine have in their molecules an acidic proton there exists the possibility that hydrogen migrates to the basic position of the molecules, either to nitrogen atom or to an oxygen atom, leading to three different tautomeric forms namely N1-H, N8-H, and O-H (**Scheme 48**). Calculations have been

performed for all these forms as indicated in the experimental section, leading to the values for their heat of formation that have been indicated in (Table 2.1).



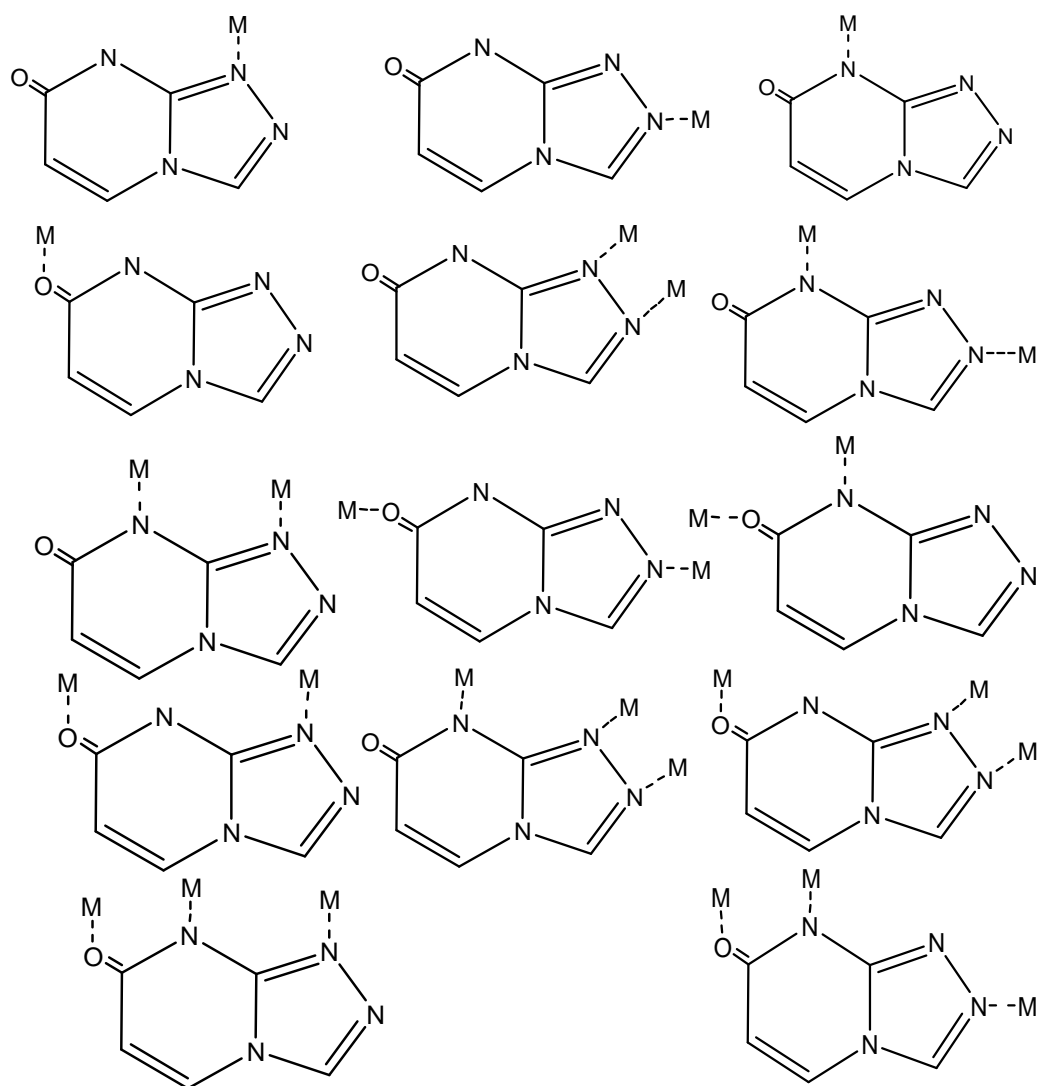
**Scheme 48**

**Table 2.1:** Theoretical heat of formation energy.

	<b>N1-H</b>	<b>N8-H</b>	<b>O-H</b>	<b>Anion</b>
<b>Energy</b>	378.91 Kj/mol	306.13 KJ/mol	334.81 KJ/mol	164.10 KJ/mol

According to these results the most stable tautomeric forms is the N8-H nevertheless the  $\Delta H_f$  value for N1-H tautomer of 7,8-dihydro-7-oxo-1,2,4-triazolo[4,3-a]pyrimidine is quite close to that of N8-H tautomer, so we may expect that this could play role in the chemistry of 7,8-dihydro-7-oxo-1,2,4-triazolo[4,3-a]pyrimidine.

Theoretically 7,8-dihydro-7-oxo-1,2,4-triazolo[4,3-a]pyrimidine is a ligand which has different possible binding site through N1, N2, N8 and O7. Metal coordination may show mono dentate actuation, bidentate bridging mode in homo and heteronuclear complex. The scheme below (**Scheme 49**) represents the sequence of the different possible site of coordination in the anionic and neutral form of the ligand.



**Scheme 49**

(Fig. 2.9) displays the calculated net charges on the atoms of the 7,8-dihydro-7-oxo-1,2,4-triazolo[4,3-a]pyrimidine ligand, theoretically most stable tautomers of the isomer in their neutral and anion forms. According to these data, the negative charge density for neutral form follows the sequence  $O7 > N8 > N4 > N1$ , while for anionic forms it follows  $O7 > N8 > N1 > N4$  sequence. From this result, it would have been expected for the metal binding to follow a similar trend. However, metal binding to oxygen, O7, is less common, as known soft and intermediate metal prefer nitrogen or oxygen as coordination site.

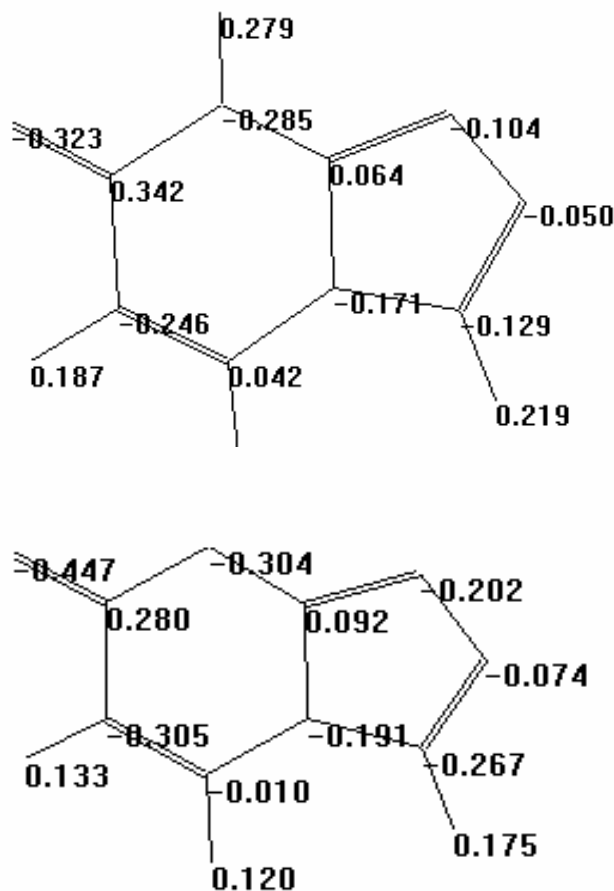


**Fig. 2.9:** Calculated charges of electrostatic potential for 7,8-dihydro-7-oxo-1,2,4-triazolo[4,3-a]pyrimidine ligand in neutral (top) and anion (bottom) forms

The total charge density is the electron density in the space surrounding the nuclei of a molecule, or the probability of finding electrons in the space around a molecule, which is the best visible representation of a molecule's shape, as determined by its electronic distribution. The Total charge density surface is calculated from scratch for each molecule.

Electron densities show the locations of electrons. Large values of the density will first reveal atomic positions and then chemical bonds, while smaller values will indicate overall molecular size. Map Property maps a color-coded visualization of a selected property onto the charge density surface. The available properties are Molecular Orbital, Spin Density, Electrostatic Potential, and Partial charges. The color scale uses red for the

highest magnitude and green for the lowest magnitude of the property. Neutral is white (**Fig.2.10 and 2.11**).

The electrostatic potential describes the interaction energy of the molecular system with a positive point charge. Electrostatic potential is useful for finding sites of reaction in a molecule: positively charged species tend to attack where the electrostatic potential is strongly negative (electrophilic attack).

Atomic charges indicate where large negative values (sites for electrophilic attack) are likely to occur. However, the largest negative value of the electrostatic potential is not necessarily adjacent to the atom with the largest negative charge. So in our ligand, the largest negative atomic charge occurs on the nitrogen, but the most negative values of the electrostatic potential occur at the oxygen lone pair sites. Protonation most favorably occurs at these sites. This illustrates the value of electrostatic potential compared to simple atomic charges in predicting reactivity.

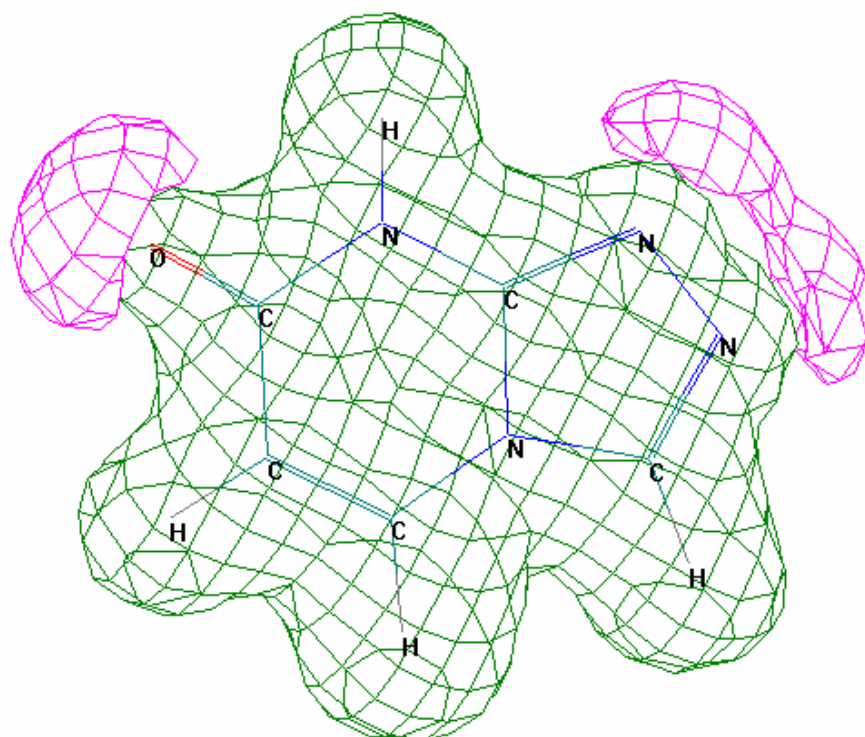


**Fig. 2.10:** Electrostatic potential diagram of 7,8-dihydro-7-oxo-1,2,4-triazolo[4,3-a] pyrimidine ligand in the neutral form using HyperChem Pro 5.1.

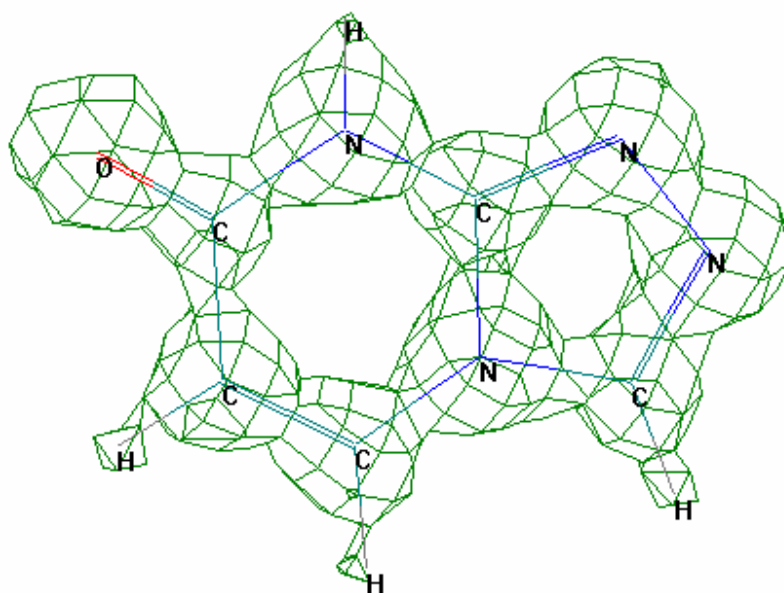


**Fig. 2.11:** Total charge density diagram for 7,8-dihydro-7-oxo-1,2,4-triazolo[4,3-a] pyrimidine ligand in the neutral form using HyperChem Pro 5.1.



Charge densities don't enough to predict the behavior of this compound as a ligand, so we must consider the molecular orbitals more likely to form bonds with atomic orbitals of metal ions. Molecular orbitals, solutions of the approximate quantum mechanical equations of electron motion, are made up of sums and differences of atomic solutions (atomic orbitals), just like molecules are made up of combinations of atoms. Molecular orbitals for very simple molecules may often be interpreted in terms of familiar chemical bonds; unoccupied molecular orbital may also provide useful information.

The MO's more likely to combine with metal atomic orbitals are those occupied with high energy and  $\sigma$  symmetry and we can see in table 2.2 the contribution of atomic orbitals of N and O atoms to the highest occupied molecular orbitals (including also the LUMO) in neutral and anionic forms are indicated that the N1, N2 and O in neutral form have main contributions to the metal, by mono or bidentate coordination. As we see in the table C atom also has high molecular orbital contributions, which give a possibility to form carbon-carbon, or organometallic compound especially with soft and intermediate metals under certain conditions.

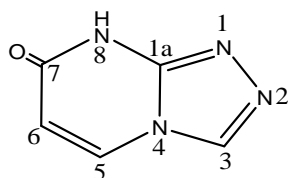


**Table 1:** Atomic orbital contributions to the highest energy occupied MO<sup>a</sup> and LUMO, from AM1 calculation for 7HtpO ligand

Orbital	N1	N2	C3	N4	C5	C6	C7	N8	C1A	O7	<sup>b</sup> sym
<b>Neutral form</b>											
$\Psi_{20}$	0.4046	0.4262	0.0069	0.0741	0.0365	0.0097	0.0033	0.0004	0.0037	0.0059	Π
$\Psi_{21}$	0.0161	<b>0.1871</b>	0.2475	0.0065	0.0014	0.0003	0.0202	0.278	0.1033	<b>0.2278</b>	σ
$\Psi_{22}$	0.2085	0.2475	0.1056	0.0303	0.0011	0.0314	0.0098	0.0259	0.0982	0.2287	Π
$\Psi_{23}$	0.1024	0.0836	0.0361	0.0194	0.0179	0.0746	0.0128	0.0784	0.0547	0.4934	Π
$\Psi_{24}$	0.1094	0.038	0.039	<b>0.2079</b>	<b>0.1622</b>	<b>0.3733</b>	0	0.0013	0.0009	0.0679	σ
$\Psi_{25}$ (HO MO)	<b>0.1886</b>	0.0919	<b>0.2449</b>	0.0186	0.0004	0.0106	0.0052	<b>0.2116</b>	0.1567	0.0714	σ
$\Psi_{26}$ (LU MO)	0.0049	0.0536	0.0792	0.0001	<b>0.3579</b>	<b>0.2738</b>	0.0458	0.0606	0.0872	0.0369	σ
<b>Ionic form</b>											
$\Psi_{20}$	0.0499	0.0107	0.0123	0.0672	0.009	0.0045	0.0293	0.2866	0.0656	0.562	σ
$\Psi_{21}$	<b>0.3599</b>	<b>0.2181</b>	0.1208	0	0.0007	0.0107	0.0024	0.083	0.1672	0.0107	σ
$\Psi_{22}$	0.0074	0.1255	0.1484	0	0.0073	0	0	0	0	0	Π
$\Psi_{23}$	0.1206	0.0356	0.0631	0.1895	0.1618	0.3507	0.0004	0.0025	0.0023	0.0737	Π
$\Psi_{24}$	0.0199	0.0052	0.0078	0.0429	0.0117	<b>0.1411</b>	0.0421	<b>0.3168</b>	0.0125	<b>0.365</b>	σ
$\Psi_{25}$ (HO MO)	0.2232	0.0327	0.2252	0.0482	0.0064	0.0331	0.0172	0.2572	0.0266	0.1302	Π
$\Psi_{26}$ (LU MO)	0.0086	0.0861	0.0503	0.009	0.3676	0.3204	0.0103	0.092	0.0459	0.0097	Π

<sup>a</sup>Calculation as the quadratic sum of the coefficients of the atomic orbitals 2s, 2px, 2py, 2pz of the atom in the linear combination which defines the MO.

<sup>b</sup>σ = Molecular plane is asymmetry plane for the MO. Π = Molecular plane is a nodal plane for MO

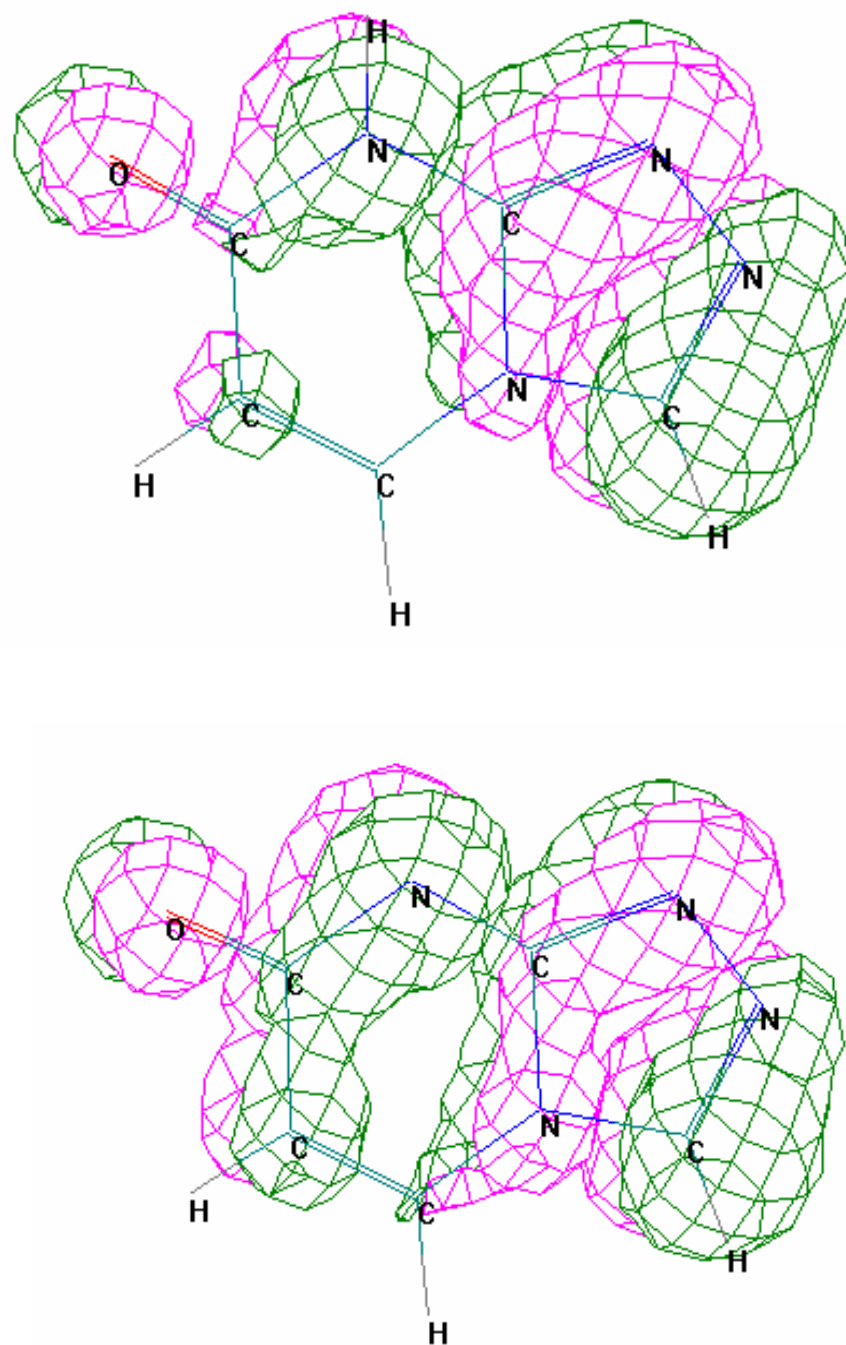


**Fig.2.12** High molecular orbital (HOMO) (green) and low molecular orbital (LUMO) (violet) in neutral (top) and anion (bottom) forms for 7,8-dihydro-7-oxo-1,2,4-triazolo[4,3-a]pyrimidine ligand in the neutral form using HyperChem Pro 5.1.

## *CHAPTER THREE*

# **The Coordination Chemistry of 7,8 dihydro-7-oxo-1,2,4-triazolo[4,3-a] pyrimidine ligand with Cu, Ni, and Ag metal**

## III.1 Introduction

The studies about the coordination chemistry of triazolopyrimidine derivatives have been focused till now in the 1,5-a series, which are examples of purine mimics. This type of compound has been used to elucidate the role of metal ions with nucleic acids biochemistry. On the other hand, we have not found in the bibliography any reference for coordination compound of any of the other arrangements (1,5-c, 4,3-a, or 4,3-c). This study is regarded as the first exploration in the coordination chemistry of 1,2,4-triazolo[4,3-a]pyrimidines. These compounds present, comparing with the corresponding 1,5-a isomers, the change in the position of one of the nitrogen atoms in the triazole ring which is now placed as separated as possible from the pyrimidine ring, with less steric hindrance and contiguous to the other external imidazole nitrogen. They are analogous and may be regarded as mimics of pyrazolo[4,3-d]pyrimidines, a family of biologically relevant compounds related to purines, the most outstanding of which is allopurinol. In the continuing studies on metal complexes of pyrimidines derivatives, we have tried to synthesis and characterize of some transition metal complexes of the less stable 7,8-dihydro-7-oxo-1,2,4-triazolo[4,3-a]pyrimidine isomer, including the crystal structure of some metal complexes.

## III.2 Experimental

### III.2.1 Material

7,8-dihydro-7-oxo-1,2,4-triazolo[4,3-a]pyrimidine ligand (L) was synthesised as described in chapter 2 according to the procedure described by Reimlinger et al. <sup>(1)</sup>, metal salts (CuCl<sub>2</sub>, NiCl<sub>2</sub>, Ni(NO<sub>3</sub>)<sub>2</sub>, AgNO<sub>3</sub>) and NH<sub>4</sub>OH and HNO<sub>3</sub> solvents were purchased from Aldrich Chemie. And used as received.

### III.2.2 Instrumentation

Microanalyses of C, H, and N were performed in a Fisons Instruments EA-1008 analyzer. <sup>1</sup>H and <sup>13</sup>C NMR spectra were recorded on a Bruker AM300 equipment using dmsO-d<sub>6</sub> as

solvent. IR spectra were recorded in the 4000-500 $\text{cm}^{-1}$  range on a Perkin Elmer 983, Shimadzu DSC-50, and Nicolet spectrophotometers, using KBr pellets. TG and DSC diagrams were studied under air flow in Shimadzu TGA-50 and Shimadzu DSC-50 equipment coupled with an IR instrument. All these equipments are sited at the Center of Scientific Instrumentation of the University of Granada in Spain.

### III.2.3 Crystallography

Data for single crystal of the nickel complex (dimensions, 0.28 x 0.15 x 0.06 mm) and silver complex ( dimensions, 0.49 x 0.19 x 0.18 mm) were collected at room temperature in a Bruker SMART APEX CCD system with MoK $\alpha$  radiation ( $\lambda = 0.7107 \text{ \AA}$ ). Data were corrected for absorption (multi-scan, transmission range, 0.6667-0.8775 (Ni), and 0.4965-0.6930 (Ag)). Structure solved by the heavy atom method and anisotropically refined in  $F^2$  using SHELXL-97<sup>2</sup>. Atom with partial occupancy has been refined isotropically and remaining non-H atoms anisotropically. Hydrogen atoms of the heterocycle were placed in ideal positions and those of the water molecule were refined with fixed O-H distance. Isotropic thermal parameters of all H atoms fixed to 1.2 times the equivalent isotropic thermal parameter of their parent atoms.

## III.3 Results and Discussion

### III.3.1 Copper(II) complexes

#### III.3.1.1 $\text{CuL}_2\text{Cl}_2(\text{H}_2\text{O})_3$ complex

##### III.3.1.1.1 Synthesis

The copper  $\text{CuL}_2\text{Cl}_2(\text{H}_2\text{O})_3$  complex was prepared by adding a clear solution of 7,8-dihydro-7-oxo-1,2,4-triazolo[4,3-a]pyrimidine (2mmol) in 30ml water, to a solution of  $\text{CuCl}_2$  (1mmol) in a minimum amount of water at room temperature. A Blue precipitates of the complex were appeared after two days. The solid was filtered off and air dried.

### III.3.1.1.2 Elemental analysis

Elemental analysis % of  $\text{CuL}_2\text{Cl}_2\cdot(\text{H}_2\text{O})_3$ : Found: C, 26.89; H, 3.82; N, 24.47 %.  
Calculated: C, 26.07; H, 3.00; N, 24.32 %.

### III.3.1.1.3 Infrared Spectroscopy

Absorption bands in the IR spectra of  $\text{CuL}_2\text{Cl}_2\cdot(\text{H}_2\text{O})_3$  complex **Fig. 3.1** show small variation with respect to the spectrum of free ligand. The spectra of the complex show very broad band centered at  $3392\text{ cm}^{-1}$  characteristic of  $\nu(\text{OH})$  from  $\text{H}_2\text{O}$  absorption, and a single band at  $1642\text{ cm}^{-1}$  associated to the vibrational activity of carbonyl group, both bands are shifted to lower wavenumber with respect to their position in the IR spectra of the free ligand, this shift is due to coordination both of the ligand and the water molecule.

The characteristic bands of pyrimidine ring skeletal vibration appeared at  $1529\text{ cm}^{-1}$ , whereas of imidazole ring skeletal vibrations at  $1477\text{ cm}^{-1}$ , (the spectra of free ligand the former band was found at  $1577$  and  $1507\text{ cm}^{-1}$  respectively), so the two bands are shifted to the lower wavenumber. This shift is due to the new electric and charge distribution over the ligand due to coordination of the triazole and pyrimidine ring

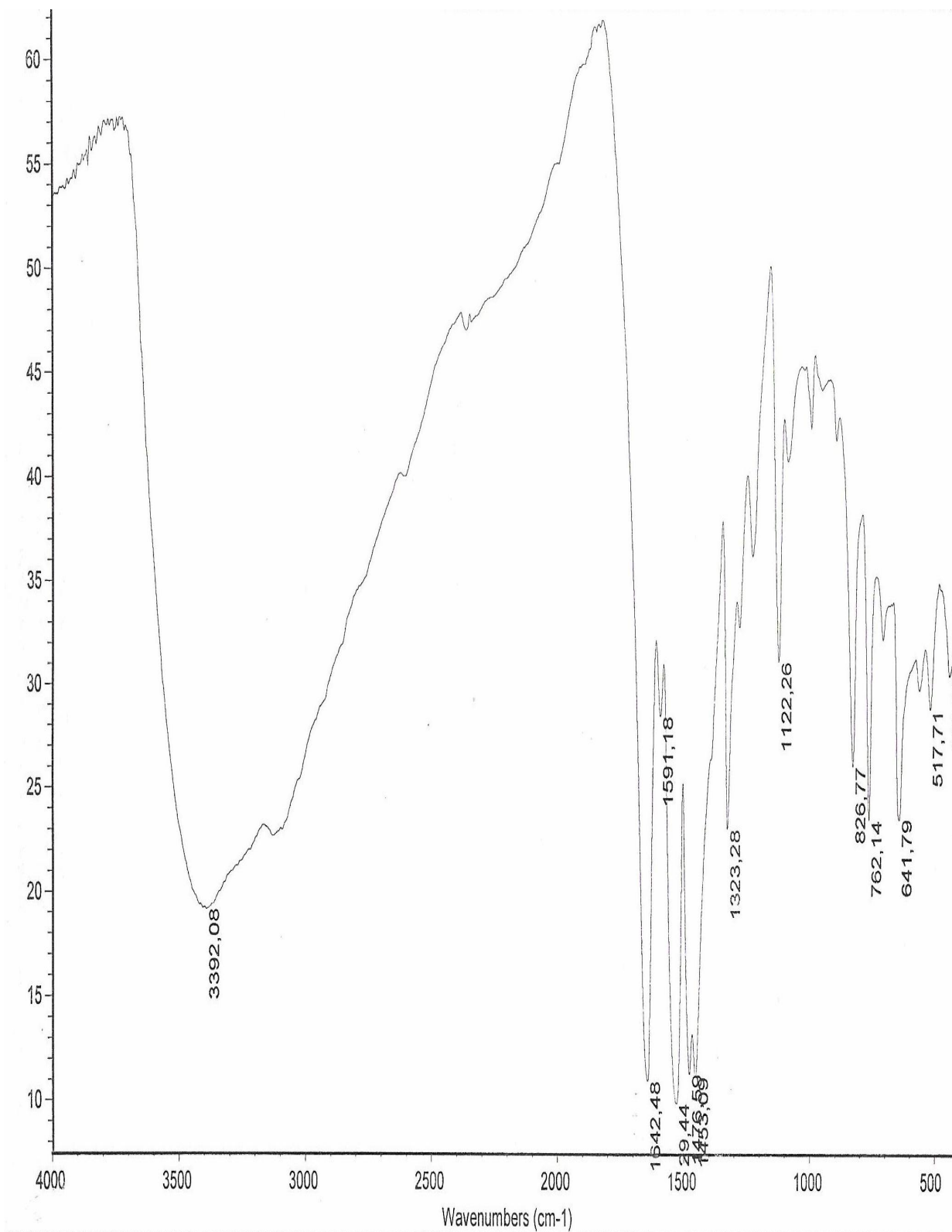


**Fig 3.1** Infrared spectrum of  $\text{CuL}_2\text{Cl}_2 \cdot (\text{H}_2\text{O})_3$  complex



#### III.3.1.1.4 Thermal analysis

Dehydration the  $\text{CuL}_2\text{Cl}_2(\text{H}_2\text{O})_3$  complex has been studied from their TG and DSC curves **Fig. 3.2** and **3.3**. Which show that the dehydration process occurs in several overlapping steps in the 62-600°C temperature range, The first step of the dehydration process appear between 62-650°C temperature range, suggesting that the three water molecules were lost in the first step (experimental weight loss percentage 13.7%, and calculated weight loss percentage 11.7 %) with an associated dehydration enthalpy of 13 kJ/mol. This process appears in the DSC curves as a broad endothermic effect, the three remaining steps are centered at 94, 171, 390 and 503 °C. From the TG diagram the pyrolytic decomposition is completed around 660 °C, leaving  $\text{CuCO}_3$  as final product (experimental percentage value of the residue 27.08% is in good agreement with the theoretical value 26.8%).

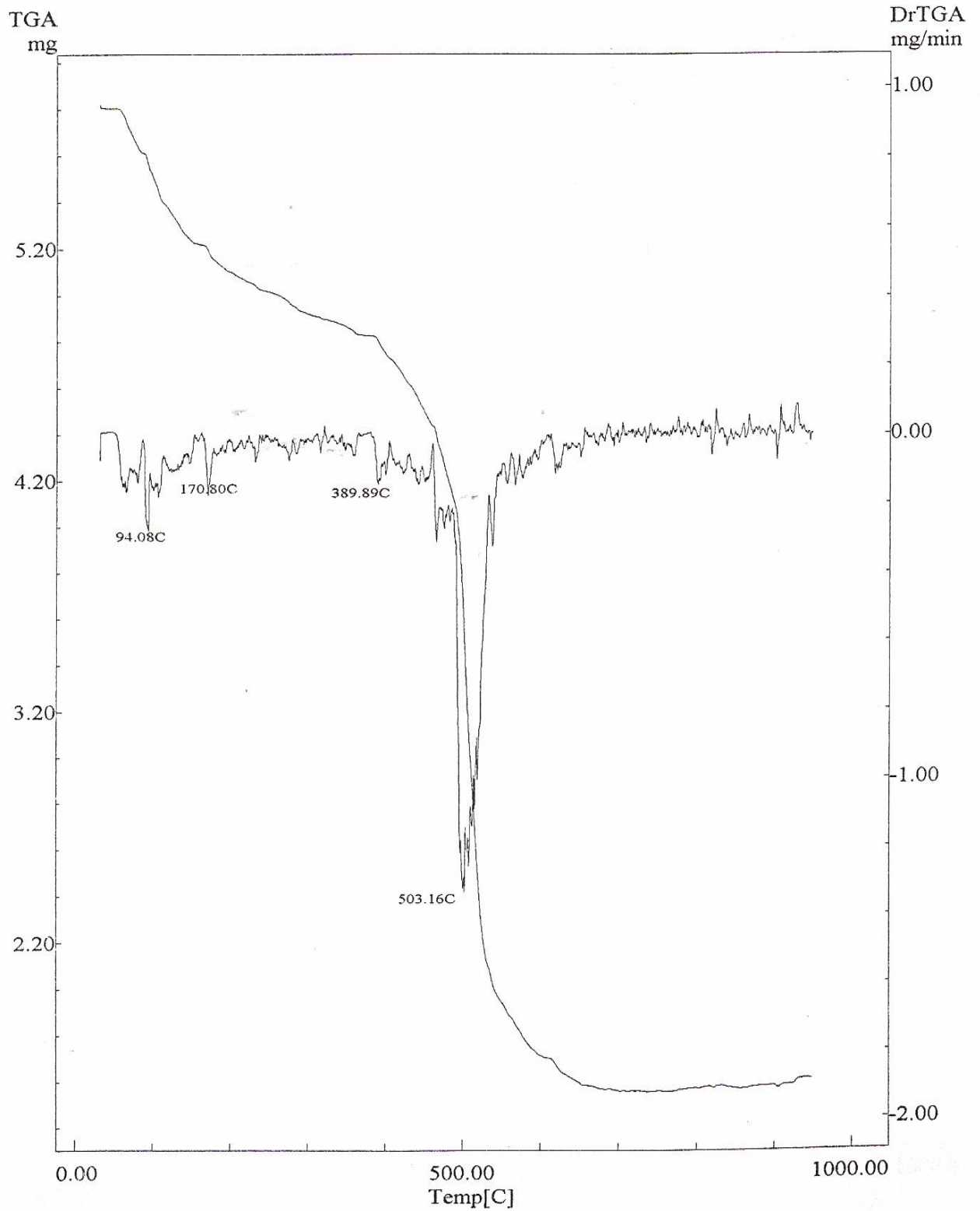


**Fig. 3.2:** TG diagram of  $\text{CuL}_2\text{Cl}_2(\text{H}_2\text{O})_3$  complex

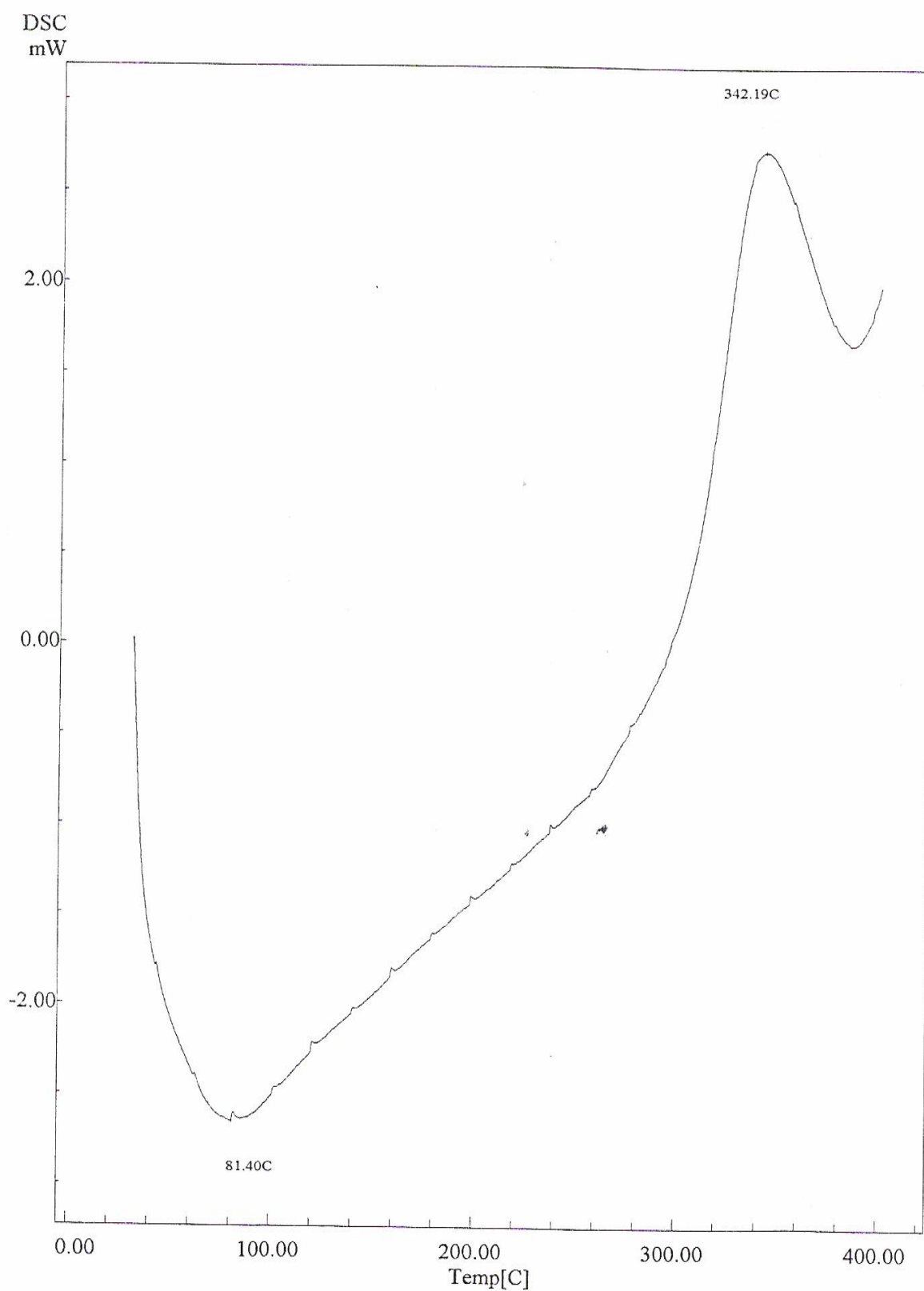


**Fig 3.3:** DSC diagram of  $\text{CuL}_2\text{Cl}_2(\text{H}_2\text{O})_3$  complex

### III.3.1.2 CuL<sub>2</sub>Cl<sub>2</sub>(H<sub>2</sub>O)<sub>5</sub> complex

#### III.3.1.2.1 Synthesis

Copper CuL<sub>2</sub>Cl<sub>2</sub>(H<sub>2</sub>O)<sub>5</sub> complex was prepared by adding a clear solution of 7,8-dihydro-7-oxo-1,2,4-triazolo[4,3-a]pyrimidine (2mmol) in 30 ml water, to a solution of CuCl<sub>2</sub> (1mmol) in a minimum amount of water at room temperature. Blue precipitates of the two complexes were appeared after two days which was filtered off and air dried

#### III.3.1.2.2 Elemental analysis

Elemental analysis percentage for CuL<sub>2</sub>Cl<sub>2</sub>(H<sub>2</sub>O)<sub>5</sub> complex: Found C, 24.75; H, 3.40; N, 22.59 %. Calculated: C, 24.17; H,3.62; N, 22.58 %.

#### III.3.1.2.3 Infrared Spectroscopy

**Fig. 3.4** show IR spectra of CuL<sub>2</sub>Cl<sub>2</sub>(H<sub>2</sub>O)<sub>5</sub> complex which show a broad band at 3414 cm<sup>-1</sup> characteristic of  $\nu(\text{O-H})$  absorption from H<sub>2</sub>O. The vibrational activity of the carbonyl group showed at 1697 cm<sup>-1</sup>, pyrimidine ring absorption appeared at 1533 cm<sup>-1</sup>, whereas the band of triazolo ring bands occurring at 1475 cm<sup>-1</sup>.

In addition the presence of aqua-metal bond is demonstrated by the identification of the absorptions associated with the vibrations of CuOH<sub>2</sub>. In the 800-400 cm<sup>-1</sup> region the Cu(II) complex shows two bands around 763 and 519 cm<sup>-1</sup>, assignable to rocking and wagging water<sup>(138)</sup>.

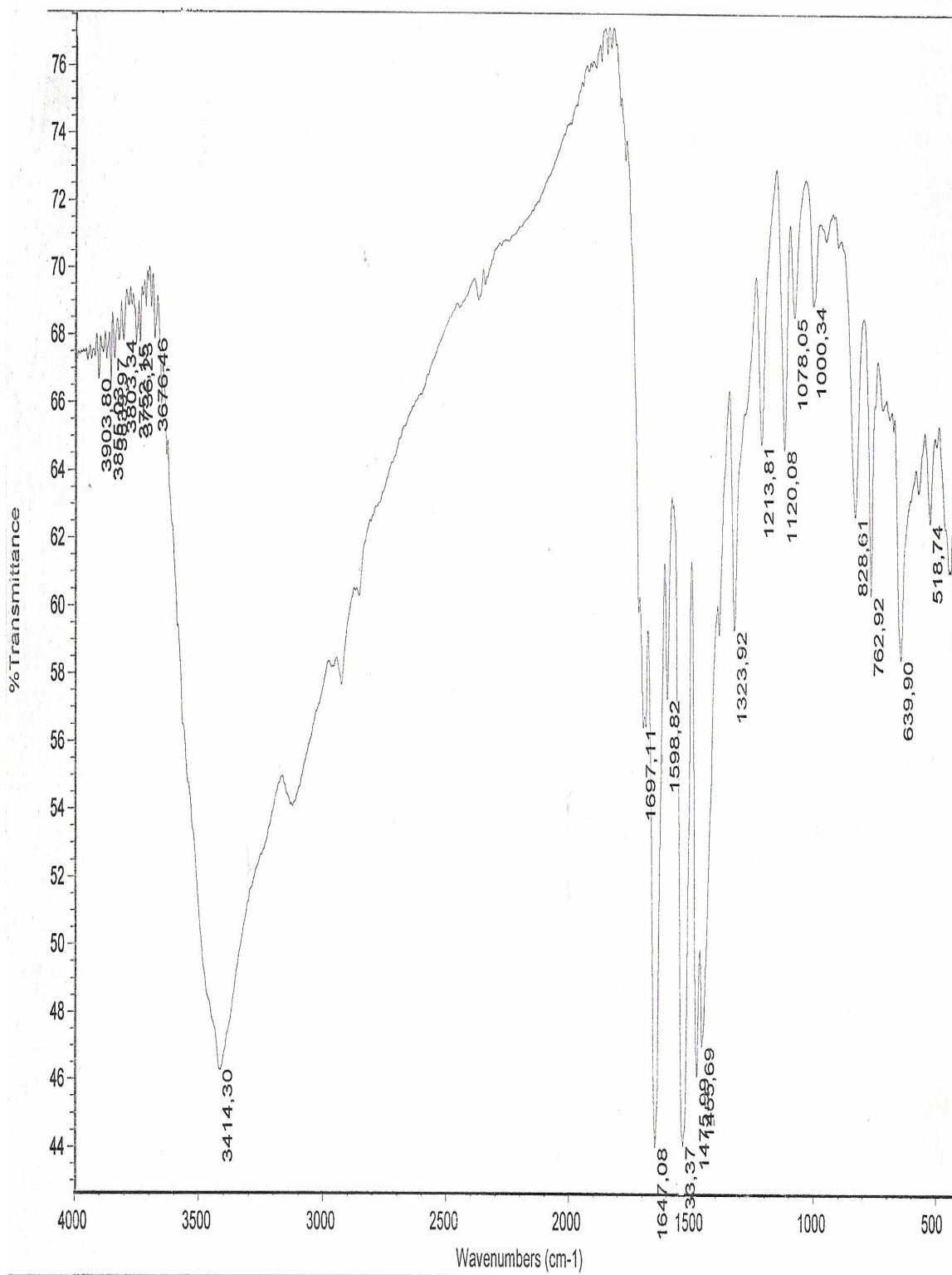


**Fig 3.4** Infrared spectrum of  $\text{CuL}_2\text{Cl}_2(\text{H}_2\text{O})_5$  complex

### III.3.1.2.4 Thermal Analysis

The thermogravimetric TG and DSC curves (**Fig. 3.5** and **3.6**) of  $\text{CuL}_2\text{Cl}_2\cdot(\text{H}_2\text{O})_5$  complex show the water molecules are lost in two steps, the first weight loss in the 53-150°C temperature range, clearly corresponding to the dehydration of the sample (the experimental weight loss 14.3%, are in good agreement with the theoretical one 14.5%), corresponding to the loss of four molecules of water, this process appeared in DSC diagram as a sharp endothermic effect centered at 58.8 °C with an associated dehydration enthalpy of 18.5 kJ/mole of water, the other endothermic step occur in the 215-250 °C temperature range with experimentally weight loss 63.5% . The pyrolysis of the compound finished at 680 °C with an experimental percentage value of the residue 19.5 % which is mixture of CuO and  $\text{CuCO}_3$  as final residue.

Both copper complexes compounds were sent to complete the characterization by magnetic methods (magnetic Susceptibility as a function of temperature and Electron Paramagnetic Resonance (EPR)), till the present day we didn't receive any data about magnetic methods, also we didn't obtain single crystal of the compound to solve it by X-ray methods.

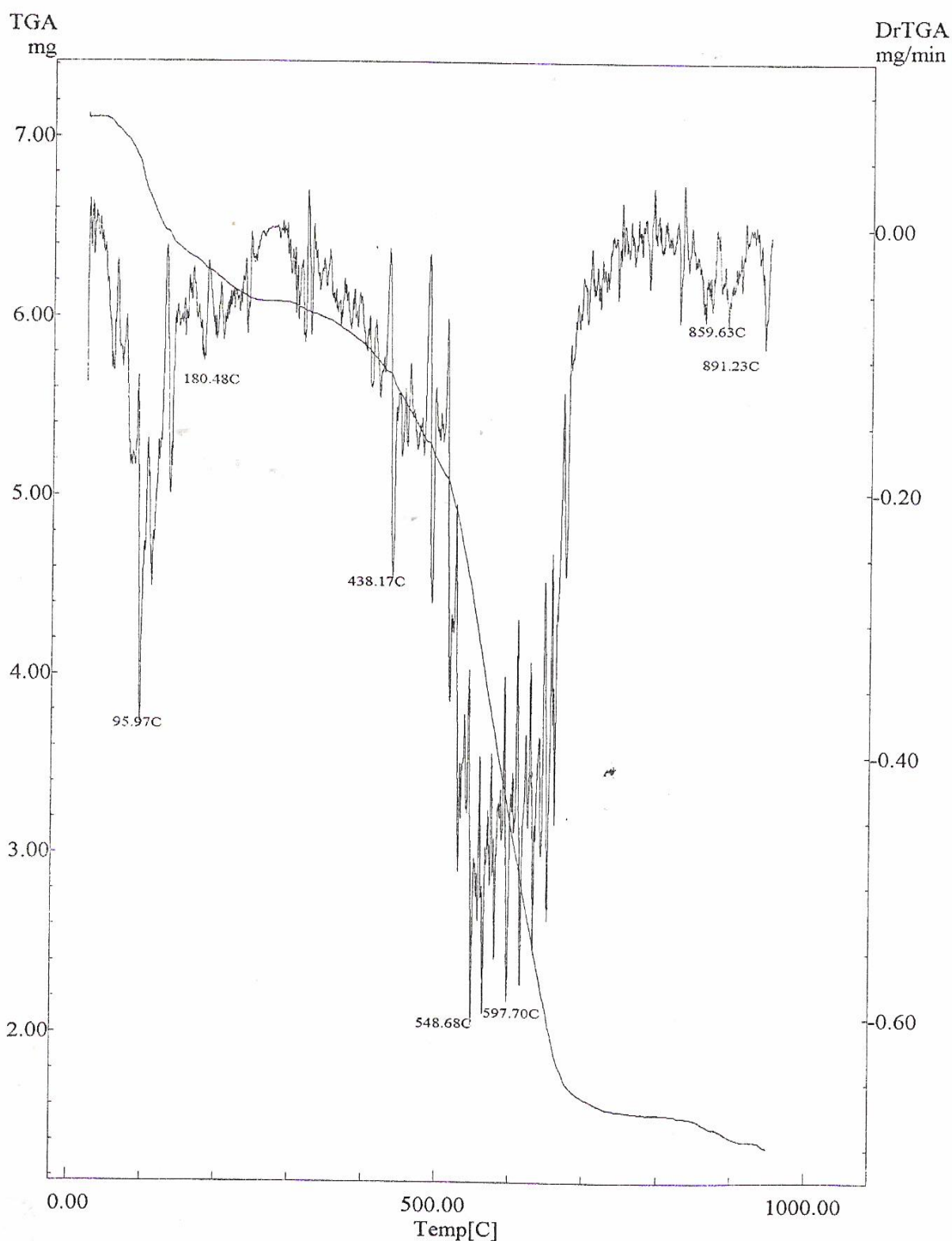


**Fig. 3.5:** TG diagram of  $\text{CuL}_2\text{Cl}_2(\text{H}_2\text{O})_5$  complex

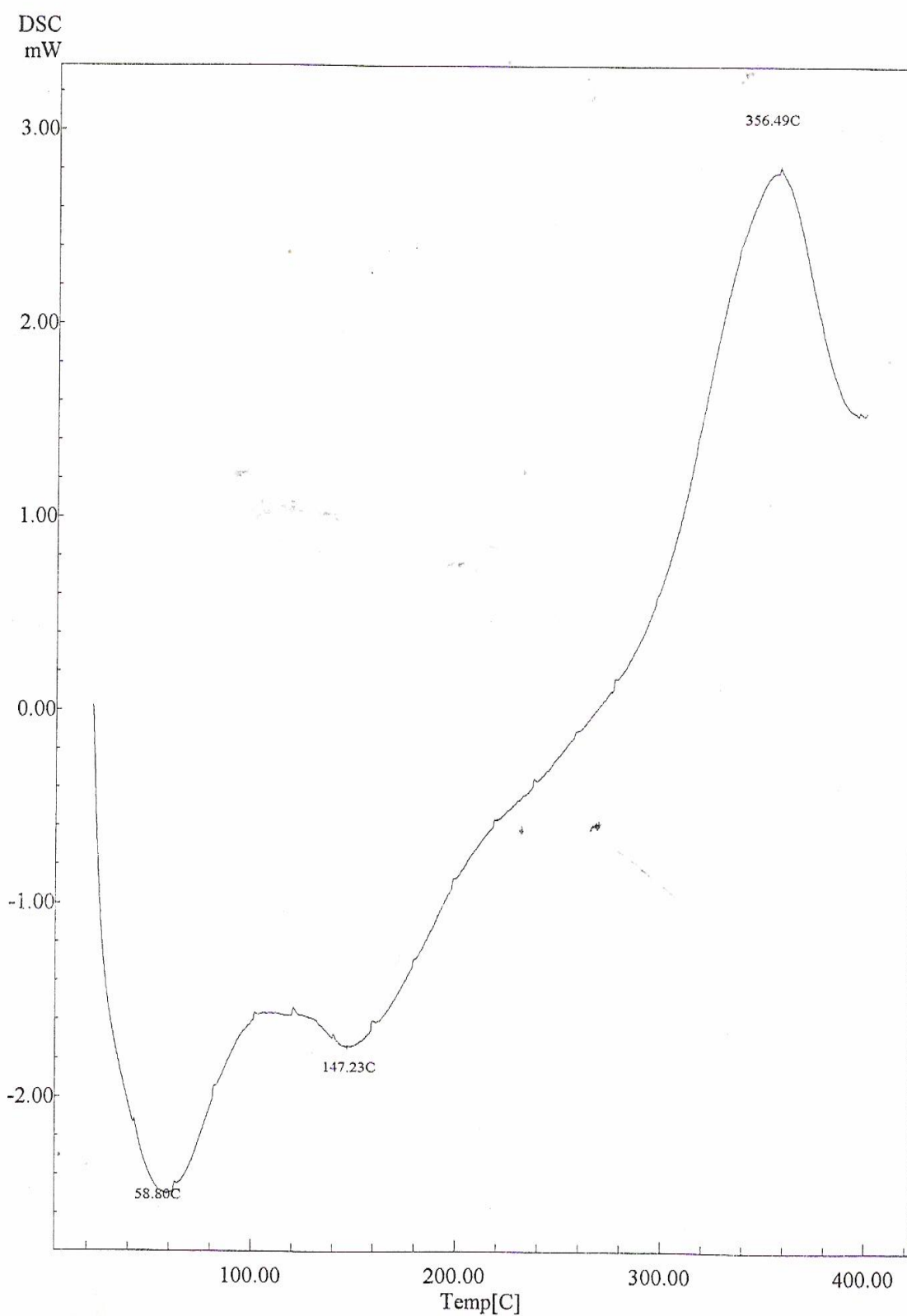


**Fig. 3.6:** DSC diagram of  $\text{CuL}_2\text{Cl}_2(\text{H}_2\text{O})_5$  complex



## III.3.2 Nickel Complexes

### III.3.2.1 NiL<sub>2</sub>(H<sub>2</sub>O)<sub>5</sub> complex

#### III.3.2.1.1 Synthesis

2mmole of 7,8-dihydro-7-oxo-1,2,4-triazolo[4,3-a]pyrimidine was dissolved in 30 ml distilled water to obtain a clear solution and then mixed with 1mmole of NiCl<sub>2</sub>, dissolved in 5ml distilled water. The solution was stirred at room temperature and left for a week, the blue precipitate was filtered off and air dried.

#### III.3.2.1.2 Elemental Analysis

Elemental analysis % for NiL<sub>2</sub>(H<sub>2</sub>O)<sub>5</sub>: Found C, 28.42; H, 3.43; N, 26.49. Calculated: C, 28.67; H, 3.85; N, 26.74.

#### III.3.2.1.3 Infrared Spectroscopy

IR spectra of NiL<sub>2</sub>(H<sub>2</sub>O)<sub>5</sub> complex **Fig. 3.7** show broad band at around 3394 cm<sup>-1</sup> assignable to ν(O-H) of water. The vibrational activity of the carbonyl group appears at 1642cm<sup>-1</sup> shifted 70 cm<sup>-1</sup> to lower frequency with respect to the free ligand (the two characteristic bands of pyrimidine and triazole ring were assigned at 1595 and 1533 cm<sup>-1</sup> respectively).

In addition the presence of aqua-metal bond is demonstrated by the identification of the absorptions associated with the vibrations of Ni(OH)<sub>2</sub>. New band at 519 cm<sup>-1</sup> are assigned to the ν(Ni-O<sub>w</sub>) (coordinated water) stretching vibrations coupled with chelated ring deformation and water deformation vibration <sup>(138)</sup>.

Bands which shown in the 3100-2300 cm<sup>-1</sup> IR spectra region, do not display in the IR spectra of this complex.

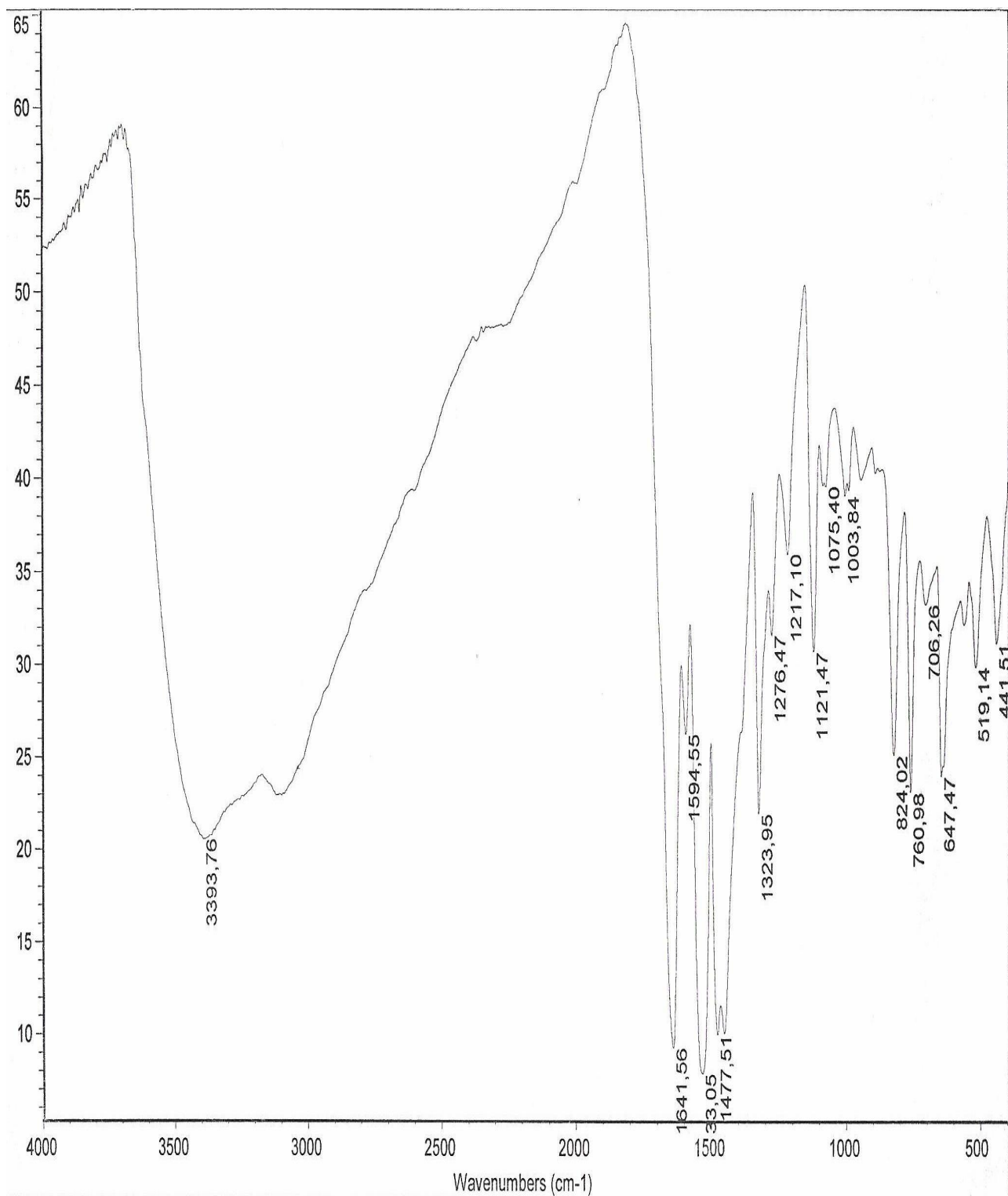


**Fig.3.7** IR Spectrum of  $\text{NiL}_2(\text{H}_2\text{O})_5$  complex

#### III.3.2.1.4 Thermal Analysis

Dehydration of the  $\text{NiL}_2(\text{H}_2\text{O})_5$  complex is reflected by the corresponding weight losses and endothermic effects in the TG and DSC curves **Fig. 3.8** and **3.9**, these indicate the water molecules are lost in several overlapping steps, water elimination started at 72 °C with experimental weight loss percentage 11.6 % and the theoretical value of 12.8%, corresponding to the loss of three molecules of water. This step is associated with dehydration enthalpy 20 kJ/mole. This endothermic step is immediately followed by an exothermic step. The pyrolysis of the complex finishes around 680°C leaving 24.3 percentage of residue which is mixture of NiO, and NiCO<sub>3</sub>.

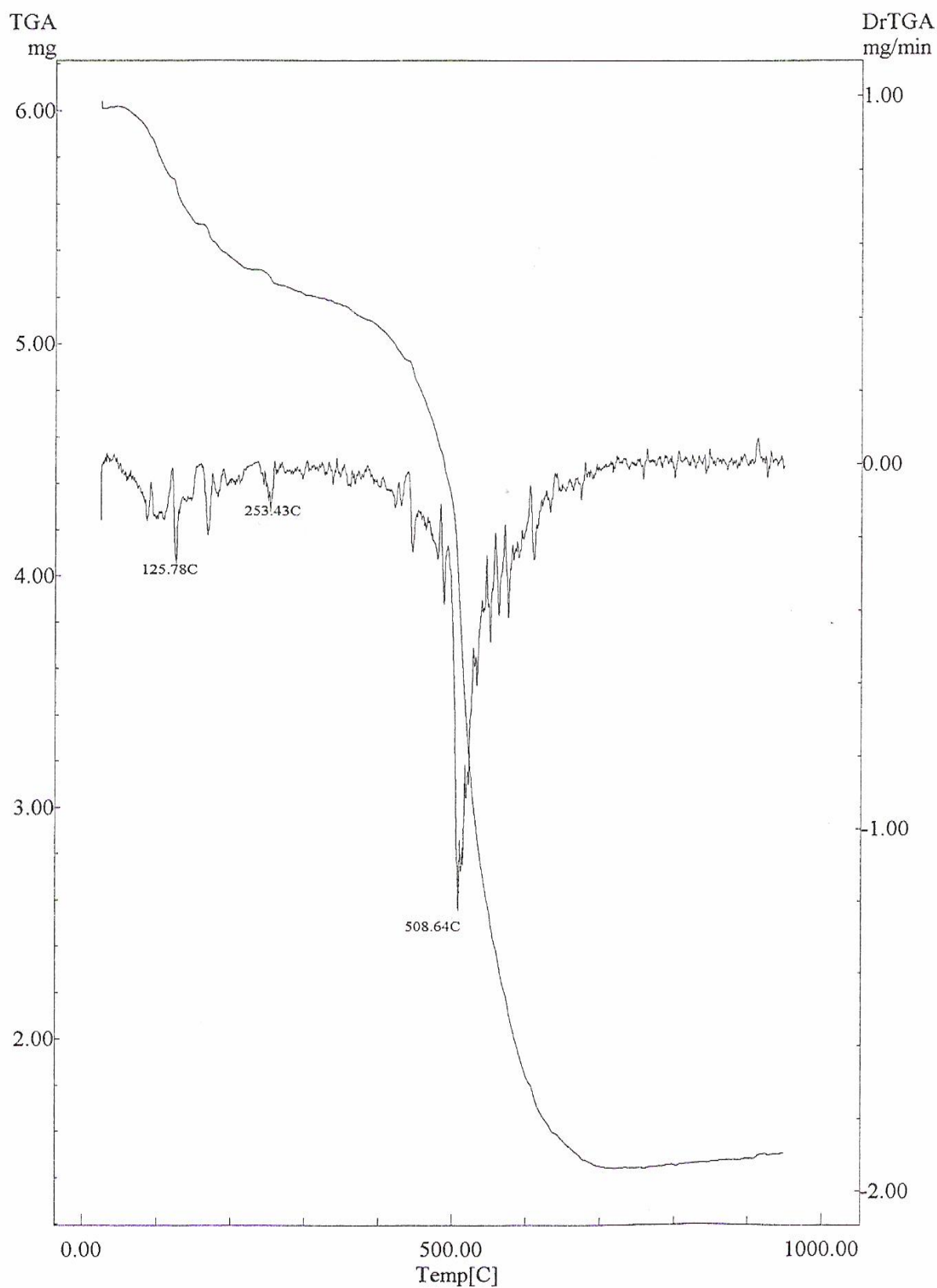


**Fig. 3.8:** TG diagraph of  $\text{NiL}_2(\text{H}_2\text{O})_5$  complex

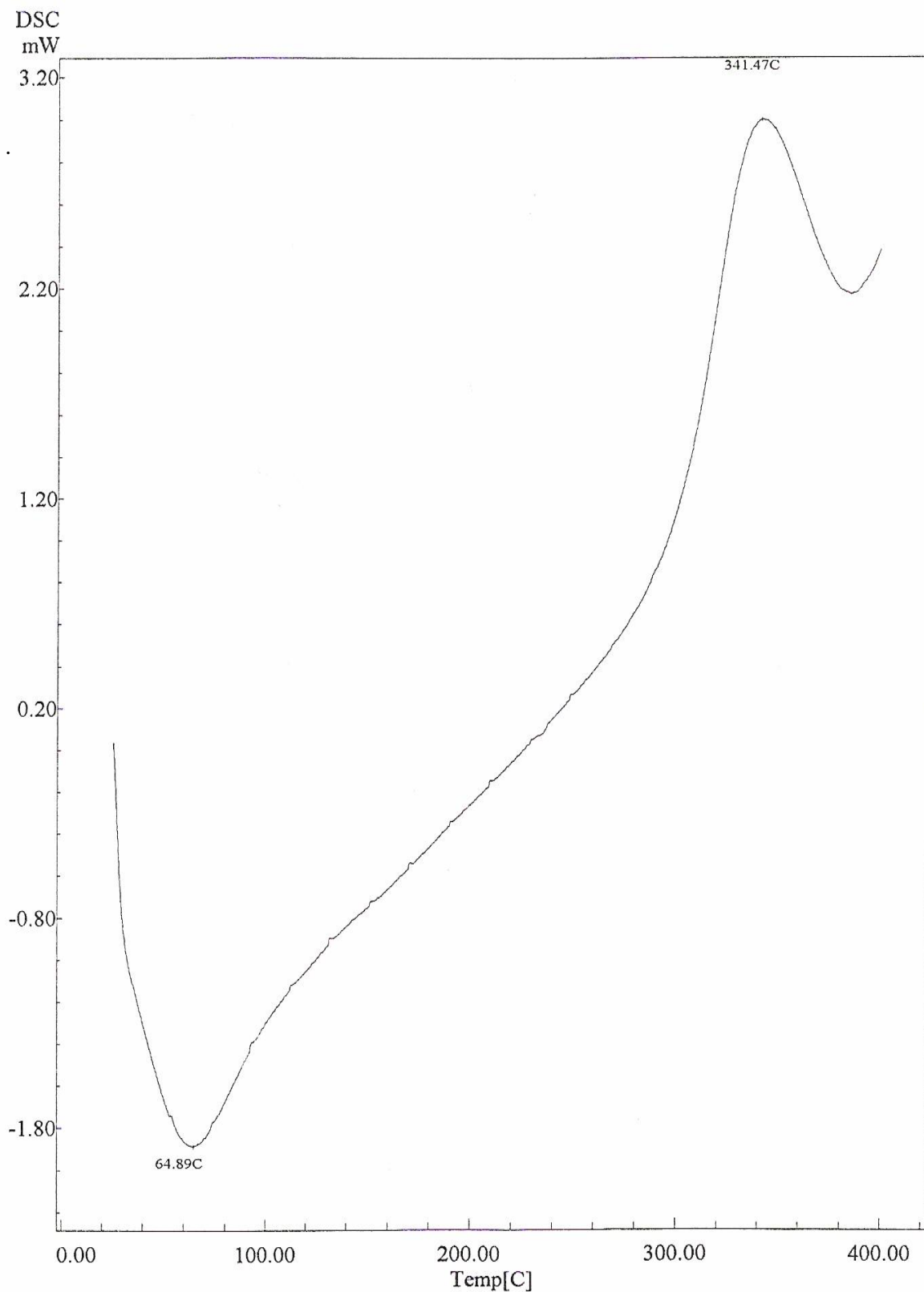


**Fig. 3.9:** DSC diagraph of  $\text{NiL}_2(\text{H}_2\text{O})_5$  complex

### III.3.2.2 Ni<sub>9</sub>(C<sub>5</sub>H<sub>3</sub>N<sub>4</sub>O)<sub>8</sub>(NO<sub>3</sub>)<sub>4</sub>(NH<sub>3</sub>)<sub>4</sub>(OH)<sub>6</sub>(H<sub>2</sub>O)<sub>16</sub> Complex

#### III.3.2.2.1 Synthesis

The nickel complex was obtained by reaction of a solution of Ni(NO<sub>3</sub>)<sub>2</sub> (1mmol) in a minimum amount of 1M NH<sub>4</sub>OH with 7,8-dihydro-7-oxo-1,2,4-triazolo[4,3-a]pyrimidine (2 mmol) in 30 ml 1 M NH<sub>4</sub>OH. The resulting solution was filtered and left to evaporate at room temperature. Blue crystals of the complex were obtained after 3 days, which were filtered off and air dried. Crystals were suitable for X-ray diffraction.

#### III.3.2.2.2 Elemental Analysis

Elemental analysis % for complex: Found C, 20.66; H, 3.51; N, 24.16. Calculated: C, 20.74; H, 3.28; N, 23.60,

#### III.3.2.2.3 Infrared Spectroscopy

The infrared spectra of the complex **Fig. 3.10**, show broad band at 3368 cm characteristic of  $\nu(\text{O-H})$  absorption, shifted  $30\text{cm}^{-1}$  to lower frequency with respect to NiL<sub>2</sub>(H<sub>2</sub>O)<sub>5</sub> complex.

The characteristic strong absorption bands in the IR spectra centered on 1649, 1598, and  $1536\text{ cm}^{-1}$  have been assigned respectively to  $\nu(\text{C=O})$ , pyrimidine ring and triazole ring stretching vibrations respectively.

In addition the presence of aqua-metal bond is demonstrated by the identification of the absorptions associated with the vibrations of Ni(OH)<sub>2</sub>. New band at  $519\text{ cm}^{-1}$  are assigned to the  $\nu(\text{Ni-Ow})$  (coordinated water) stretching vibrations coupled with chelated ring deformation and water deformation vibration <sup>(138)</sup>.

New bands at  $1325\text{ cm}^{-1}$  and  $825\text{ cm}^{-1}$  corresponding respectively to  $\nu_1$  and  $\nu_2$  vibration modes of a D<sub>3h</sub> NO<sub>3</sub><sup>-</sup> group. Bands which shown in the  $3100\text{-}2300\text{ cm}^{-1}$  IR spectra region, do not display in the IR spectra of this complex.

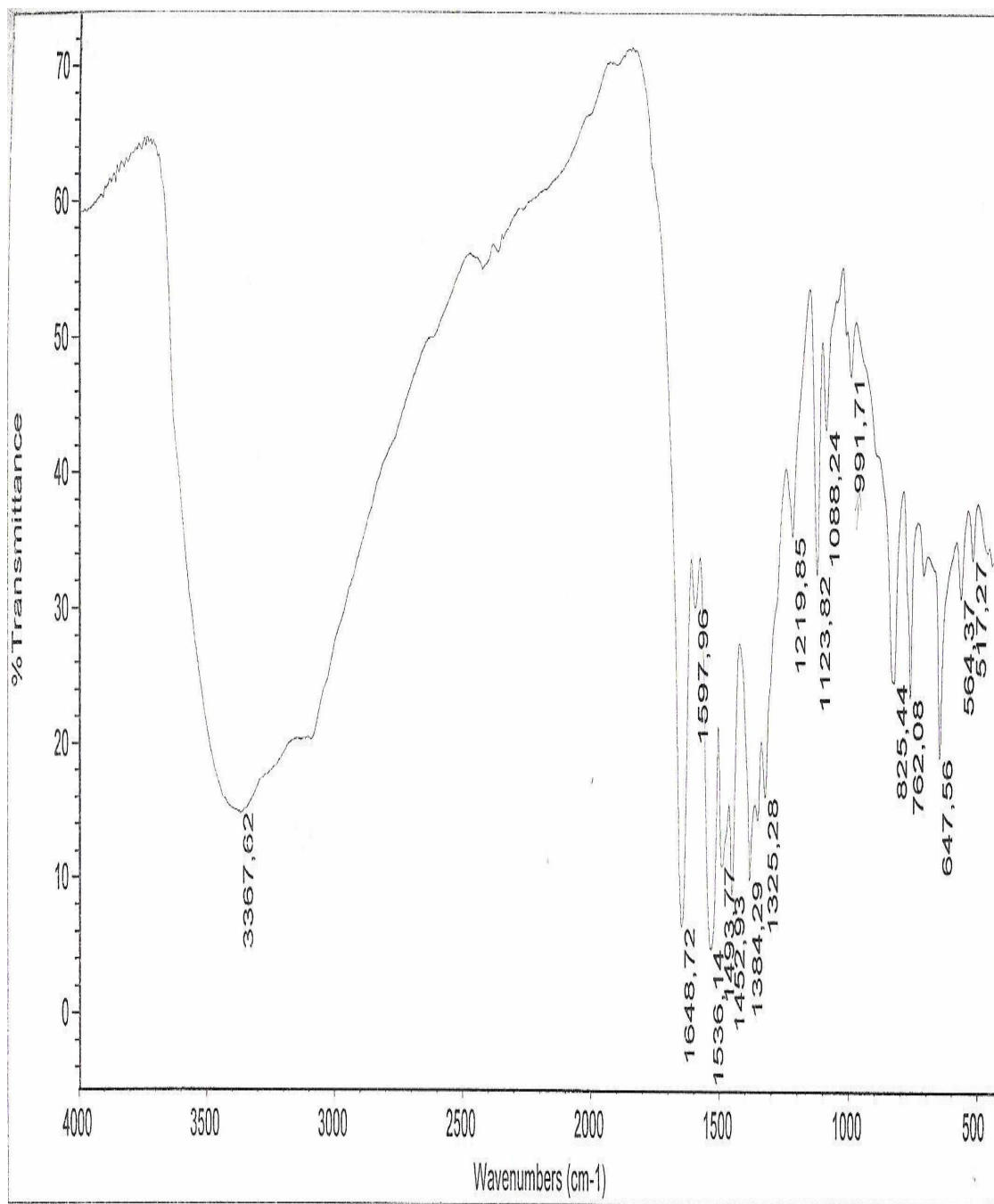


**Fig. 3.10** Infrared Spectroscopy of  $\text{Ni}_9(\text{C}_5\text{H}_3\text{N}_4\text{O})_8(\text{NO}_3)_4(\text{NH}_3)_4(\text{OH})_6(\text{H}_2\text{O})_{16}$  complex

### III.3.2.2.3 Thermal analysis

The thermal behavior of the isolated  $\text{Ni}_9(\text{C}_5\text{H}_3\text{N}_4\text{O})_8(\text{NO}_3)_4(\text{NH}_3)_4(\text{OH})_6(\text{H}_2\text{O})_{16}$  complex has been studied from the TG and DSC curves (**Fig. 3.11** and **3.12**). The latter study showed that the dehydration process is rather complicated, involving four steps, the first overlapping with the second and the third overlapping with the fourth. The elimination started at 75 °C suggesting that 15.5 water molecules are lost, accumulated weight loss are 12.2% after the third step and with the theoretical value 12.1%. The DSC curve shows two endothermic effects appeared at 60.17 °C and 199.6 °C followed by an exothermic one centered at 365.4 °C. The pyrolysis is finished around 500 °C leaving 27.7 % of the residue.



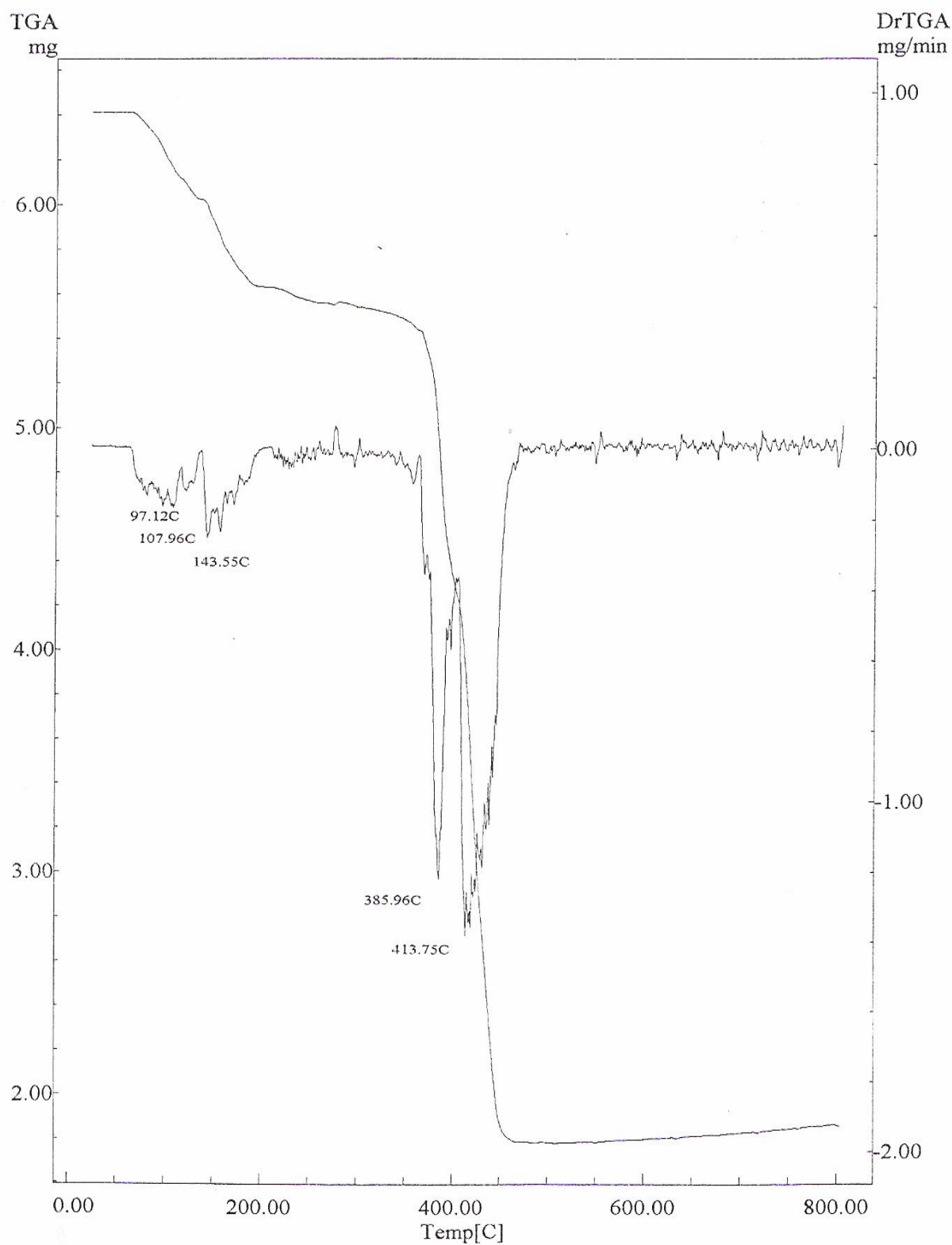


**Fig. 3.11:** TG diagraph of a  $\text{Ni}_9(\text{C}_5\text{H}_3\text{N}_4\text{O})_8(\text{NO}_3)_4(\text{NH}_3)_4(\text{OH})_6(\text{H}_2\text{O})_{16}$  complex

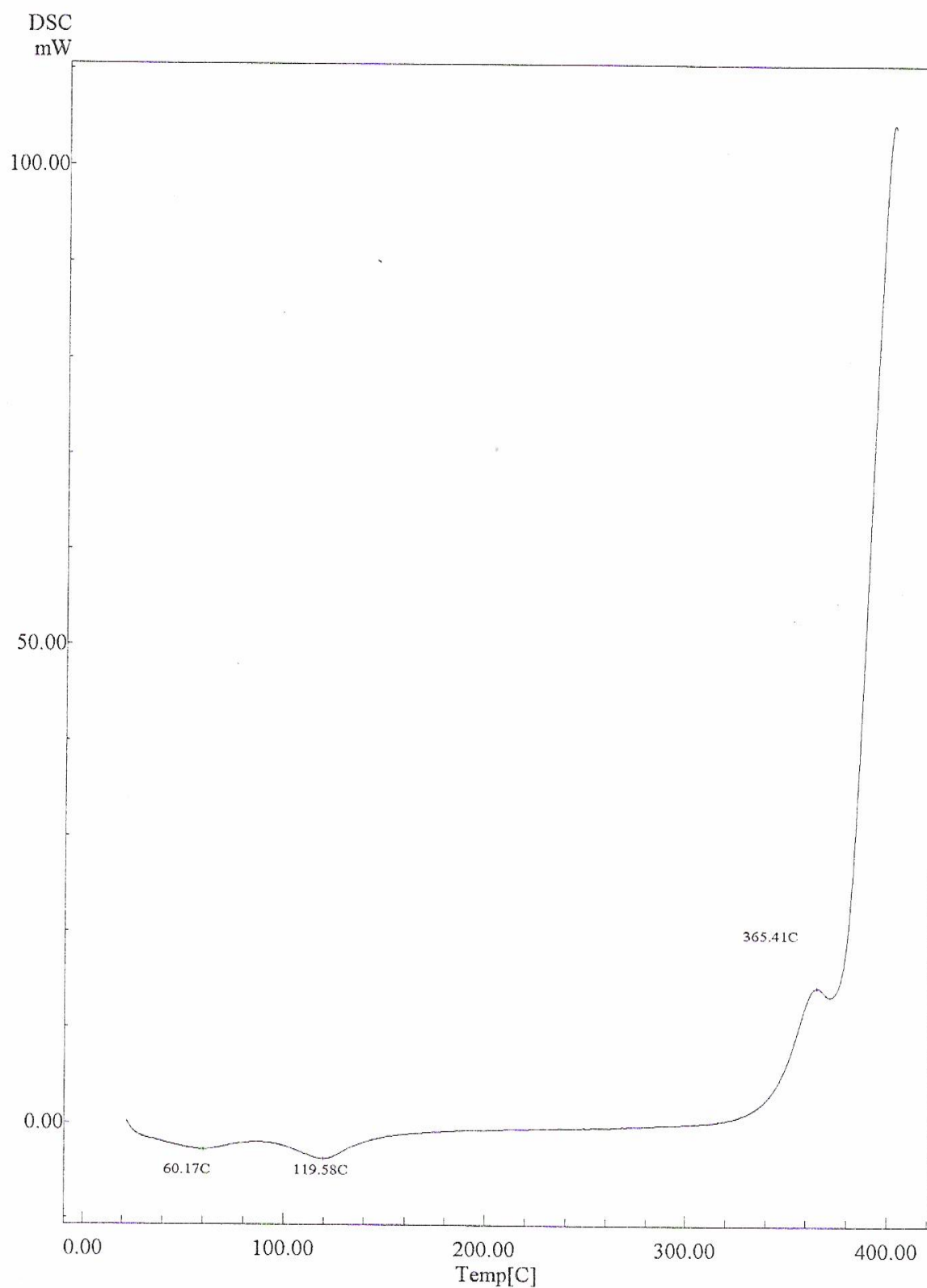


**Fig. 3.12:** DSC diagraeme of  $\text{Ni}_9(\text{C}_5\text{H}_3\text{N}_4\text{O})_8(\text{NO}_3)_4(\text{NH}_3)_4(\text{OH})_6(\text{H}_2\text{O})_{16}$  complex

### III.3.2.2.4 Crystal structure for $\text{Ni}_9(\text{C}_5\text{H}_3\text{N}_4\text{O})_8(\text{NO}_3)_4(\text{NH}_3)_4(\text{OH})_6(\text{H}_2\text{O})_{16}$ complex

Empirical formula	$\text{C}_{40}\text{H}_{72}\text{N}_{40}\text{Ni}_9\text{O}_{42}$
Formula weight	2313.77
Wavelength	0.71073 °A
Crystal system	Triclinic
Space group	P -1
Unit cell dimensions	
a	11.0481(5) °A
b	18.2700(8) °A
c	21.3860(9) °A
$\alpha$	65.9660(10)°
$\beta$	83.2870(10)°
$\gamma$	86.0430(10)°
Volume	3914.4(3) A <sup>3</sup>
Z	2
Calculated density	1.963 Mg/m <sup>3</sup>
Absorption coefficient	2.237 mm <sup>-1</sup>
F(000)	2360
Crystal size	0.28 x 0.15 x 0.06 mm
Reflections collected / unique	45862 / 17819 [R(int)= 0.0461]
Final R indices [I>2sigma(I)]	R1 = 0.0808, wR2 = 0.2202
R indices (all data)	R1 = 0.1142, wR2 = 0.2454

The nickel cluster is composed of nine atoms of nickel, the central nickel (Ni1) is situated in inversion center and is united to 6 atoms N2 from six ligands anion. Three of these six ligands are coordinated through N1 with a second nickel atom Ni2 and the other three are related through the symmetry center. In addition every one of these ligands is coordinated through N8 with other different atoms (Ni3, Ni4 and Ni5 and the symmetry related ones). With this we have the nine atoms. Also Ni2 forms OH bridging with Ni3, Ni4 and Ni5. In addition to the six ligands exists another two ligand in the cluster that are united with Ni4 and Ni5 through N1 and N2.

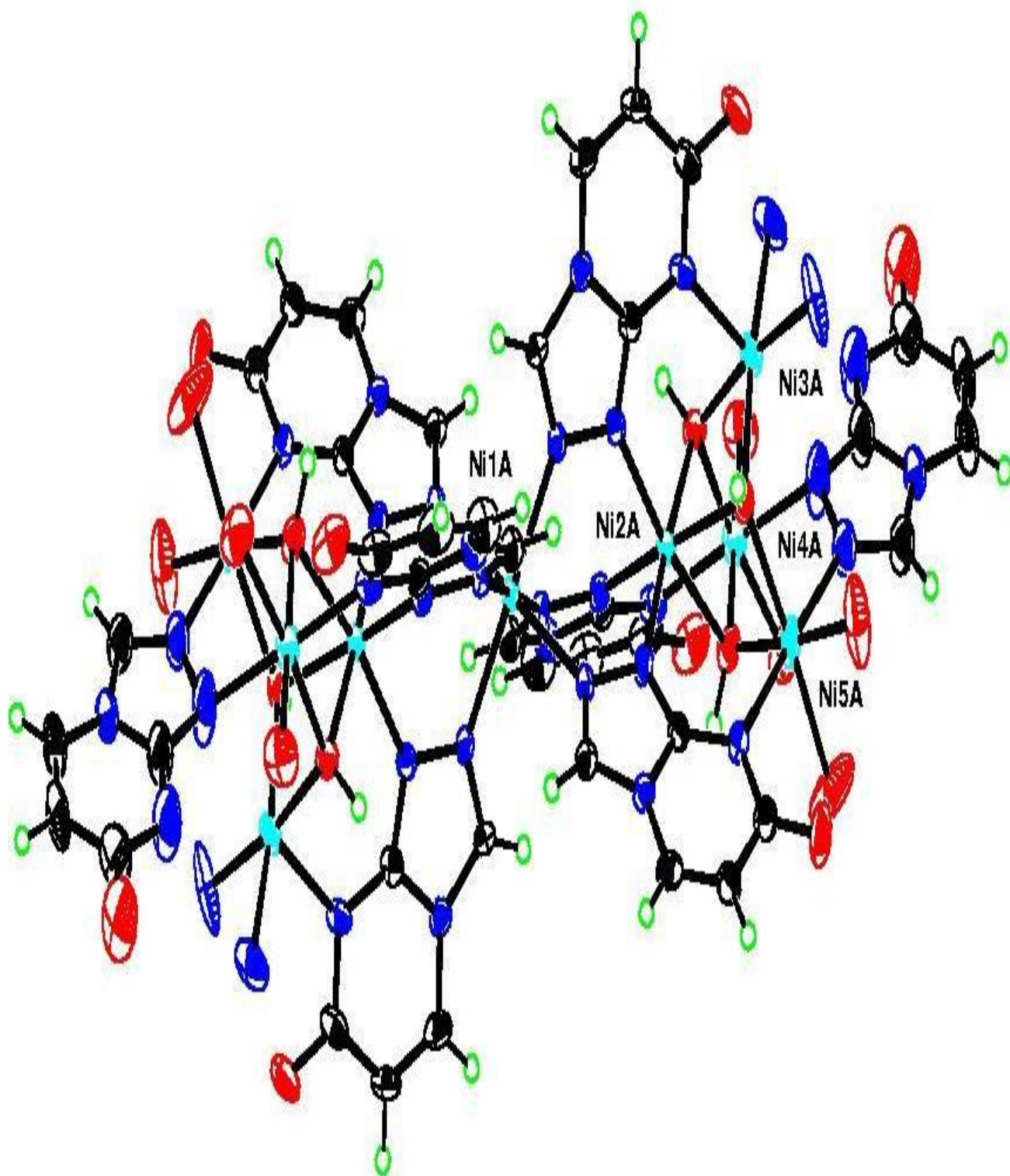


**Fig. 3.13:** Ionic structure of  $\text{Ni}_9(\text{C}_5\text{H}_3\text{N}_4\text{O})_8(\text{NO}_3)_4(\text{NH}_3)_4(\text{OH})_6(\text{H}_2\text{O})_{16}$  cluster according to X-ray analysis, Non  $\text{H}_2\text{O}$ ,  $\text{NO}_3$  and  $\text{NH}_3$  molecules are present

**Table 3.1:** bond lengths [°A] of Ni<sub>9</sub>(C<sub>5</sub>H<sub>3</sub>N<sub>4</sub>O)<sub>8</sub>(NO<sub>3</sub>)<sub>4</sub>(NH<sub>3</sub>)<sub>4</sub>(OH)<sub>6</sub>(H<sub>2</sub>O)<sub>16</sub> complex

Ni(1A)-N(2B)	2.084(5)		Ni(2B)-O(4)	2.041(5)
Ni(1A)-N(2A)	2.090(5)		Ni(2B)-O(6)	2.046(5)
Ni(1A)-N(2C)	2.092(5)		Ni(2B)-O(5)	2.068(4)
Ni(2A)-N(1C)	2.019(5)		Ni(3B)-O(4)	1.993(5)
Ni(2A)-N(1B)	2.023(5)		Ni(3B)-O(5)	2.040(5)
Ni(2A)-N(1A)	2.036(5)		Ni(3B)-N(4M)	2.044(6)
Ni(2A)-O(1)	2.039(4)		Ni(3B)-N(3M)	2.067(6)
Ni(2A)-O(2)	2.055(5)		Ni(3B)-N(8E)	2.087(6)
Ni(2A)-O(3)	2.081(4)		Ni(4B)-O(4)	2.016(5)
Ni(3A)-O(1)	2.008(5)		Ni(4B)-O(6)	2.042(5)
Ni(3A)-O(2)	2.025(5)		Ni(4B)-O(6M)	2.086(6)
Ni(3A)-N(1M)	2.047(7)		Ni(4B)-N(8F)	2.111(6)
Ni(3A)-N(2M)	2.064(7)		Ni(4B)-O(5M)	2.112(6)
Ni(3A)-N(8A)	2.087(5)		Ni(4B)-N(1H)	2.139(8)
Ni(4A)-O(1)	2.005(4)		Ni(5B)-O(6)	2.033(5)
Ni(4A)-O(3)	2.057(5)		Ni(5B)-O(5)	2.054(4)
Ni(4A)-O(2M)	2.071(6)		Ni(5B)-O(8M)	2.067(6)
Ni(4A)-O(1M)	2.091(6)		Ni(5B)-N(2H)	2.069(8)
Ni(4A)-N(8B)	2.108(6)		Ni(5B)-O(7M)	2.118(5)
Ni(4A)-N(1D)	2.162(8)		Ni(5B)-N(8G)	2.165(6)
Ni(5A)-O(3)	2.015(5)		N(1E)-C(8AE)	1.308(8)
Ni(5A)-O(2)	2.038(5)		N(1E)-N(2E)	1.371(7)
Ni(5A)-O(3M)	2.064(7)		N(2E)-C(3E)	1.292(8)
Ni(5A)-O(4M)	2.084(6)		C(3E)-N(4E)	1.365(8)
Ni(5A)-N(2D)	2.096(6)		N(4E)-C(8AE)	1.367(8)
Ni(5A)-N(8C)	2.187(6)		N(4E)-C(5E)	1.393(8)
N(1A)-C(8AA)	1.317(8)		C(5E)-C(6E)	1.308(10)
N(1A)-N(2A)	1.374(7)		C(6E)-C(7E)	1.470(10)
N(2A)-C(3A)	1.299(8)		C(7E)-O(7E)	1.251(8)
C(3A)-N(4A)	1.360(8)		C(7E)-N(8E)	1.372(8)
N(4A)-C(8AA)	1.370(8)		N(8E)-C(8AE)	1.354(8)
N(4A)-C(5A)	1.398(8)		N(1F)-C(8AF)	1.318(8)
C(5A)-C(6A)	1.331(10)		N(1F)-N(2F)	1.372(7)
C(6A)-C(7A)	1.438(10)		N(2F)-C(3F)	1.286(8)

C(7A)-O(7A)	1.259(8)		C(3F)-N(4F)	1.369(8)
C(7A)-N(8A)	1.381(9)		N(4F)-C(8AF)	1.363(8)
N(8A)-C(8AA)	1.340(8)		N(4F)-C(5F)	1.380(8)
N(1B)-C(8AB)	1.324(8)		C(5F)-C(6F)	1.322(11)
N(1B)-N(2B)	1.379(7)		C(6F)-C(7F)	1.451(12)
N(2B)-C(3B)	1.287(9)		C(7F)-O(7F)	1.261(10)
C(3B)-N(4B)	1.367(9)		C(7F)-N(8F)	1.375(10)
N(4B)-C(8AB)	1.365(9)		N(8F)-C(8AF)	1.339(8)
N(4B)-C(5B)	1.390(9)		N(1G)-C(8AG)	1.326(8)
C(5B)-C(6B)	1.313(12)		N(1G)-N(2G)	1.384(7)
C(6B)-C(7B)	1.464(12)		N(2G)-C(3G)	1.295(8)
C(7B)-O(7B)	1.259(9)		C(3G)-N(4G)	1.363(8)
C(7B)-N(8B)	1.361(9)		N(4G)-C(8AG)	1.375(8)
N(8B)-C(8AB)	1.346(8)		N(4G)-C(5G)	1.384(8)
N(1C)-C(8AC)	1.319(8)		C(5G)-C(6G)	1.320(10)
N(1C)-N(2C)	1.385(7)		C(6G)-C(7G)	1.458(11)
N(2C)-C(3C)	1.299(8)		C(7G)-O(7G)	1.237(8)
C(3C)-N(4C)	1.365(8)		C(7G)-N(8G)	1.370(9)
N(4C)-C(8AC)	1.368(8)		N(8G)-C(8AG)	1.349(8)
N(4C)-C(5C)	1.391(8)		N(1H)-C(8AH)	1.316(11)
C(5C)-C(6C)	1.325(10)		N(1H)-N(2H)	1.382(12)
C(6C)-C(7C)	1.457(10)		N(2H)-C(3H)	1.294(11)
C(7C)-O(7C)	1.240(8)		C(3H)-N(4H)	1.327(15)
C(7C)-N(8C)	1.362(9)		N(4H)-C(8AH)	1.326(15)
N(8C)-C(8AC)	1.344(8)		N(4H)-C(5H)	1.460(14)
N(1D)-C(8AD)	1.329(10)		C(5H)-C(6H)	1.243(17)
N(1D)-N(2D)	1.385(10)		C(6H)-C(7H)	1.431(17)
N(2D)-C(3D)	1.293(9)		C(7H)-O(7H)	1.305(14)
C(3D)-N(4D)	1.373(10)		C(7H)-N(8H)	1.399(14)
N(4D)-C(8AD)	1.347(10)		N(8H)-C(8AH)	1.255(14)
N(4D)-C(5D)	1.371(9)		N(1N)-O(1N)	1.228(9)
C(5D)-C(6D)	1.327(13)		N(1N)-O(2N)	1.231(9)
C(6D)-C(7D)	1.450(14)		N(1N)-O(3N)	1.253(11)
C(7D)-O(7D)	1.253(12)		N(2N)-O(4N)	1.136(14)
C(7D)-N(8D)	1.364(11)		N(2N)-O(5N)	1.260(18)
N(8D)-C(8AD)	1.355(12)		N(2N)-O(6N)	1.348(18)
Ni(1B)-N(2F)	2.072(5)		N(3N)-O(8N)	1.269(9)

Ni(1B)-N(2E)	2.090(5)		N(3N)-O(7N)	1.273(9)
Ni(1B)-N(2G)	2.106(5)		N(3N)-O(9N)	1.276(9)
Ni(2B)-N(1G)	2.017(5)		N(4N)-O(10N)	1.260(9)
Ni(2B)-N(1E)	2.022(5)		N(4N)-O(11N)	1.265(9)
Ni(2B)-N(1F)	2.032(5)		N(4N)-O(12N)	1.288(9)

**Table 3.2** bond angle [°] of Ni<sub>9</sub>(C<sub>5</sub>H<sub>3</sub>N<sub>4</sub>O)<sub>8</sub>(NO<sub>3</sub>)<sub>4</sub>(NH<sub>3</sub>)<sub>4</sub>(OH)<sub>6</sub>(H<sub>2</sub>O)<sub>16</sub> complex

N(2B)-Ni(1A)-N(2A)	92.0(2)		N(1M)-Ni(3A)-N(8A)	95.3(2)
N(2B)-Ni(1A)-N(2C)	91.3(2)		N(2M)-Ni(3A)-N(8A)	91.8(3)
N(2A)-Ni(1A)-N(2C)	90.6(2)		O(1)-Ni(4A)-O(3)	84.97(18)
N(1C)-Ni(2A)-N(1B)	92.7(2)		O(1)-Ni(4A)-O(2M)	94.4(2)
N(1C)-Ni(2A)-N(1A)	93.0(2)		O(3)-Ni(4A)-O(2M)	178.9(2)
N(1B)-Ni(2A)-N(1A)	93.6(2)		O(1)-Ni(4A)-O(1M)	173.6(2)
N(1C)-Ni(2A)-O(1)	176.0(2)		O(3)-Ni(4A)-O(1M)	94.5(2)
N(1B)-Ni(2A)-O(1)	90.1(2)		O(2M)-Ni(4A)-O(1M)	86.1(2)
N(1A)-Ni(2A)-O(1)	89.59(19)		O(1)-Ni(4A)-N(8B)	94.4(2)
N(1C)-Ni(2A)-O(2)	94.5(2)		O(3)-Ni(4A)-N(8B)	90.8(2)
N(1B)-Ni(2A)-O(2)	169.46(19)		O(2M)-Ni(4A)-N(8B)	90.1(2)
N(1A)-Ni(2A)-O(2)	93.7(2)		O(1M)-Ni(4A)-N(8B)	92.0(2)
O(1)-Ni(2A)-O(2)	82.34(18)		O(1)-Ni(4A)-N(1D)	85.3(3)
N(1C)-Ni(2A)-O(3)	93.56(19)		O(3)-Ni(4A)-N(1D)	87.6(2)
N(1B)-Ni(2A)-O(3)	92.88(19)		O(2M)-Ni(4A)-N(1D)	91.5(3)
N(1A)-Ni(2A)-O(3)	170.5(2)		O(1M)-Ni(4A)-N(1D)	88.3(3)
O(1)-Ni(2A)-O(3)	83.51(18)		N(8B)-Ni(4A)-N(1D)	178.4(2)
O(2)-Ni(2A)-O(3)	79.03(19)		O(3)-Ni(5A)-O(2)	80.95(19)
O(1)-Ni(3A)-O(2)	83.86(19)		O(3)-Ni(5A)-O(3M)	173.8(2)
O(1)-Ni(3A)-N(1M)	94.3(3)		O(2)-Ni(5A)-O(3M)	97.0(3)
O(2)-Ni(3A)-N(1M)	169.4(2)		O(3)-Ni(5A)-O(4M)	93.0(3)
O(1)-Ni(3A)-N(2M)	171.8(3)		O(2)-Ni(5A)-O(4M)	174.0(3)
O(2)-Ni(3A)-N(2M)	89.7(3)		O(3M)-Ni(5A)-O(4M)	89.1(4)
N(1M)-Ni(3A)-N(2M)	91.1(3)		O(3)-Ni(5A)-N(2D)	87.6(2)
O(1)-Ni(3A)-N(8A)	93.8(2)		O(2)-Ni(5A)-N(2D)	89.0(2)
O(2)-Ni(3A)-N(8A)	95.25(19)		O(3M)-Ni(5A)-N(2D)	86.6(3)
O(4M)-Ni(5A)-N(2D)	91.0(3)		O(7B)-C(7B)-N(8B)	120.5(8)
O(3)-Ni(5A)-N(8C)	95.72(19)		O(7B)-C(7B)-C(6B)	120.1(7)

O(2)-Ni(5A)-N(8C)	92.37(18)		N(8B)-C(7B)-C(6B)	119.4(7)
O(3M)-Ni(5A)-N(8C)	90.2(2)		C(8AB)-N(8B)-C(7B)	115.9(6)
O(4M)-Ni(5A)-N(8C)	87.9(2)		C(8AB)-N(8B)-Ni(4A)	121.4(4)
N(2D)-Ni(5A)-N(8C)	176.6(2)		C(7B)-N(8B)-Ni(4A)	122.6(5)
Ni(4A)-O(1)-Ni(3A)	113.9(2)		N(1B)-C(8AB)-N(8B)	126.8(6)
Ni(4A)-O(1)-Ni(2A)	94.79(18)		N(1B)-C(8AB)-N(4B)	108.4(5)
Ni(3A)-O(1)-Ni(2A)	94.42(19)		N(8B)-C(8AB)-N(4B)	124.7(6)
Ni(3A)-O(2)-Ni(5A)	123.7(2)		C(8AC)-N(1C)-N(2C)	106.9(5)
Ni(3A)-O(2)-Ni(2A)	93.43(19)		C(8AC)-N(1C)-Ni(2A)	129.5(4)
Ni(5A)-O(2)-Ni(2A)	95.88(19)		N(2C)-N(1C)-Ni(2A)	123.4(4)
Ni(5A)-O(3)-Ni(4A)	120.6(2)		C(3C)-N(2C)-N(1C)	108.8(5)
Ni(5A)-O(3)-Ni(2A)	95.8(2)		C(3C)-N(2C)-Ni(1A)	127.4(4)
Ni(4A)-O(3)-Ni(2A)	92.05(18)		N(1C)-N(2C)-Ni(1A)	123.8(4)
C(8AA)-N(1A)-N(2A)	107.5(5)		N(2C)-C(3C)-N(4C)	109.0(6)
C(8AA)-N(1A)-Ni(2A)	128.3(4)		C(3C)-N(4C)-C(8AC)	106.3(5)
N(2A)-N(1A)-Ni(2A)	124.1(4)		C(3C)-N(4C)-C(5C)	132.9(6)
C(3A)-N(2A)-N(1A)	108.8(5)		C(8AC)-N(4C)-C(5C)	120.8(5)
C(3A)-N(2A)-Ni(1A)	127.9(4)		C(6C)-C(5C)-N(4C)	116.5(6)
N(1A)-N(2A)-Ni(1A)	123.2(4)		C(5C)-C(6C)-C(7C)	122.5(6)
N(2A)-C(3A)-N(4A)	108.7(5)		O(7C)-C(7C)-N(8C)	121.6(7)
C(3A)-N(4A)-C(8AA)	106.7(5)		O(7C)-C(7C)-C(6C)	119.1(6)
C(3A)-N(4A)-C(5A)	133.0(6)		N(8C)-C(7C)-C(6C)	119.3(6)
C(8AA)-N(4A)-C(5A)	120.3(6)		C(8AC)-N(8C)-C(7C)	116.8(6)
C(6A)-C(5A)-N(4A)	116.7(6)		C(8AC)-N(8C)-Ni(5A)	121.6(4)
C(5A)-C(6A)-C(7A)	122.4(6)		C(7C)-N(8C)-Ni(5A)	121.6(5)
O(7A)-C(7A)-N(8A)	119.5(7)		N(1C)-C(8AC)-N(8C)	126.8(6)
O(7A)-C(7A)-C(6A)	120.8(6)		N(1C)-C(8AC)-N(4C)	109.1(5)
N(8A)-C(7A)-C(6A)	119.7(6)		N(8C)-C(8AC)-N(4C)	124.1(6)
C(8AA)-N(8A)-C(7A)	116.3(6)		C(8AD)-N(1D)-N(2D)	106.9(7)
C(8AA)-N(8A)-Ni(3A)	120.8(4)		C(8AD)-N(1D)-Ni(4A)	124.3(7)
C(7A)-N(8A)-Ni(3A)	122.8(5)		N(2D)-N(1D)-Ni(4A)	116.0(6)
N(1A)-C(8AA)-N(8A)	127.2(6)		C(3D)-N(2D)-N(1D)	108.2(7)
N(1A)-C(8AA)-N(4A)	108.2(5)		C(3D)-N(2D)-Ni(5A)	132.1(6)
N(8A)-C(8AA)-N(4A)	124.5(6)		N(1D)-N(2D)-Ni(5A)	119.4(5)
C(8AB)-N(1B)-N(2B)	107.4(5)		N(2D)-C(3D)-N(4D)	109.3(7)
C(8AB)-N(1B)-Ni(2A)	127.8(4)		C(8AD)-N(4D)-C(5D)	119.8(7)
N(2B)-N(1B)-Ni(2A)	124.9(4)		C(8AD)-N(4D)-C(3D)	106.3(6)



C(3B)-N(2B)-N(1B)	108.6(5)		C(5D)-N(4D)-C(3D)	133.7(7)
C(3B)-N(2B)-Ni(1A)	128.7(4)		C(6D)-C(5D)-N(4D)	118.6(8)
N(1B)-N(2B)-Ni(1A)	122.7(4)		C(5D)-C(6D)-C(7D)	121.4(7)
N(2B)-C(3B)-N(4B)	109.4(6)		O(7D)-C(7D)-N(8D)	119.2(10)
C(8AB)-N(4B)-C(3B)	106.2(5)		O(7D)-C(7D)-C(6D)	122.1(8)
C(8AB)-N(4B)-C(5B)	120.5(6)		N(8D)-C(7D)-C(6D)	118.7(8)
C(3B)-N(4B)-C(5B)	133.3(7)		C(8AD)-N(8D)-C(7D)	117.0(8)
C(6B)-C(5B)-N(4B)	116.7(8)		N(1D)-C(8AD)-N(4D)	109.2(7)
C(5B)-C(6B)-C(7B)	122.3(7)		N(1D)-C(8AD)-N(8D)	126.2(8)
N(4D)-C(8AD)-N(8D)	124.5(7)		O(8M)-Ni(5B)-N(2H)	86.8(3)
N(2F)-Ni(1B)-N(2E)	92.5(2)		O(6)-Ni(5B)-O(7M)	91.8(2)
N(2F)-Ni(1B)-N(2G)	90.87(19)		O(5)-Ni(5B)-O(7M)	171.4(2)
N(2E)-Ni(1B)-N(2G)	91.14(19)		O(8M)-Ni(5B)-O(7M)	88.8(3)
N(1G)-Ni(2B)-N(1E)	92.1(2)		N(2H)-Ni(5B)-O(7M)	88.7(2)
N(1G)-Ni(2B)-N(1F)	94.0(2)		O(6)-Ni(5B)-N(8G)	96.11(19)
N(1E)-Ni(2B)-N(1F)	93.6(2)		O(5)-Ni(5B)-N(8G)	94.24(19)
N(1E)-Ni(2B)-O(4)	90.3(2)		O(8M)-Ni(5B)-N(8G)	88.7(3)
N(1F)-Ni(2B)-O(4)	88.9(2)		N(2H)-Ni(5B)-N(8G)	175.4(3)
N(1G)-Ni(2B)-O(6)	93.88(19)		O(7M)-Ni(5B)-N(8G)	90.2(2)
N(1E)-Ni(2B)-O(6)	171.62(19)		Ni(3B)-O(4)-Ni(4B)	114.9(2)
N(1F)-Ni(2B)-O(6)	91.8(2)		Ni(3B)-O(4)-Ni(2B)	94.8(2)
O(4)-Ni(2B)-O(6)	83.39(19)		Ni(4B)-O(4)-Ni(2B)	94.58(19)
N(1G)-Ni(2B)-O(5)	94.71(19)		Ni(3B)-O(5)-Ni(5B)	125.5(2)
N(1E)-Ni(2B)-O(5)	93.95(19)		Ni(3B)-O(5)-Ni(2B)	92.62(19)
N(1F)-Ni(2B)-O(5)	168.2(2)		Ni(5B)-O(5)-Ni(2B)	94.73(18)
O(4)-Ni(2B)-O(5)	82.05(19)		Ni(5B)-O(6)-Ni(4B)	120.6(2)
O(6)-Ni(2B)-O(5)	79.73(18)		Ni(5B)-O(6)-Ni(2B)	96.0(2)
O(4)-Ni(3B)-O(5)	83.96(19)		Ni(4B)-O(6)-Ni(2B)	93.64(19)
O(4)-Ni(3B)-N(4M)	165.7(2)		C(8AE)-N(1E)-N(2E)	107.2(5)
O(5)-Ni(3B)-N(4M)	92.2(2)		C(8AE)-N(1E)-Ni(2B)	128.4(4)
O(4)-Ni(3B)-N(3M)	91.5(2)		N(2E)-N(1E)-Ni(2B)	124.2(4)
O(5)-Ni(3B)-N(3M)	171.0(2)		C(3E)-N(2E)-N(1E)	108.9(5)
N(4M)-Ni(3B)-N(3M)	90.3(3)		C(3E)-N(2E)-Ni(1B)	128.1(4)
O(4)-Ni(3B)-N(8E)	96.5(2)		N(1E)-N(2E)-Ni(1B)	122.9(4)
O(5)-Ni(3B)-N(8E)	93.3(2)		N(2E)-C(3E)-N(4E)	109.0(5)
N(4M)-Ni(3B)-N(8E)	97.5(3)		C(3E)-N(4E)-C(8AE)	105.6(5)
N(3M)-Ni(3B)-N(8E)	95.0(2)		C(3E)-N(4E)-C(5E)	132.7(6)

O(4)-Ni(4B)-O(6)	84.11(19)		C(8AE)-N(4E)-C(5E)	121.7(6)
O(4)-Ni(4B)-O(6M)	178.6(2)		C(6E)-C(5E)-N(4E)	116.3(7)
O(6)-Ni(4B)-O(6M)	96.1(2)		C(5E)-C(6E)-C(7E)	123.1(6)
O(4)-Ni(4B)-N(8F)	94.6(2)		O(7E)-C(7E)-N(8E)	120.9(7)
O(6)-Ni(4B)-N(8F)	90.8(2)		O(7E)-C(7E)-C(6E)	120.6(6)
O(6M)-Ni(4B)-N(8F)	86.8(3)		N(8E)-C(7E)-C(6E)	118.5(6)
O(4)-Ni(4B)-O(5M)	89.7(2)		C(8AE)-N(8E)-C(7E)	116.9(6)
O(6)-Ni(4B)-O(5M)	173.2(2)		C(8AE)-N(8E)-Ni(3B)	119.8(4)
O(6M)-Ni(4B)-O(5M)	90.1(3)		C(7E)-N(8E)-Ni(3B)	122.9(5)
N(8F)-Ni(4B)-O(5M)	92.5(2)		N(1E)-C(8AE)-N(8E)	127.5(6)
O(4)-Ni(4B)-N(1H)	86.9(3)		N(1E)-C(8AE)-N(4E)	109.2(5)
O(6)-Ni(4B)-N(1H)	87.2(3)		N(8E)-C(8AE)-N(4E)	123.3(5)
O(6M)-Ni(4B)-N(1H)	91.7(3)		C(8AF)-N(1F)-N(2F)	106.5(5)
N(8F)-Ni(4B)-N(1H)	177.3(3)		C(8AF)-N(1F)-Ni(2B)	128.7(4)
O(5M)-Ni(4B)-N(1H)	89.7(3)		N(2F)-N(1F)-Ni(2B)	124.4(4)
O(6)-Ni(5B)-O(5)	80.37(19)		C(3F)-N(2F)-N(1F)	109.8(5)
O(6)-Ni(5B)-O(8M)	175.2(3)		C(3F)-N(2F)-Ni(1B)	127.4(4)
O(5)-Ni(5B)-O(8M)	98.6(3)		N(1F)-N(2F)-Ni(1B)	122.9(4)
O(6)-Ni(5B)-N(2H)	88.4(3)		N(2F)-C(3F)-N(4F)	108.5(5)
O(5)-Ni(5B)-N(2H)	87.5(2)		C(8AF)-N(4F)-C(3F)	106.1(5)
C(8AF)-N(4F)-C(5F)	121.9(6)		N(8G)-C(8AG)-N(4G)	124.2(6)
C(3F)-N(4F)-C(5F)	132.1(6)		C(8AH)-N(1H)-N(2H)	103.2(8)
C(6F)-C(5F)-N(4F)	116.1(7)		C(8AH)-N(1H)-Ni(4B)	132.2(9)
C(5F)-C(6F)-C(7F)	122.4(7)		N(2H)-N(1H)-Ni(4B)	119.1(5)
O(7F)-C(7F)-N(8F)	120.4(8)		C(3H)-N(2H)-N(1H)	110.6(9)
O(7F)-C(7F)-C(6F)	120.2(7)		C(3H)-N(2H)-Ni(5B)	130.0(8)
N(8F)-C(7F)-C(6F)	119.4(7)		N(1H)-N(2H)-Ni(5B)	119.3(5)
C(8AF)-N(8F)-C(7F)	116.2(6)		N(2H)-C(3H)-N(4H)	107.6(11)
C(8AF)-N(8F)-Ni(4B)	120.8(5)		C(8AH)-N(4H)-C(3H)	107.4(8)
C(7F)-N(8F)-Ni(4B)	123.0(5)		C(8AH)-N(4H)-C(5H)	126.1(12)
N(1F)-C(8AF)-N(8F)	127.1(6)		C(3H)-N(4H)-C(5H)	126.5(11)
N(1F)-C(8AF)-N(4F)	109.1(6)		C(6H)-C(5H)-N(4H)	107.3(14)
N(8F)-C(8AF)-N(4F)	123.8(6)		C(5H)-C(6H)-C(7H)	129.8(13)
C(8AG)-N(1G)-N(2G)	106.7(5)		O(7H)-C(7H)-N(8H)	118.8(12)
C(8AG)-N(1G)-Ni(2B)	129.6(4)		O(7H)-C(7H)-C(6H)	124.1(11)
N(2G)-N(1G)-Ni(2B)	123.7(4)		N(8H)-C(7H)-C(6H)	117.0(11)
C(3G)-N(2G)-N(1G)	109.4(5)		C(8AH)-N(8H)-C(7H)	116.5(11)

C(3G)-N(2G)-Ni(1B)	127.7(4)		N(8H)-C(8AH)-N(1H)	125.5(12)
N(1G)-N(2G)-Ni(1B)	122.9(4)		N(8H)-C(8AH)-N(4H)	123.3(10)
N(2G)-C(3G)-N(4G)	08.8(5)		N(1H)-C(8AH)-N(4H)	111.2(10)
C(3G)-N(4G)-C(8AG)	106.6(5)		O(1N)-N(1N)-O(2N)	120.4(8)
C(3G)-N(4G)-C(5G)	132.8(6)		O(1N)-N(1N)-O(3N)	121.1(8)
C(8AG)-N(4G)-C(5G)	120.6(6)		O(2N)-N(1N)-O(3N)	118.2(9)
C(6G)-C(5G)-N(4G)	116.9(7)		O(4N)-N(2N)-O(5N)	128.1(19)
C(5G)-C(6G)-C(7G)	122.6(6)		O(4N)-N(2N)-O(6N)	121.7(18)
O(7G)-C(7G)-N(8G)	121.2(7)		O(5N)-N(2N)-O(6N)	110.2(13)
O(7G)-C(7G)-C(6G)	19.6(7)		O(8N)-N(3N)-O(7N)	124.7(14)
N(8G)-C(7G)-C(6G)	119.2(6)		O(8N)-N(3N)-O(9N)	116.4(13)
C(8AG)-N(8G)-C(7G)	116.4(6)		O(7N)-N(3N)-O(9N)	114.3(13)
C(8AG)-N(8G)-Ni(5B)	120.7(4)		O(10N)-N(4N)-O(11N)	122.0(12)
C(7G)-N(8G)-Ni(5B)	122.9(5)		O(10N)-N(4N)-O(12N)	112.2(12)
N(1G)-C(8AG)-N(8G)	127.2(6)		O(11N)-N(4N)-O(12N)	111.7(12)
N(1G)-C(8AG)-N(4G)	108.6(5)		N(1E)-Ni(2B)-O(4)	90.3(2)

### III.3.2.2.5 Preliminary results of Magnetic Studies.

The magnetic study of the clusters show interesting ferromagnetic and antiferromagnetic interaction at lower temperature, the graph of  $\chi$  vs. T (**Fig. 3.15**) indicate this behavior, the compound is still under farther magnetic studies to enable to calculate coupling constant and give the accurate information about the ferromagnetic and antiferromagnetic behavior.

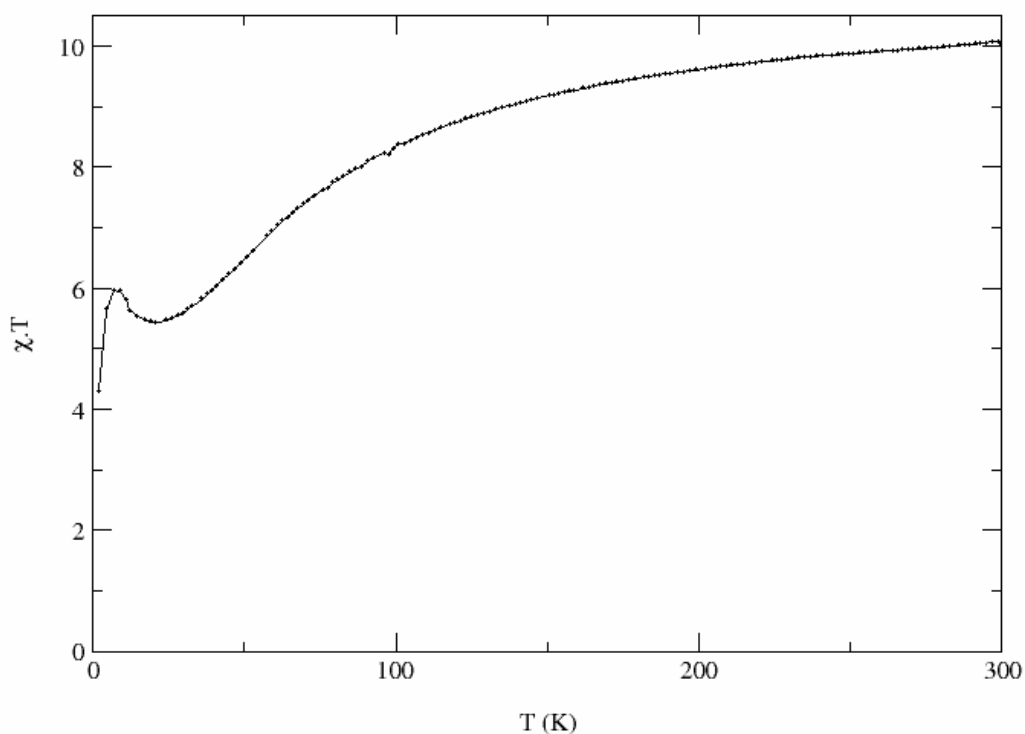


**Fig.3.15:** Magnetic susceptibility of  $\text{Ni}_9(\text{C}_5\text{H}_3\text{N}_4\text{O})_8(\text{NO}_3)_4(\text{NH}_3)_4(\text{OH})_6(\text{H}_2\text{O})_{16}$  cluster as a function of temperature

### III.3.3 Silver complex

#### III.3.3.1 Synthesis of $\text{Ag}_2\text{L}_2(\text{NO}_3)_2(\text{H}_2\text{O})_2$ complex

1 mmol of  $\text{AgNO}_3$  was dissolved in a solution of 10 ml 5M  $\text{HNO}_3$  and added to a clear solution of 1 mmol ligand solid dissolved in 30 ml 5M  $\text{HNO}_3$ , the solution was filtered off and allow to stranded at room temperature for 3 days, large colorless crystals suitable for X-ray work, were obtained..

#### III.3.3.2 Elemental analysis

Elemental analysis % for  $\text{Ag}_2\text{L}_2(\text{NO}_3)_2(\text{H}_2\text{O})_2$  complex: Found C,18.49; H,1.82; N,21.55. Calculated. C, 18.53; H, 1.85; N, 21.61

#### III.3.3.3 Infrared spectroscopy

The IR spectrum of  $\text{Ag}_2\text{L}_2(\text{NO}_3)_2(\text{H}_2\text{O})_2$  complex (**Fig 3.16**) is almost identical to that of free ligand  $\nu(\text{O-H})$  of water and N-H of pyrimidine ring showed at  $3449\text{ cm}^{-1}$ , the presence of the acidic hydrogen atom is shown in the characteristic set in the  $2700\text{-}3100\text{ cm}^{-1}$  region. Comparing with free ligand, the only appreciable difference is a  $35\text{ cm}^{-1}$  shifted to lower frequency of the C=O vibration mode and ( at  $1678\text{ cm}^{-1}$ ) and the appearance of new bands at  $1384\text{ cm}^{-1}$  (v. strong) and  $857$  (weak), corresponding respectively to  $\nu_3$  and  $\nu_2$  vibration modes of  $\text{D}_{3h}$   $\text{NO}_3^-$  group.

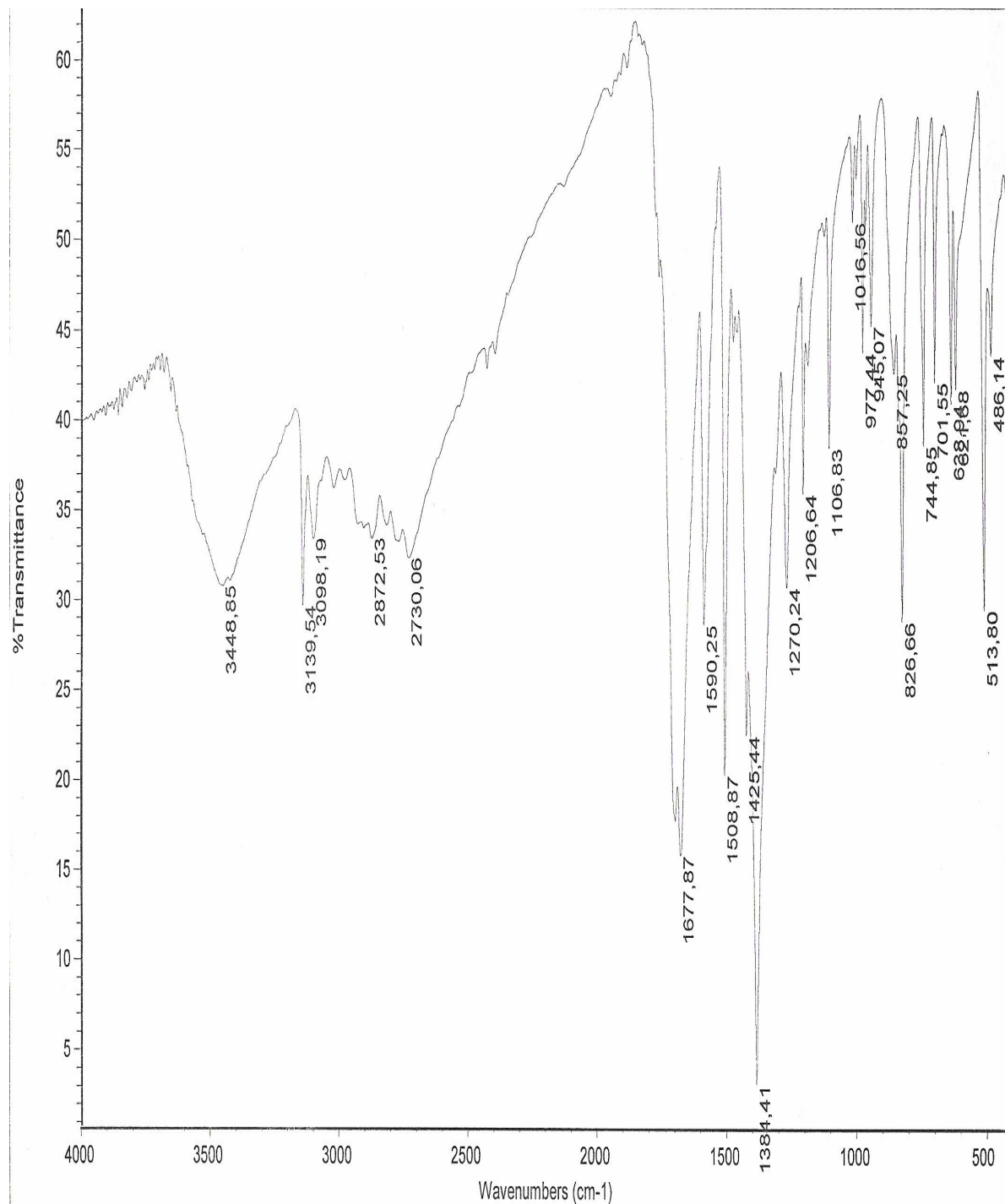


**Fig 3.16** IR Spectrum of  $\text{Ag}_2\text{L}_2(\text{NO}_3)_2(\text{H}_2\text{O})_2$  complex

### III.3.3.4 thermal analysis

Dehydration of  $[\text{Ag}_2\text{L}_2(\text{NO}_3)_2] \cdot 2\text{H}_2\text{O}$  complex is reflected by the corresponding weight losses and endothermic effect in the TG and DSC curves (**Fig 3.17 and 3.18**), which shows that the dehydration process takes place at high temperature (DSC endothermic peak at 161 °C) due to the strong interaction of the water molecule with the rest of the structure, this dehydration overlapping with another process since the weight loss is much higher than expected and the endothermic effect is immediately followed by an exothermically one. Pyrolytic decomposition of the compound ends at 500°C leaving silver metals final residue with the experimental weight percentage 35.52 % and calculated percentage 35.49%.

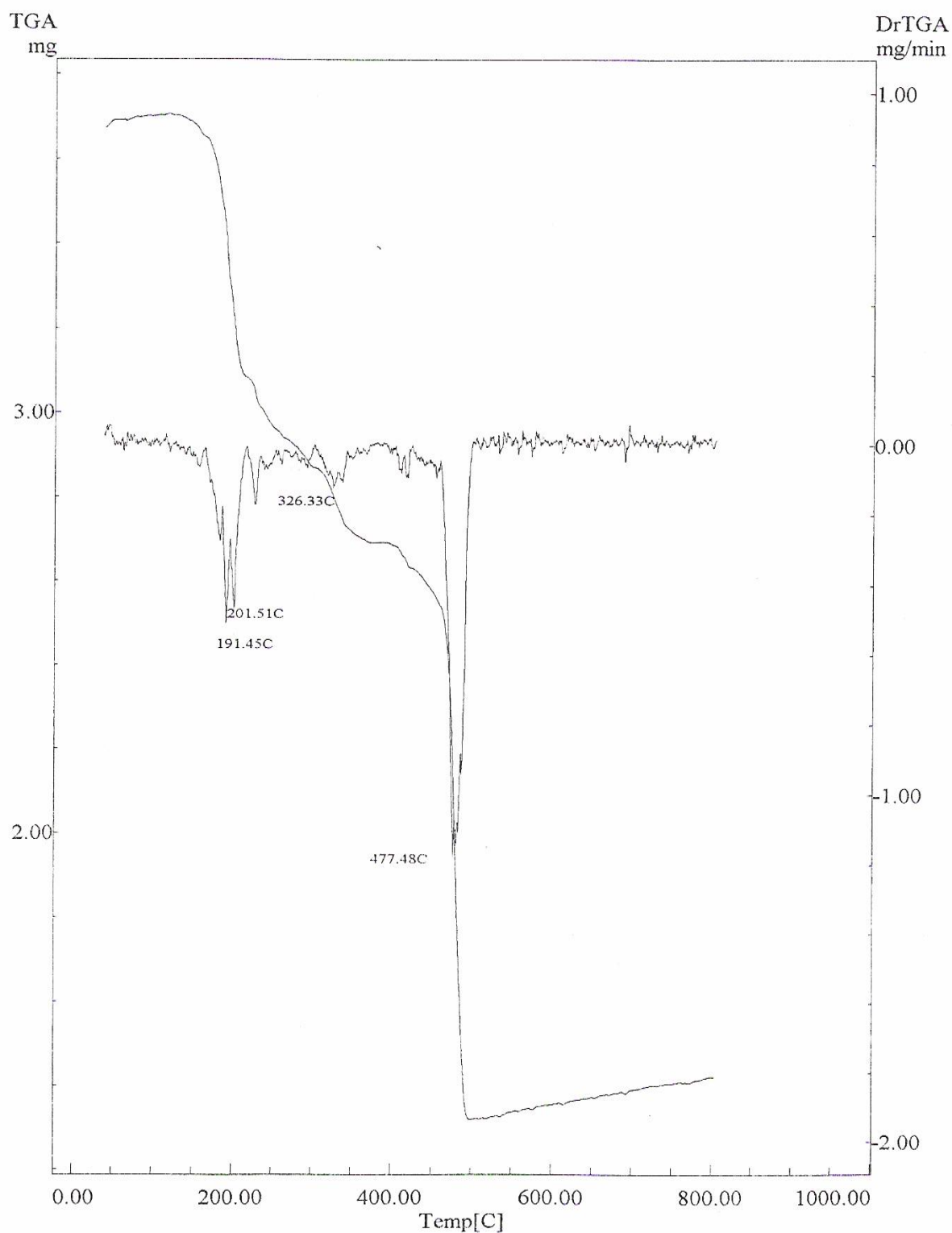


**Fig 3.17:** TG curve of  $\text{Ag}_2\text{L}_2(\text{NO}_3)_2(\text{H}_2\text{O})_2$  complex



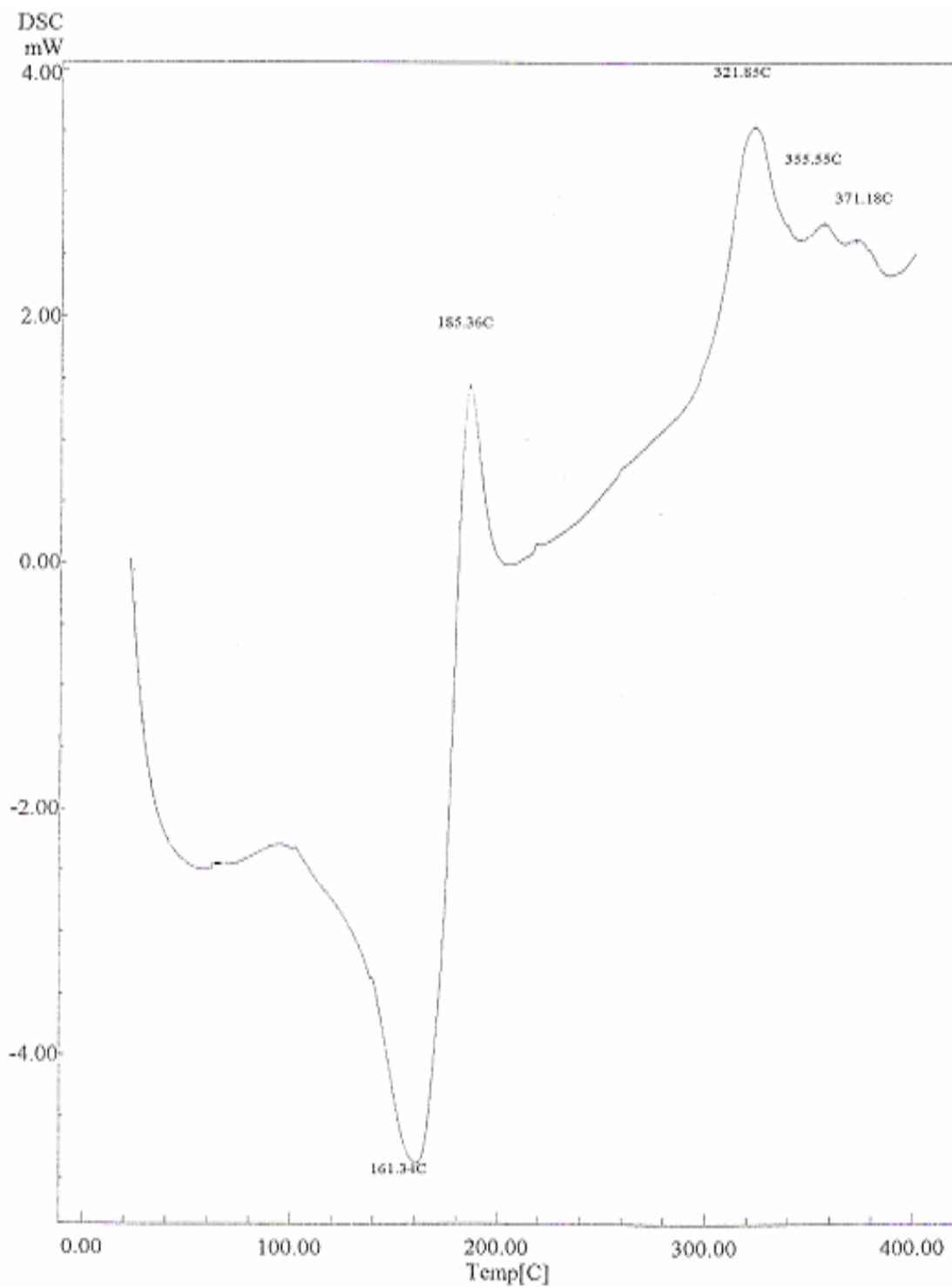


**Fig 3.18:** DSC curve of  $\text{Ag}_2\text{L}_2(\text{NO}_3)_2(\text{H}_2\text{O})_2$  complex

### III.3.3.5 Crystallography

Empirical formula	C <sub>10</sub> H <sub>12</sub> Ag <sub>2</sub> N <sub>10</sub> O <sub>10</sub>
Formula weight	648.04
Wavelength	0.71073 Å°
Crystal system	Monoclinic
Space group	P 2 <sub>1</sub> /c
Unit cell dimensions	
a	10.5297(6) Å°
b	12.6897(8) Å°
c	6.9432(4) Å°
β	94.782(1)°
Volume	924.51(9) Å <sup>3</sup>
Z	2
Calculated density	2.328 Mg/m <sup>3</sup>
Absorption coefficient	2.199 mm <sup>-1</sup>
F(000)	632
Crystal size	0.49 x 0.19 x 0.18 mm
Reflections collected / unique	5595 / 2080 [R(int)= 0.0155]
Final R indices [I>2σ(I)]	R1 = 0.0507, wR2 = 0.1396
R indices (all data)	R1 = 0.0607, wR2 = 0.1498
Largest diff. peak and hole	0.599 and -0.405 e. Å <sup>-3</sup>

The crystal structure is built by dinuclear centrosymmetric units (**Figure 3.19**) in which both silver atoms are bridged by two heterocycles, which are linked to the metal atoms through both external nitrogen atoms (N1 and N2) of the triazole ring. This defines a hexagonal Ag<sub>2</sub>N<sub>4</sub> core for which there are a number of other examples In the bibliography, involving pyrazole<sup>(139)</sup>, 1,2,4-triazolo and tetrazole<sup>(140)</sup> derivatives as well as piridazines<sup>(141)</sup>, but we have not found any for a 5+6 bicyclic ligand. This behaviour is very different to that of 1,2,4-triazolo[1,5-a]pyrimidines, which also form with Ag(I) dinuclear compounds but with a N3-N4 (N1-N8 translated to the [4,3-a] numbering

scheme) bridging mode that leads to a eight member  $\text{Ag}_2\text{C}_2\text{N}_4$  core <sup>(142)</sup>. As a consequence, the intermetallic distance (**Table 3.2**) is much higher in the compound described here.

The geometry of the cluster makes it impossible for the silver atom to adopt its usual linear coordination; instead, a flat trigonal geometry is observed, the third coordination position being occupied by a nitrate anion and the distortion of the triangle not being too severe (see bond distances and angles atoms in **Table 3.3** and **3.4**). A weak interaction with second oxygen of nitrate is also indicated in **Table 3.3**. The  $\text{Ag}_2\text{L}_2$  moiety is planar within  $0.025 \text{ \AA}$  with O1-N clearly displaced from this plane ( $0.983(3) \text{ \AA}$ ) and the water oxygen dose to it ( $0.223(4) \text{ \AA}$ ); the nitrate plane is rotated  $60.25(8)^\circ$  respect to the  $\text{Ag}_2\text{L}_2$  plane.

The strongly acidic media prevents deprotonation of N8, probably avoiding the formation of species with higher nuclearity (likely to be polymeric). The ligand is clearly in its amido tautomeric form and N8-H forms a rather strong hydrogen bond towards the water molecule which, in turn, forms another hydrogen bond with the nitrate anion defining in this wave an eight member pseudochelate ring. Again, the behaviour is different from that observed for the most similar member of the [1,5-a] series, for which the stability of the N4-Ag bond is able to displace the acidic proton to the exocyclic oxygen atom, giving rise to the formation of the unusual iminophenolic tautomer <sup>(143)</sup>.

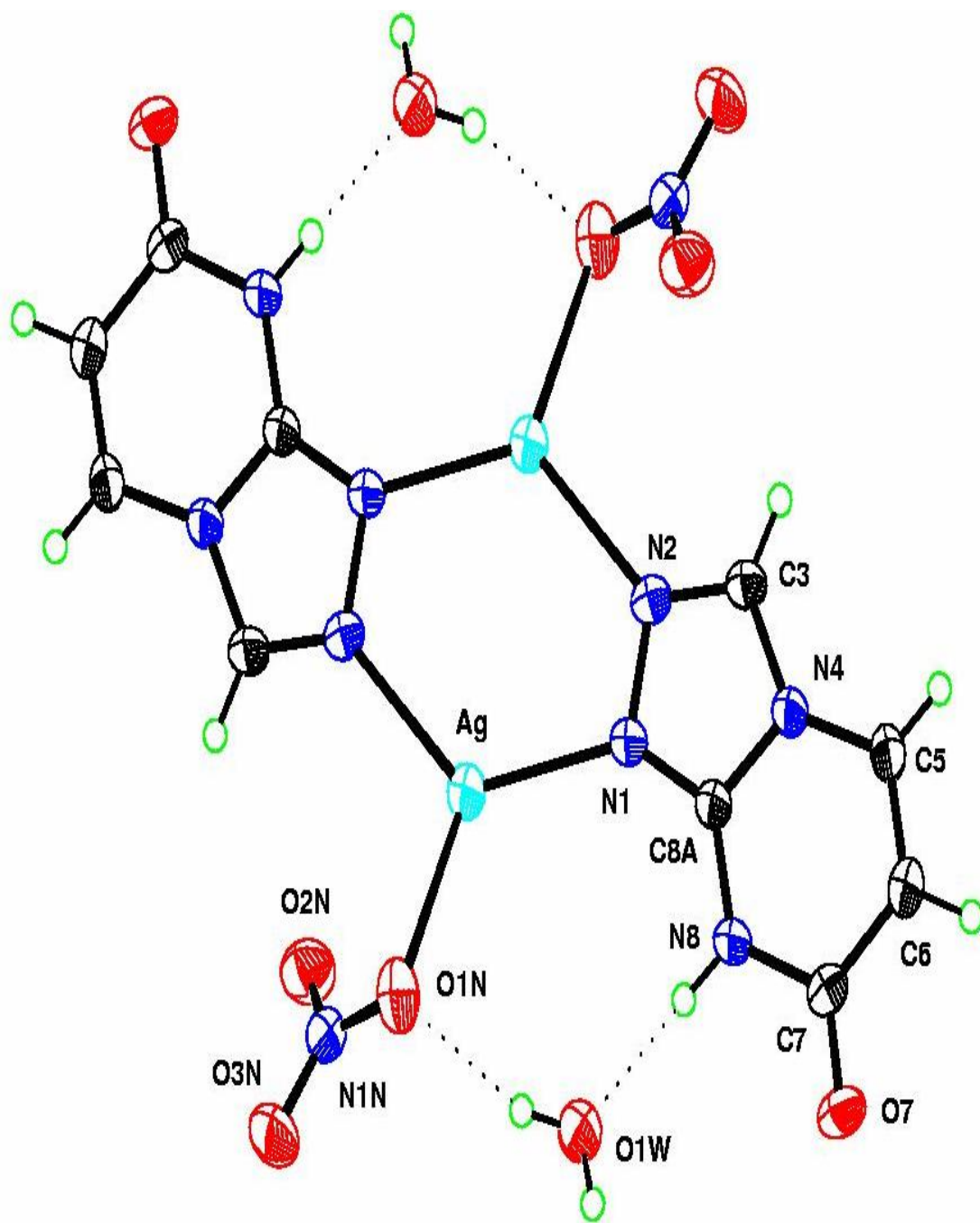


**Fig. 3.19:** Molecular structure of the dinuclear compound  $\text{Ag}_2\text{L}_2(\text{NO}_3)_2(\text{H}_2\text{O})_2$  according to X-ray analysis

**Table 3.3:** bond lengths [°A] of [Ag<sub>2</sub>L<sub>2</sub>(NO<sub>3</sub>)<sub>2</sub>].2H<sub>2</sub>O complex

Ag-N(1)	2.2423(18)		C(4)-C(5)	1.336(3)
Ag-N(2) # 1	2.2680(19)		C(5)-C(6)	1.451(3)
Ag-O(1N)	2.492(2)		C(6)-O(6)	1.221(3)
N(1)-C(7A)	1.304(3)		C(6)-N(7)	1.384(3)
N(1)-N(2)	1.405(3)		N(7)-C(7A)	1.360(3)
N(2)-C(3)	1.295(3)		N(1N)-O(2N)	1.235(3)
C(3)-N(3A)	1.371(3)		N(1N)-O(3N)	1.240(3)
N(3A)-C(7A)	1.363(3)		N(1N)-O(1N)	1.266(3)
N(3A)-C(4)	1.390(3)			

**Table 3.4:** bond angles [°] of [Ag<sub>2</sub>L<sub>2</sub>(NO<sub>3</sub>)<sub>2</sub>].2H<sub>2</sub>O complex

N(1)-Ag-N(2) #1	125.20(6)		C(6)-C(5)-N(4)	118.0(2)
N(1)-Ag-O (1N)	121.04(6)		C(5)-C(6)-C(7)	122.3(2)
N(2) #1-Ag-O(1N)	109.94(7)		O(7)-C(7)-N(7)	120.3(2)
C(8A)-N(1)-N(2)	105.80(17)		O(7)-C(7)-C(6)	123.7(2)
C(8A)-N(1)-Ag	139.76(15)		N(8)-C(7)-C(6)	115.91(19)
N(2)-N(1)-Ag	114.42(13)		C(8A)-N(8)-C(7)	122.00(18)
C(3)-N(2)-N(1)	108.38(18)		N(1)-C(8A)-N(8)	129.4(2)
C(3)-N(2)-Ag #1	131.29(15)		N(1)-C(8A)-N(4)	111.12(18)
N(1)-N(2)-Ag #1	120.28(14)		N(7)-C(8A)-N(4)	119.50(19)
N(2)-C(3)-N(3A)	109.65(19)		O(2N)-N(1N)-O(3N)	120.6(2)
C(8A)-N(4)-C(3)	105.04(17)		O(2N)-N(1N)-O(1N)	119.2(2)
C(8A)-N(4)-C(5)	122.17(18)		O(3N)-N(1N)-O(1N)	120.2(2)
C(3)-N(4)-C(5)	132.78(19)		N(1N)-O(1N)-Ag	103.45(15)

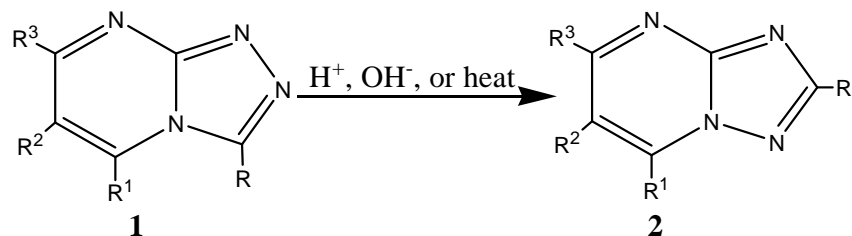
## *CHAPTER FOUR*

# **Dimroth rearrangement and the crystal structure of 7,8-dihydro-7-oxo-1,2,4-triazolo[4,3-a]pyrimidine ligand**

## IV.1 Introduction

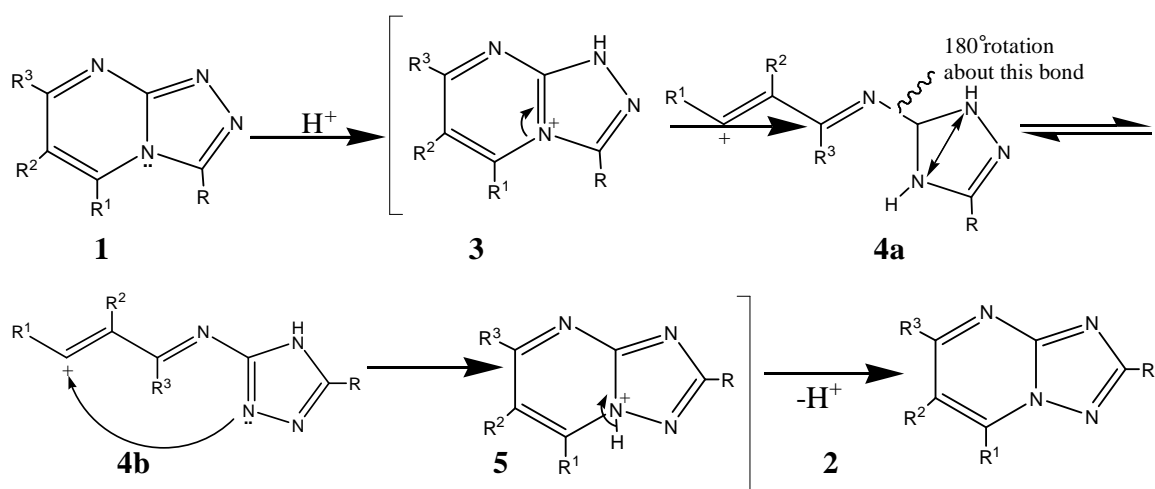
The Dimroth rearrangement <sup>(144)</sup> including 1,2,4-triazolo[4,3-a]pyrimidine generally proceeds rather easily; therefore these compounds, when prepared, are often not isolable (or only by very carefully handling).

This type of Dimroth rearrangement is strongly influenced primarily by inductive to a lesser extent by steric effects; Dimroth reactions, usually reversible, almost always proceed, in the case of triazolopyrimidines, from the kinetically favored [4,3-a] **1** product to the thermodynamically more stable [1,5-a] isomer **2** <sup>(8, 12)</sup> (**Scheme 50**). This isomerization may be induced by acids <sup>(5, 7, 18, 20, 131, 145, 146)</sup>, bases <sup>(7, 18, 20, 145)</sup>, or by heating <sup>(145)</sup>.



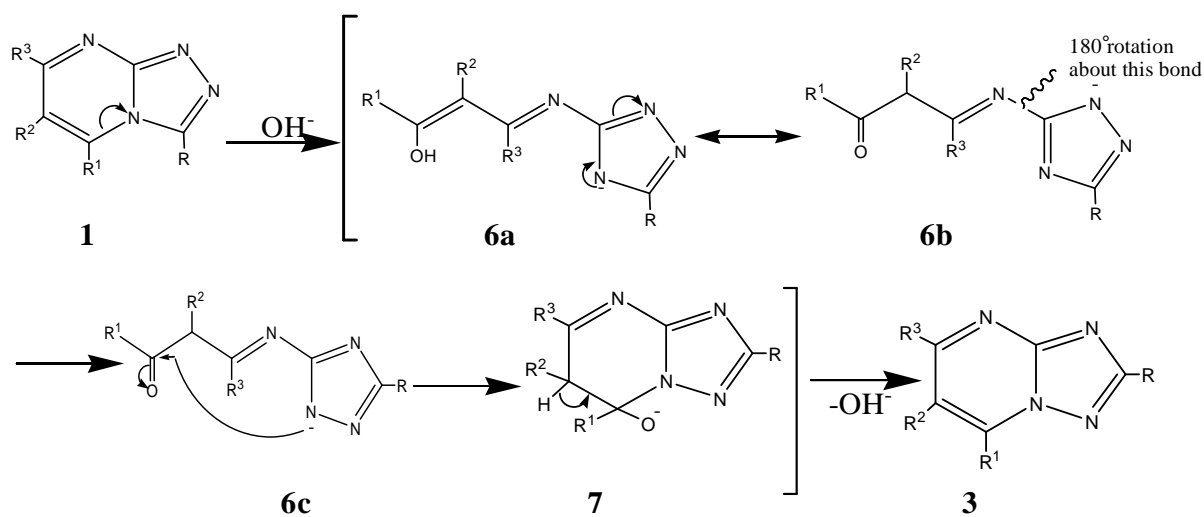
**Scheme 50**

The mechanism of this isomerization in acid media involves protonation of **1** followed by pyrimidine-ring opening of **3** to form the carbocation **4a**. Nucleophilic attack of the triazole N1 onto the positively charged carbon of the tautomeric structure **4b** gives the protonated cyclic isomer **5**, which deprotonates to the 1,2,4-triazolo[1,5-a]pyrimidine **2** <sup>(146)</sup> (**Scheme 51**).



**Scheme 51**

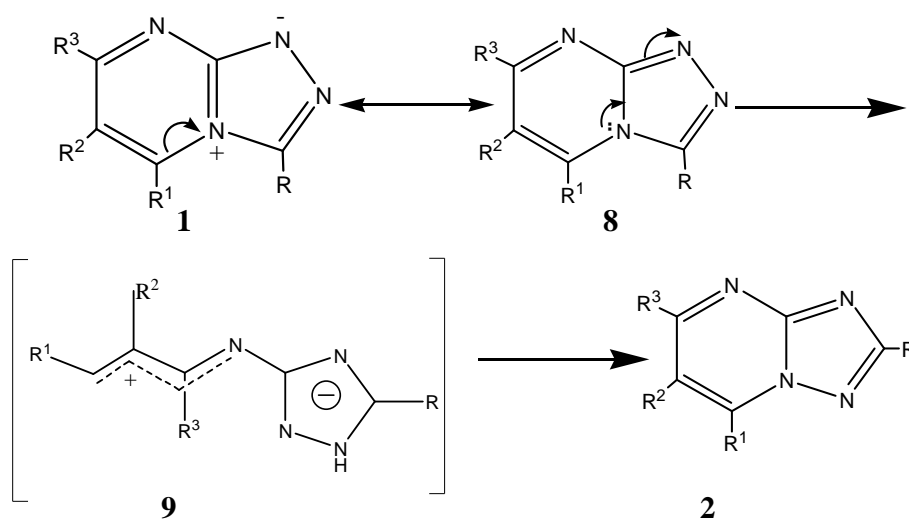
In basic media, the rearrangement of **1** most probably occurs by the nucleophilic attack of the base onto C5 causing pyrimidine-ring rupture to form **6a** and **6b**. Recyclization of the side-chain carbonyl carbon with the triazole N1 of the tautomeric structure **6c** and elimination of the base gave **2** (Scheme 52).



**Scheme 52**



Whereas there is no experimental proof for thermally induced isomerization of **1**, good arguments suggested to take place through the formation of the zwitterionic intermediate **9**<sup>(145)</sup>. Recyclization of the latter gives the isomer 1,2,4-triazolo[1,5-a]pyrimidine **2**<sup>(18, 20)</sup> (Scheme 53).



**Scheme 53**

Brown and Nagamatsu<sup>(132)</sup> reported kinetic studies on Dimroth rearrangements to triazolopyrimidine in two pH ranges. Isomerization rates in alkali increase steeply in the range pH 10-12.5. In acid, they obtain maxima at pH values corresponding approximately to the  $pK_a$  of each substance (in the range pH 1.5-2.5).

## IV.2 Results and Discussion

During one of the reactions to prepare cobalt complex with the desired ligand, an organic compound had precipitated in the form of mono crystal. This compound was resolved by X-ray diffraction. And came out to be a derivative thermodynamically stable [1,5-a].

Empirical formula	C <sub>9</sub> H <sub>9</sub> N <sub>4</sub> O <sub>3</sub>
Formula weight	231.45
Wavelength	0.71073Å°
Crystal system	triclinic
Space group	P1

### Unit cell dimensions

a	3.8164(2)Å°
b	9.9868(6)Å°
c	25.9722(15)Å°
$\alpha$	80.5010(10)°
$\beta$	88.6440(10)°
$\gamma$	86.8900(10)°
Volume	974.78(10)Å <sup>3</sup>
Z	4
Calculated density	1.577Mg/m <sup>3</sup>
Absorption coefficient	0.125 mm <sup>-1</sup>
F(000)	481
Crystal size	0.41 x 0.28 x 0.25 mm
Reflections collected / unique	8327/ 2080 [R(int)=0.0161]

The structure contains residues on one of the nitrogen of the pentagon. Carbon in position 2 bonded to hydrogen. The residue is bonded to nitrogen in position 3, this implies that when N4 lost the hydrogen site of the double bond had changed. El residue -CH=CH-CO-O-CH<sub>3</sub> came from a second atom of the ligand that was destroyed; these atoms are C7-C6-C5-O5. N4 had been hydrolyzed and in its place a methoxide group had situated (methanol was in the reaction medium). There are four equal and independent in the unit cell.

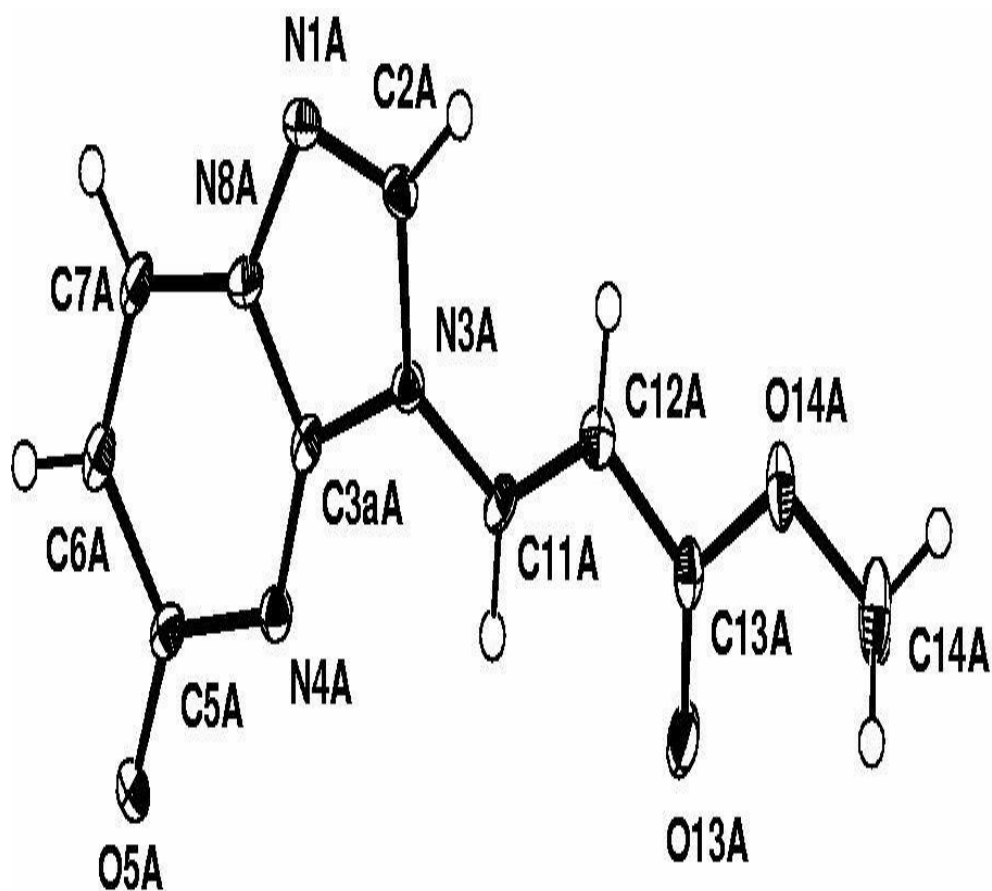


**Fig. 4.1** The crystal structure of the rearranged compound

**Table 4.1:** bond length [ $^{\circ}\text{A}$ ] of the rearranged compound

N1A-C2A	1.307(3)		N1C-C2C	1.295(3)
N1A-N8A	1.385(3)		N1C-N8C	1.393(3)
C2A-N3A	1.383(3)		C2C-N3C	1.392(3)
N3A-C3AA	1.376(3)		N3C-C3AC	1.377(3)
N3A-C11A	1.408(3)		N3C-C11C	1.412(3)
C3AA-N4A	1.297(3)		C3AC-N4C	1.304(3)
C3AA-N8A	1.353(3)		C3AC-N8C	1.346(3)
N4A-C5A	1.387(3)		N4C-C5C	1.385(3)
C5A-O5A	1.235(3)		C5C-O5C	1.239(3)
C5A-C6A	1.465(3)		C5C-C6C	1.461(3)
C6A-C7A	1.345(4)		C6C-C7C	1.350(4)
C7A-N8A	1.382(3)		C7C-N8C	1.377(3)
C11A-C12A	1.322(3)		C11C-C12C	1.325(3)
C12A-C13A	1.476(3)		C12C-C13C	1.473(3)
C13A-O13A	1.207(3)		C13C-O13C	1.215(3)
C13A-O14A	1.341(3)		C13C-O14C	1.331(3)
O14A-C14A	1.451(3)		O14C-C14C	1.455(3)
N1B-C2B	1.306(3)		N1D-C2D	1.296(3)
N1B-N8B	1.393(3)		N1D-N8D	1.396(3)
C2B-N3B	1.392(3)		C2D-N3D	1.392(3)
N3B-C3AB	1.375(3)		N3D-C3AD	1.381(3)
N3B-C11B	1.407(3)		N3D-C11D	1.399(3)
C3AB-N4B	1.296(3)		C3AD-N4D	1.305(3)
C3AB-N8B	1.359(3)		C3AD-N8D	1.354(3)
N4B-C5B	1.387(3)		N4D-C5D	1.394(3)
C5B-O5B	1.235(3)		C5D-O5D	1.236(3)
C5B-C6B	1.472(3)		C5D-C6D	1.457(3)
C6B-C7B	1.343(4)		C6D-C7D	1.350(4)
C7B-N8B	1.373(3)		C7D-N8D	1.371(3)
C11B-C12B	1.332(4)		C11D-C12D	1.336(4)
C12B-C13B	1.490(3)		C12D-C13D	1.475(4)
C13B-O13B	1.213(3)		C13D-O13D	1.214(3)
C13B-O14B	1.326(3)		C13D-O14D	1.338(3)
O14B-C14B	1.451(3)		O14D-C14D	1.450(3)

**Table 4.2:** Bond angle [°] of the rearranged compound

C2A-N1A-N8A	103.1(2)		C13D-O14D-C14D	116.0(2)
N1A-C2A-N3A	112.5(2)		C2C-N1C-N8C	103.3(2)
C3AA-N3A-C2A	106.9(2)		N1C-C2C-N3C	112.5(2)
C3AA-N3A-C11A	124.2(2)		C3AC-N3C-C2C	106.7(2)
C2A-N3A-C11A	128.7(2)		C3AC-N3C-C11C	125.1(2)
N4A-C3AA-N8A	127.4(2)		C2C-N3C-C11C	128.0(2)
N4A-C3AA-N3A	128.5(2)		N4C-C3AC-N8C	127.4(2)
N8A-C3AA-N3A	104.1(2)		N4C-C3AC-N3C	128.3(2)
C3AA-N4A-C5A	116.2(2)		N8C-C3AC-N3C	104.3(2)
O5A-C5A-N4A	119.6(2)		C3AC-N4C-C5C	115.7(2)
O5A-C5A-C6A	122.5(2)		O5C-C5C-N4C	119.8(2)
N4A-C5A-C6A	117.9(2)		O5C-C5C-C6C	121.7(2)
C7A-C6A-C5A	122.5(2)		N4C-C5C-C6C	118.5(2)
C6A-C7A-N8A	116.0(2)		C7C-C6C-C5C	121.9(2)
C3AA-N8A-C7A	120.0(2)		C6C-C7C-N8C	116.1(2)
C3AA-N8A-N1A	113.3(2)		C3AC-N8C-C7C	120.3(2)
C7A-N8A-N1A	126.7(2)		C3AC-N8C-N1C	113.2(2)
C12A-C11A-N3A	122.9(2)		C7C-N8C-N1C	126.5(2)
C11A-C12A-C13A	118.3(2)		C12C-C11C-N3C	122.5(2)
O13A-C13A-O14A	123.6(2)		C11C-C12C-C13C	119.4(2)
O13A-C13A-C12A	125.7(2)		O13C-C13C-O14C	123.4(2)
O14A-C13A-C12A	110.6(2)		O13C-C13C-C12C	125.9(2)
C13A-O14A-C14A	114.5(2)		O14C-C13C-C12C	110.6(2)
C2B-N1B-N8B	103.5(2)		C13C-O14C-C14C	115.84(19)
N1B-C2B-N3B	112.1(2)		C2D-N1D-N8D	103.8(2)
C3AB-N3B-C2B	107.3(2)		N1D-C2D-N3D	112.5(2)
C3AB-N3B-C11B	125.1(2)		C3AD-N3D-C2D	106.6(2)
C2B-N3B-C11B	127.5(2)		C3AD-N3D-C11D	124.9(2)
N4B-C3AB-N8B	127.1(2)		C2D-N3D-C11D	128.4(2)
N4B-C3AB-N3B	128.8(2)		N4D-C3AD-N8D	126.6(2)
N8B-C3AB-N3B	104.2(2)		N4D-C3AD-N3D	128.8(2)
C3AB-N4B-C5B	116.3(2)		N8D-C3AD-N3D	104.6(2)
O5B-C5B-N4B	119.8(2)		C3AD-N4D-C5D	116.0(2)

O5B-C5B-C6B	121.8(2)		O5D-C5D-N4D	119.3(2)
N4B-C5B-C6B	118.4(2)		O5D-C5D-C6D	122.0(2)
C7B-C6B-C5B	121.1(2)		N4D-C5D-C6D	118.7(2)
C6B-C7B-N8B	117.3(2)		C7D-C6D-C5D	121.4(2)
C3AB-N8B-C7B	119.8(2)		C6D-C7D-N8D	116.9(2)
C3AB-N8B-N1B	112.9(2)		C3AD-N8D-C7D	120.4(2)
C7B-N8B-N1B	127.3(2)		C3AD-N8D-N1D	112.5(2)
C12B-C11B-N3B	122.2(2)		C7D-N8D-N1D	127.1(2)
C11B-C12B-C13B	120.7(2)		C12D-C11D-N3D	122.3(2)
O13B-C13B-O14B	124.7(2)		C11D-C12D-C13D	119.7(2)
O13D-C13D-C12D	126.2(2)		O13D-C13D-O14D	124.0(2)
O14D-C13D-C12D	109.8(2)		C2C-N1C-N8C	103.3(2)
			N1C-C2C-N3C	112.5(2)

*CHAPTER FIVE*

*CONCLUSION*

1. This research and investigation of the coordination chemistry of triazolopyrimidine were the center of our thesis; a complete bibliography revision was done including all previous work of all investigation group in this field of study mainly the work of the group in Granada University (Spain) and Leiden University (Holland). All previous work about the coordination chemistry had focused on 1,5-a derivative, we have not found any reference for the coordination compound of any of any of the other arrangements (1,5-c, 4,3-a, or 4,3-c).
2. Following this line of investigation a new a new derivative 7,8-dihydro-7-oxo-1,2,4-triazolo[4,3-a]pyrimidine was synthesized and characterized, the only references were about the synthesis of this ligand. In this thesis we chose the best method through the synthesis and modification to obtain maximum yield.

The compound was characterize by usual methods and the results indicated that the most stable tautomer form is when the acidic hydrogen was on N8 position, pka value was determined and it was more acidic than analogues purine bases. On the other hand, theoretical study of the ligand was done in molecular and ionic form. This study indicates that the most stable tautomer is that when the acidic hydrogen is on N8. this was supported by  $^1\text{H-NMR}$  and  $^{13}\text{C-NMR}$  and from MO calculation there was no preference site of coordination. Characterization was completed by IR, elemental analysis, and theoretical studies.

3. Synthesis of metal complexes of the first and second row transition metals was carried out, some of these complexes were isolated in pure crystal form, others need further investigation, the complexes were characterize by X-ray crystallography showing that the retain 4,3-a isomer which is less favored thermodynamically.
4. For Ni cluster the ligand coordination in its anionic form through N1, N2 and O7 without preference of one site over another as was concluded from theoretical



calculation at lower temperature and also need further investigation since this type of compound could be used in the field of electronics as data storage materials.

5. the cation  $\text{Ag}^+$  show dimeric complex with the ligand in its molecular form and coordination mode N1 and N2 atoms, the acidic hydrogen was situated on N8 the same as in the free ligand.
6. The most stable thermodynamic 1,5-a compound was also obtained during the experiment and the isolated product is in agreement with Dimroth rearrangement

*CHAPTER SIX*

*REFERENCES*

1. C. Bulow and, K. Haas, *Chem. Ber.* **42**, 4638 (1909).
2. W. L. Moseby, *Chem. Heterocycl. Comp.* **15**, 878 (1961).
3. K. Sirakawa, *Yakugaku Zasshi* **78**, 1395 (1958), [CA **53**, 8150 (1959)]
4. Y. Makisumi, H. Watanabe, and K. Tori, *Chem. Pharm. Bull.* **12**, 204 (1964). C.
5. C. F. H. Allen, H. R. Beilfuss, D. M. Burness, G. A. Reynolds, J. F. Tinker, and L. A. Williams, *J. Org. Chem.* **25**, 361 (1960).
6. Ya. A. Levin and V. A. Kukhtin, *Zh. Obshch. Khim.* **34**, 502 (1964) [CA **60**, 13243 (1964)].
7. A. Kreutzberger, *Chem. Ber* **99**, 2237 (1966).
8. H. Reimlinger and M. A. Peiren, *Chem. Ber.* **103**, 3266 (1970).
9. J. Reiter, L. Pongó, and I. Lukovits, *Monatsh. Chem.* **119**, 341 (1988).
10. Fischer, *Adv. Heterocycl. Chem.* **57**, 81(1993).
11. V. A. Kovtunencko, V. V. Ishchenko, A. K. Tyltin, and F. S. Babichev, *Ukr, Khim. Zh.* **57**, 172 (1991) [CA **115**, 29155 (1991)].
12. M. Tisler, *Pure Appl. Chem.* **52**, 1611 (1980).
13. A. V. Ivashchenko and O. N. Garicheva, *Khim. Geterosikl. Soedin.*, 579 (1982) [CA **97**, 109889 (1982)].
14. M. A. E. Shaban, M. A. M. Taha, and E. M. Sharshira, *Adv. Heterocycl. Chem.* **52**, 1 (1991)
15. G. Maury, *Chem. Heterocycl. Comp.* **30**, 179 (1977).
16. E. S. H. El Ashry, Y El Kilany, N. Rashed, and H. R. Assafir, *Adv., Heterocycl. Chem.* **73** (1999).
17. J. D. Bower and F. P. Doyle, *J. Chem. Soc.*, 727 (1957)
18. T. Novinson, T. Okabe, R. K. Robins, and P. Dea, *J. Heterocycl. Chem.*, **12**. 1187 (1975)

19. S. Ishiguro, T. Kojima, and A. Mitsui, Ger. Pat., 3,308.203 (1983) [CA **100**, 59576 (1984)].
20. R. G. W. Spickett and S. H. B. Wright, *J. Chem. Soc. C*, 498 (1967).
21. H. S. El Khadem, J. Kawai, and D. L. Swartz, *Heterocycles* **28**, 239 (1989).
22. P. Nagy, I. Gorbe, V. Pany, and L. Fodor, Rom. Pat. 63,828 (1978) [CA **92**, 41980 (1980)]
23. T. La Noce and A. M. Giuliani, *Tetrahedron* **34**, 2927 (1978).
24. H. A. Daboun and A. M. El-Reedy, *Z. Naturforsch., B: Anorg. Chem., Org. Chem.* **38B**, 1686 (1983).
25. S. M. Hussain, A. M. El-Reedy, A. M. H. Rezk, and Kh. A. S. El-Dien, *J Heterocycl. Chem.* **24**, 1605 (1987)
26. S. M. Hussain, A. M El-Reedy, and A. S. Ali, *Sulfur Lett.* **7**, 203 (1988).
27. N. H. Eshba, *Alex. J. Pharm. Sci.* **9**, 31(1995) [CA **123**, 313858 (1995)].
28. B. E. Bayoumy, S. El-Bahie, M. El-Mobayed, and El. Abd El-Latif, *Rev. Roum. Chim.* **38**, 701 (1993).
29. T. Okabe, E. Taniguchi, and K. Maekawa, *Agric. Biol. Chem.* **37**, 441 (1973) [CA **79**, 5307 (1973)].
30. G. M. Golubushina, G. N. Poshtaruk, and V.A. Chuiguk, *Khim. Geterosikl. Soedin.*, 565 (1974) [CA **81**, 49629 (1974)]
31. M. El-Borai, A. A. El-Barbary, M. Fahmy, and H.H. El-Naggar, *DeltaJ. Sci.* **12**, 93 (1988) [CA **112**, 235227 (1990)]
32. Shionogi & Co., Ltd. (H. Kano, Y. Makikado, and S. Takahashi), Jpn. Pat. 61/14,724 (1961) [CA **56**, 10165 (1962)].
33. G. Jaenecke, L. Meister, L. Dressel, R. Richter, and H. Voigt, *Z. Chem.* **29**, 378 (1989).
34. A. Hassoun and J. Liebscher, Ger. (East) Pat. 270,711 (1989) [CA **112**, 98556 (1990)].

35. J. J. Hlavka, P. Bitha, and Y. Lin, U.S. Pat. 4,546,181 (1985) [CA **104**, 225051(1986)].
36. Y. Tamura, J. H. Kim, and M. Ikeda, *J. Heterocycl. Chem.* **12**, 107 (1975).
37. B. Stanovnik, A. Stimac, M. Tisler, and B. Vercek, *J. Heterocycle. Chem.* **19**, 577 (1982).
38. S. Polanc, B. Vercek, B. Stanovnik, and M. Tisier, *Tetrahedron Lett.*, 1677 (1973).
39. Y. Qu and W. Zhang, *Zhonguo Yiyao Gongye Zazhi* **23**,538 (1992) [CA **119**, 117200 (1993)].
40. K. Wermann and M. Hartmann, *Synthesis*, 189 (1991).
41. S. M. Desenko, V. D. Orlov, N. V. Getmanskii, O. V. Shishkin, S. V Lindeman, and Yu. T. Struchkov, *Dokl. Akad. Nauk SSSR* **324**, 801 (1991).
42. A. Kreutzberger and G. Risse, *Arch. Pharm. (Weinheim, Ger.)* **313**, 244 (1980).
43. A. -S. M. Abdel-Fattah, S. M. Sherif, M. M. Youssef, and N. S. E. Ahmed, *J. Chem. Res., Synop.*, 412 (1994).
44. F. Yoneda and T. Nagamatsu, *Chem. Pharm. Bull.* **23**, 1885 (1975)
45. B. Jenko, B. Stanovnik, and M. Tisier, *Synthesis*, 833 (1976).
46. T. K. Liao, F. Baiocchi, and C. C. Cheng, *J. Org. Chem.* **31**, 900 (1996)
47. Farmaceutici Italia Soc. Anon. (B. Camerino and T. La Noce), Ger. Pat. 1,074,589 (1960) [CA **55**, 19967 (1961)].
48. D. Loaks, D. M. Brown, and S. A. Salisbury, *Tetraheadron Lett.* **39**, 3865 (1998).
49. D. J. Brown and J. R. Kershaw, *J. Chem. Soc., Perkin Trans.* **1** ,2316 (1972).
50. O. Rousseaux, D. Blondeau, and H. Sliwa, *Heterocycles* **31**, 277 (1990).
51. C. Temple, Jr., R. L. McKee, and J. A. Montgomery, *J. Org. Chem.* **28**, 2257 (1963).
52. G. W. Miller and F. L. Rose, *J. Chem. Soc.*, 3357 (1965)

53. G. D. Searle and Co. (H. A. Wagner), Ger. Pat. Offen. 3,029,871 (1981) [CA **94**, 175163 (1981)]
54. G. D. Searle and Co. (H. Wagner), U.S. Pat. 4,405,780 (1983) [CA **100**, 6550 (1984)].
55. H. S. El-Khadem, J. Kawai, and D. L. Swartz, *Heterocycles* **28**, 239 (1989)
56. W. Ried and J. Nenninger, *Chem. Ber.* **119**, 129 (1986).
57. M. T. Cocco, C. Congiu, A. Maccioni, and V. Onnis, *J. Heterocycl. Chem.* **29**, 1341 (1992).
58. C. Yamazaki, *J. Org. Chem.* **46**, 3956 (1981).
59. C. Yamazaki, *Bull. Chem. Soc. Jpn.* **54**, 1767 (1981).
60. Y. Miyamoto, *Chem. Pharm. Bull.* **33**, 2678 (1985).
61. M. L. Benklioud, II. Mraihl, and B. Baccar, *J. Soc. Chim. Tunis.*, **2**, 3 (1989) [CA **114**, 81750 (1991)].
62. F.K. Mohamed, *Bull. Fac. Sci., Assiut Univ.* **21**, 81(1992) [CA **118**, 80897 (1993)].
63. N.V. Volkova, V N. Konyukhov, T. G. Koksharova, L. N. Dianova, and Z. V. Pushkareva, *Khirn. Geterotsikl. Soedin.*, 262 (1979).
64. M. L. Benkhoud, H. Mraih, and B. Baccar, *J. Soc. Chim. Tunis.* **3**, 145 (1992) [CA **119**, 180731 (1993)].
65. M. Pohl, U. Bechstein, M. Paetzel, J. Liebscher, and P. G. Jones, *J. Prakt. Chem./Chem. Ztg.* **334**, 630 (1992) [CA **118**, 191705 (1993)]
66. F. Gatta, M. R. Del Giudice, A. Borioni, C. Mustazza, and C. Fazio, *J. Heterocycl. Chem.* **31**, 1171 (1994).
67. M. R. Del Giudice, A. Borioni, G. Mustazza, F. Gatta, *J. Heterocycl. Chem.* **31**, 1503 (1994).
68. J. E. Francis, W. D. Cash, B. S. Barabaz, P. S. Bernard, R. L. Lovell, G. C. Mazzenga, R. C. Friedmann, J. L. Hyun, A. F. Braunwalder, P. S. Loo, and D. A. Bennet, *J. Med. Chem.* **34**, 281 (1991).

69. R. A. Bowie, D. A. Thomason, and J. A. J. Jarvis, *Tetrahedron Lett.*, 1643 (1973).
70. R. Neidlein and W. D. Ober, *Monash. Chem.* **107**, 1241 (1976) [*CA* **86**, 89772 (1977)].
71. N. Guillot, H. G. Viehe, B. Tinant, and J. P. Declercq, *Tetrahedron* **46**, 3897 (1990).
72. J.B. Medwid, R. Paul, J. S. Baker, J. A. Brockman, M. T. Du, W. A. Hallett, J. W. Hanifin, R. A. Hardy, Jr., M. E. Tarrant, W. Torley, and S. Wrenn, *J. Med. Chem.* **33**, 1230 (1990).
73. J.M. Salas, A. Rahmani, M.A. Romero, M. Quirös, E.R.T. Tiekink, *J. Chem. Cryst.* **24**, 669 (1994).
74. J.M. Salas, M.A. Romero, J.A. Rodriguez, R. Faure, *J. Chem. Cryst.* **26**, 847 (1996).
75. A.T.H. Lenstra, H.J. Bruins-Slot, P.T. Beurskens, J.G. Haasnoot, J. Reedijk, *Recl. Trav. Chim. Pays-Bas* **108**, 133 (1989).
76. J.M. Salas, J. A. R. Navarro, M. Romero, M. Quirös, *An. Quim. Int. Ed.* **93**, 55 (1997).
77. J.M. Salas, M.A. Romero, A. Rahmani, R. Faure, G. Alvarez de Cienfuegos, E.R.T. Tiekink, *J. Inorg. Biochem.* **64** 259 (1996).
78. J.M. Salas, A. Rahmani, M.A. Romero, A.D. Rae, A.C. Willis, E.R.T. Tiekink, *Z. Krist.* **213** 302 (1998).
79. J.A.R. Navarro, M.A. Romero, J.M. Salas, E.R.T. Tiekink, *Z. Krist.* **212**, 682 (1997).
80. T.L.F. Favre, J.G. Haasnoot, J. Reedijk, *Polyhedron* **5**, 1405 (1986).
81. J.A.R. Navarro, M.A. Romero, J.M. Salas, J. Molina, E.R.T. Tiekink, *Inorg. Chim. Acta* **274**, 53 (1998).
82. M. Abul Haj, M. Quirös, J.M. Salas, Communication presented to the 4th European Biological Inorganic Chemistry Conference, Seville, Spain, 1998.

83. M.A. Romero, J.M. Salas, M. Quirós, M.P. Sanchez, J. Romero, D. Martín, *Inorg. Chem.* **33**, 5477 (1994).
84. M. Biagini-Cingi, A.M. Manotti-Lanfredi, A. Tiripicchio, J.P. Cornelissen, J.G. Haasnoot, J. Reedijk, *Inorg. Chim. Acta* **129**, 217 (1987).
85. M. Biagini-Cingi, A.M. Manotti-Lanfredi, A. Tiripicchio, J.P. Cornelissen, J.G. Haasnoot, J. Reedijk, *Acta Cryst.* **C4** 21296 (1986).
86. S. B. Sanni, H. Behm, P.T. Beurskens, J.P. J.P. Cornelissen, J.G. Haasnoot, A. T. H. Lenstra, *J. Cryst. Spec. Res.* **17**, 81 (1987).
87. M. Abul Haj, M. Quirós, J.M. Salas, R. Faure, Communication presented to the X Symposium del Grupo Especializado de Cristalografía, Andorra la Vella, Andorra, (1998).
88. M. Biagini-Cingi, A.M. Manotti-Lanfredi, A. Tiripicchio, J.G. Haasnoot, J. Reedijk, *Inorg. Chim. Acta.* **101** 49 (1985).
89. M. Biagini-Cingi, A.M. Manotti-Lanfredi, A. Tiripicchio, J.G. Haasnoot, J. Reedijk, *Inorg. Chim. Acta* **86** (1984) 137—143.
90. M. Biagini-Cingi, A.M. Manotti-Lanfredi, A. Tiripicchio, J. Reedijk, J.G. Haasnoot, *Acta Cryst.* **C42** 427 (1986).
91. M. Abul Haj, M. Quirós, J.M. Salas, R. Faure, *J. Chem. Soc. Dalton Trans.* 1798, (2001).
92. J.A.R. Navarro, M.A. Romero, J.M. Salas, R. Faure, X. Solans, *J. Chem. Soc. Dalton Trans.* 2321 (1997).
93. M. Abul Haj, M. Quirós, J.M. Salas, R. Faure, *J. Chem. Commu.* **4** 254 (2001).
94. J.G. Haasnoot, T.L.F. Favre, W. Hinrichs, J. Reedijk, *Angew. Chem. Int. Ed. Engl.* **27**, 856 (1988).
95. A.H. Velders, L. Pazderski, F. Ugozzoli, M. Biagini-Cingi, A.M. Manotti-Lanfredi, J.G. Haasnoot, J. Reedijk, *Inorg. Chim. Acta.* **273**, 259 (1998).



96. M. Biagini-Cingi, A.M. Manotti-Lanfredi, A. Tiripicchio, J.G. Haasnoot, J. Reedijk, *Inorg. Chim. Acta.* **72**, 81 (1983).
97. J.A.R. Navarro, J.M. Salas, M.A. Romero, R. Vilaplana, F. Gonzalez-Vilchez, R. Faure, *J. Med. Chem.* **41**, 332 (1998).
98. J.A.R. Navarro, M.A. Romero, J.M. Salas, M. Quirós, *Inorg. Chem.* **36**, 3277 (1997).
99. J.A.R. Navarro, M.A. Romero, J.M. Salas, M. Quires, J. El Bahraoui, J. Molina, *Inorg. Chem.* **35**, 7829 (1996).
100. T. L. Pilicheva, V L. Rusinov, L. G. Egorova, O. N. Chupakhin, G. V. Viadyko, L. V. Korobchenko, and E. I. Boreko, *Khim. Farm. Zh.* **24**, 41(1990).
101. M. Nakazawa, H. Iwagami, M. Yatagai, A. Hosoi, H. Naora, T. Oonuki, K. Kato, and K. Murakami, Eur. Pat. 292,230 (1988) [CA **110**, 231332 (1989)].
102. K. Singh, A. Hasan, R. Pratap, P.Y. Guru, and D. S. Bhakuni, *J. Indian Chem. Soc.* **66**, 686 (1989).
103. J. J. Wade, U. S. Pat. 4,528,288 (1985) [CA **104**, 5889 (1986)].
104. J.J. Wade, U.G. Pat., 4,591,588 (1986) [CA **105**, 97494 (1986)].
105. Mitsui Petrochemical Industries, Ltd., Jpn. Kokai Pat. 59/29,689 (1984) [CA **101**, 72749 (1984)].
106. Mochida Pharmaceutical Co. Ltd., Jpn. Kokai Pat. 81/127, 383 (1981) [CA **96**, 85572 (1982)].
107. A. Eriguchi, T. Mimura, M. Tomikawa, and K. Nishida, Jpn. Kokai Pat. 03/118,383 (1991) [CA **115**, 208011 (1991)].
108. K. Atwal, Ger. Pat. 3,839,711 (1989) [CA **112**, 55902 (1990)].
109. E. Nicolai, El. Cure, J. Eloyard, M. Kirchner, J. M. Teulon, A. Ver signy, M. Gazes, F. Caussade, A. Virone-Oddos, and A. Cloarec, *J. Med. Chem.* **37**, 2371 (1994)].
110. A. Ookubo, T. Minegishi, I. Shimoyama, H. Sato, and T. Mizuta, Jpn. Kokai Pat. 07/157,485 (1995) [CA **123**, 256758 (1995)].
111. N. Bru-Magniez, T. Guengor, and J. M. Teulon, U.S. Pat. 5,387,747 (1995) [CA **123**, 228204 (1995)].

112. H. Wagner, Eur. Pat. 152,841 (1985) [CA **104**, 34103 (1986)].
113. A. Dlugosz, *Pol. J. Chem.* **66**, 131 (1992).
114. A. P. Novikova, L.A. Chechulina, G.M. Anoshina, and A. S. Bary bin, *Khim. Farm. Zh.* **15**, 31(1981).
115. D. J. Heal, M. I. Fernandez, and B. G. Sargent, PCT Pat. 9,510,521 (1995) [CA **123**, 313997 (1995)].
116. MA. Romero, J.M. Salas, M. Quirós, D.J. Williams, J. Molina, *Trans. Met. Chem.* **18**, 595 (1993).
117. F. Luque, C. Fernández-Ramos, E. Guerrero, J.M. Molina, A. Doña, J.M. Salas, M. Sanchez Moreno, Communication presented to the 1st COST B-9 Congress on Anitprotozoal Chemoterapy, Sierra Nevada, (1998).
118. F. Luque, C. Fernández-Ramos, S. Azzouz, M.J. Rosales, C. Mascaró, J.M. Salas, M. Sanchez Moreno, Communication presented to the 1st COST B-9 Congress on Anitprotozoal Chemoterapy, Sierra Nevada, (1998).
119. A.H. Velders, L. Pazderski, F. Ugozzoli, M. Biagini-Cingi, A.M. Manotti-Lanfredi, J.G. Haasnoot, J. Reedijk, *Inorg. Chim. Acta.* **273**, 259 (1998).
120. M. J. Costales, J. C. Van Heertum, W. A. Kleschick, R. J. Ehr, and P. El. Ray, U.S. Pat. 5,201,938 [CA **119**, 180806 (1993)].
121. W.A. Kleschick, M. J. Costales, B. C. Gerwick, J. B. Holtwick, R. W. Meikle, W. T. Monte, N. R. Pearson, S. W. Snider, NI. V Subramanian et al., *ACS Symp. Ser.* **504**, 10 (1992) [CA **117**, 228373 (1992)].
122. W. A. Kleschick, M. J. Costales, J. E. Dunbar, R. W. Meikle, W T. Monte, N. R. Pearson, S. W. Snider, and A. P. Vinogradoff, *Pestic. Sci.* **29**, 341 (1990) [CA **113**, 206633 (1990)].
123. K. Jeich, H. J. Santel, R. R. Schmidt, and H. Strang, Eur. Pat, 337,232 (1989) [CA **112**, 139042 (1990)]
124. K. J. Pees and H. M. Becher, PCT Pat. 9,420,501 (1994) [CA **122**, 133227 (1995)].

125. K. Eichen, K. Soheib, H. Theobald, E. H. Pommer, and E. Amman, Ger. Pat., 3, 130,633 (1983) [CA **98**, 215609 (1983)].
126. A. Kleschick, R. J. Ehr, M. J. Costales, B. C. Gerwick, J. B. Holtwick, R. W. Meikie, W. T. Monte, and N. R. Pearson, U.S. Pat. 4,818,273 (1985) [CA **103**, 196117 (1985)].
127. H. Nakamura, Y. Hosoi, and J. Fukawa, Jap. Kokai Pat. 03/13,934 (1991) [CA **115**, 266657 (1991)].
128. K. H. Bedemann, G. Fischer, M. Klepel, S. Kuehne, H. J. Michel, F. Schulze, and G. Schwarz, Ger. (East) Pat. 276,620 (1990) [CA **114**, 39451 (1991)].
129. L. A. Williams, *J. Chem. Soc.*, **1829** (1960).
130. I. Krezel, *pharmazie* **43**, 723 (1988).
131. W. W. Paudler and L. S. Helmick, *J. Heterocycle. Chem.* **3**, 269 (1966).
132. J. M. Salas, C. Enrique, M. A. Romereo, K. Takagi, K. Auki, Y. Miyashita, and IL-Hawan Suh, *J. Polyhedron*. **11**. 22, (1992), 2903-2912
133. D. J. Brown and T. Nagamatsu, *Aust. J. Chem.* **30**, 2515 (1977).
134. H. Reimlinger, *Chem. Ber.* **103**, 3278 (1970).
135. ChemOffice Ultra(R) version 7.0.1 CambridgeSoft Corporation, 2002.
136. J. J. Christensen, J. H. Rytting, R. M. Izatt, *Biochemistry* **9**, 4907 (1970).
137. HyperChem, "Tools for molecular Modeling", Computational Chemistry, HyperCub, Inc. 1996.
138. M. Sabat, D. Zglinska, B. Jazowska-Trzebiato Wska, *Acta crystallogr., Sect. B* **36** (1980) 1187.
139. G. A. Ardizzola, G. La Monica, A. Maspero, N. Moret, N. Masciochi, *Inorg. Chem.* **36** (1997) 2321
140. L. Carlucci, G. Ciani, D. M. Proserpio, *Angew. Chem. Int. Ed. Engl.* **38** (1999) 3488.
141. L. Carlucci, G. Ciani, D. M. Proserpio, A. Sironi, *Inorg. Chem.* **37** (1998) 5941.

142. J.M. Salas, M.A. Romero, A.Rahmani, M. Quirô's, *An. Quim. Int. Ed.* **92** (1996) 249.
143. M. Abul Haj, M. Quiros, J.M. Salas, R. Faure, *J. Chem., Soc., Dalton Trans.* (2001) 1798
144. M. Wahren, *Z. Chem.* **9**, 242 (1969).
145. J. A. Bee and F.L. Rose, *J. Chem. Soc. C*, 2031 (1966).
146. M. Kuentlinger and E. Breitmaier, *Synthesis*, **44** (1983).